ÅBO AKADEMI

INSTITUTIONEN FÖR
KEMITEKNIK

DEPARTMENT OF CHEMICAL
ENGINEERING

Processkemiska centret

Process Chemistry Centre

REPORT 14-01

Fate of Fuel-Bound Nitrogen and Sulfur in Biomass-Fired Industrial Boilers

Emil Vainio

Doctoral Thesis

Laboratory of Inorganic Chemistry

Emil Vainio

M.Sc. 2009

Laboratory of Inorganic Chemistry

Department of Chemical Engineering

Åbo Akademi University

Fate of Fuel-Bound Nitrogen and Sulfur in Biomass-Fired Industrial Boilers

Emil Vainio

Doctoral Thesis

Laboratory of Inorganic Chemistry
Process Chemistry Centre
Department of Chemical Engineering
Åbo Akademi University
2014

Supervisors

Docent Anders Brink
Åbo Akademi University

Professor Mikko Hupa
Åbo Akademi University

Opponent and reviewer

Professor Peter Glarborg
Technical University of Denmark

Reviewer

Docent Lars-Erik Åmand
Chalmers University of Technology

Preface

I would like to thank my supervisors, Docent Anders Brink and Professor Mikko Hupa, for all their guidance and support during my doctoral studies. I would like to express my gratitude for the continuous support I have got from Anders. It is amazing how he always found time for me when I got stuck in my research. Anders had an especially big role in the modeling work presented in this thesis. I am also grateful to him for involving me into projects that have become a big part of this thesis.

I am grateful to Professor Hupa for giving me the opportunity to carry out this work. Mikko has motivated and inspired me throughout this work. Despite his really tight schedule he always had time to answer my questions. I appreciate all the discussions we have had, sometimes very late in the evening. His knowledge has been invaluable for this thesis.

I have been very fortunate to have had the opportunity to work with people with different fields of expertise. I want to thank D.Sc. Nikolai DeMartini, D.Sc. Patrik Yrjas, D.Sc. Maria Zevenhoven, and Lic.Sc. Tor Laurén for all their contributions to this work and for the fruitful discussions we had.

The full-scale measurement campaigns have involved a large number of people. I want to thank Hannu Vesala, Tuula Kajolinna, Kauko Tormonen and D.Sc. Pasi

Åbo, January 2014

Abstract

The use of biomass as an energy source for the production of heat and power is one way to decrease dependency on fossil fuels and increase energy self-sufficiency. The utilization of fossil fuels in energy production is also the major source of CO_2 emissions, and CO_2 is the main anthropogenic greenhouse gas. Biomass, on the other hand, is regarded as a CO_2-neutral energy source. However, the nitrogen and sulfur in the biomass forms pollutants such as NO_X and SO_2. These must meet the stringent emission limits set by emission directives. Furthermore, the sulfur in the fuel can both cause and prevent corrosion of an incinerator, depending on the fuel and combustion.

The main objective of this work was to gain knowledge about the fate of fuel-bound nitrogen and sulfur in industrial-scale biomass combustors during combustion of various biofuels. This was achieved by full-scale measurement campaigns: in a bubbling fluidized bed (BFB) boiler combusting various fuel mixtures and in a Kraft recovery boiler. A four-meter-long quenching probe connected to a Fourier transform infrared (FTIR) gas analyzer was used to determine the gas composition in the furnace measurements. In-furnace measurements of NO, NH_3, HCN and HNCO were carried out, to understand how the fuel-bound nitrogen is released and to learn how and where the reduction of the released nitrogen species occur. This kind of information is essential for the validation of models, e.g., those based on computational fluid dynamics (CFD), to enable the construction of cleaner and more efficient boilers.

The measurements in the BFB boiler showed that NH_3 was the main reactive nitrogen species at reducing conditions in the furnace, and the highest concentrations of NH_3 were measured above the fuel inlet. No significant reduction of the nitrogen species to N_2 took place in the lower furnace, however, a drastic reduction was observed over the secondary air jet level. The final reduction of fuel bound nitrogen to N_2 was over 90%, although only air-staging was applied to minimize the NO_X emissions. Furthermore, the reduction of reactive nitrogen species in the air jets in the bubbling fluidized bed boiler was studied with kinetic modeling using a detailed reaction mechanism. The modeling work showed the

importance of mixing the combustion gases with the air jets, when modeling the NO_X formation and final emissions of a boiler.

Another objective was to gain knowledge about the formation of SO_2 and sulfation of ash components during combustion of biofuels with different ash properties. This was done by in-furnace measurements of the gaseous sulfur species and by detailed sampling and analysis of the fuel mixtures, ashes, and fine particles. All the fuels combusted in the BFB boiler had a high sulfur capturing potential, i.e., a high Ca/S ratio, and the emissions of SO_2 were low. Furthermore, the sulfur in the fuel played an important role in sulfating alkali chlorides, which are known for enhancing deposit formation and may also accelerate superheater corrosion. Deposit formation on heat transfer surfaces reduces the boiler efficiency and may result in unplanned shutdowns of the boiler. Sulfation of alkali chlorides was observed in the co-firing case with bark, sludge, and solid recovered fuel (SRF). The SRF had a fairly high chlorine content, while sludge had the highest sulfur content. Most of the chlorine was found as gaseous HCl in the measurements, which implies that sulfation of alkali chlorides occurred. This was seen in the furnace measurements as a rise in the HCl concentration and a decrease in SO_2 when moving up in the freeboard. The work showed the benefits of co-combustion of fuels with different properties. Despite the high sulfur content and low heating value of sludge, the ash components in the sludge play an important role in combustion. The sulfur has the positive effect of sulfating alkali chlorides when chlorine is present in biomass combustion.

The measurement campaign at the Kraft recovery boiler resulted in valuable data regarding the nitrogen and sulfur species in the furnace. The main nitrogen species at reducing conditions was NH_3. Considerable amounts of HCN were measured at the black liquor spraying level. This HCN is believed to be formed via re-burning of NO, since HCN has not been found as a pyrolysis species in earlier laboratory studies. The main sulfur intermediates close to the fuel inlet were H_2S and methyl mercaptan. In the flue gases, the only nitrogen species measured was NO and virtually all the sulfur was captured in the ash.

The presence of gaseous sulfuric acid (H_2SO_4) in the cold end of a Kraft and sulfite recovery boiler was also studied, due to low temperature corrosion seen in these boilers. A small part of the SO_2 formed in combustion forms SO_3, which reacts with

water vapor to form H_2SO_4 as the flue gas temperature drops. Sulfuric acid in the flue gas may lead to severe corrosion of components, such as economizers, air preheaters, and the flue gas duct, if their material temperature is below the sulfuric acid dew point temperature. If the H_2SO_4 concentration in the flue gas is known, the dew point temperature can be calculated. The objective was first to evaluate various SO_3/H_2SO_4 measurement techniques in the Chalmers 100 kW_{th} oxy-fuel test unit during air-fired and oxy-fuel conditions. The SO_3 in these experiments was generated by combusting propane and injecting SO_2 in the feed gas. A salt method showed promising results in these measurements. In this method a salt is used to capture H_2SO_4 in the form of sulfate, and the amount of sulfate formed in the salt is determined after the measurement. The salt method was further studied and developed in laboratory conditions. Various salts´ - NaCl, KCl, K_2CO_3, and $CaCl_2$ – ability to capture H_2SO_4, without the interference from SO_2, was studied. In this case, a synthetic flue gas was used and H_2SO_4 was generated by evaporating a weak solution of sulfuric acid. Both NaCl and KCl proved to be suitable for the measurement of low quantities of H_2SO_4 in a flue gas environment. Furthermore, an in-situ implementation of the salt method was used to study the presence of H_2SO_4 in the cold end of a Kraft and sulfite recovery boiler. The measurements revealed that during normal operation of these boilers, there existed no risk of low temperature corrosion due to condensation of H_2SO_4.

Keywords: In-furnace measurements, full-scale measurements, BFB boiler, Recovery boiler, NH_3, HCN, HNCO, NO, SO_2, SO_3, H_2SO_4, acid dew point

Svensk sammanfattning

Användning av biomassa som energikälla för produktion av el och värme är ett sätt att minska beroendet av fossila bränslen och höja självförsörjningen av energi. Fossila bränslen i energiproduktionen är den främsta källan till antropogena CO_2 utsläpp och CO_2 är den huvudsakliga antropogena växthusgasen. Biomassa, å andra sidan, betraktas som en CO_2-neutral energikälla. Svavlet och kvävet i biomassan bildar dock föroreningar såsom NO_X och SO_2. Dessa måste uppfylla de stränga utsläppsgränsvärden som fastställts av utsläppsdirektiv. Svavlet i bränslet kan även både förorsaka och förhindra korrosion i en förbränningsanläggning, vilket beror på förbränningen och bränslet.

Huvudsyftet med detta arbete var att få kunskap om vad som händer med bränslebundet kväve och svavel i eldstaden i industriella förbränningsanläggningar vid förbränning av olika biobränslen. Detta mål uppnåddes genom att utföra fullskaliga mätkampanjer: i en bubblande fluidiserad bädd (BFB) panna, vid förbränning av olika bränsleblandningar, och i en sodapanna. En fyra meter lång sond ansluten till en Fourier transform infraröd (FTIR) spektrometer användes för att bestämma gassammansättningen i eldstaden. Mätningarna utfördes för att förstå hur det bränslebundna kvävet frigörs och för att lära sig hur och var reduktionen av de frigjorda kvävespecierna sker i eldstaden. Denna typ av information är viktig för validering av modeller, till exempel de som är baserade på datorstödd strömningsdynamik "Computational Fluid Dynamics" (CFD), för att möjliggöra utvecklandet av renare och effektivare förbränningsanläggningar.

Mätningarna i BFB-pannan visade att NH_3 var den viktigaste reaktiva kväveföreningen under reducerande förhållandena i eldstaden. De högsta koncentrationerna av NH_3 mättes ovanför bränsleinloppet, men även HCN, HNCO, och NO kunde kvantifieras. Ingen betydande reduktion av reaktivt kväve till N_2 ägde rum i eldstadens nedre del. En avsevärd reduktion observerades vid den sekundära luftnivån. Den slutliga reduktionen av det bränslebundna kvävet till N_2 var över 90%, med endast fördelning av förbränningsluften för att minimera NO_X-utsläppen. I arbetet studerades även reduktionen av de reaktiva kväveföreningarna till N_2 vid luftnivåerna med kinetisk modellering med en detaljerad reaktionsmekanism. Modelleringsarbetet visade betydelsen av omblandningen av förbränningsgaserna med förbränningsluften för att minimera NO_X-utsläppen.

Ett annat syfte med arbetet var att öka förståelsen om bildningen av SO_2 och sulfatering av askkomponenter vid förbränning av biobränslen med olika askegenskaper i BFB-pannan. Detta mål uppnåddes genom att utföra gasmätningar i eldstaden och genom detaljerad provtagning och analys av bränsleblandningarna, askorna, och finpartiklarna. Samtliga bränslen hade en hög svavelupptagningsförmåga, det vill säga ett högt Ca/S-förhållande, och följaktligen var utsläppen av SO_2 låga. Svavlet i bränslet spelade en viktig roll i att sulfatera alkaliklorider. Alkaliklorider förorsakar beläggningsbildning och kan också påskynda korrosion. Avlagringar på värmeöverföringsytor minskar effektiviteten av förbränningsanläggningen och kan leda till oplanerade driftstopp. Utifrån de experimentella testerna observerades sulfatering av alkaliklorider till mindre korrosiva alkalisulfater vid samförbränningen med bark, slam, och utsorterat avfallsbränsle (SRF). Avfallsbränslet hade en relativt hög klorhalt, medan slammet hade den högsta svavelhalten. Största delen av kloret mättes som gasformig HCl i eldstadsmätningarna, vilket antydde att sulfatering av alkaliklorider inträffat. Detta sågs som en ökning av HCl-koncentrationen och en minskning av SO_2-koncentrationen längre upp i eldstaden. En viktig slutsats från arbetet är att det är fördelaktigt att samelda vissa bränslen. Trots slammets höga svavelhalt och det låga värmevärdet, spelar askkomponenterna i slammet en viktig roll i förbränningen. Svavlet har den positiva effekten att sulfater alkaliklorider när klorhaltiga bränslen sameldas med biomassa.

Mätkampanjen vid sodapannan gav värdefull information om kväve- och svavelföreningar i eldstaden. Vid reducerande förhållanden i eldstaden var NH_3 den huvudsakliga reaktiva kväveföreningen. Betydande mängder HCN mättes vid lutinsprutningsnivån. Detta HCN tros bildas genom reaktioner mellan NO och kolväten, eftersom HCN inte har påträffats som en primär pyrolysgas i tidigare laboratoriestudier. De huvudsakliga svavelgaserna vid lutsprutorna var H_2S och metylmerkaptan. I rökgaserna var den enda reaktiva kväveföreningen NO och all SO_2 hade bundits till askan.

Närvaron av gasformig svavelsyra (H_2SO_4) i den kalla ändan av en sodapanna och en sulfitpanna studerades också, på grund av lågtemperaturkorrosion som påträffats i dessa pannor. En liten del av den SO_2 som bildas i förbränningen bildar SO_3. När temperaturen sjunker i rökgaserna reagerar SO_3 med vattenånga för att bilda H_2SO_4.

Svavelsyra i rökgasen kan leda till korrosion av bl.a. economisern, luftförvärmaren och rökgaskanalen, om deras materialtemperatur är under svavelsyradaggpunkten. Om H_2SO_4-koncentrationen i rökgasen är känd, kan daggpunktstemperaturen beräknas. I arbetet var målet först att utvärdera olika SO_3/H_2SO_4 mättekniker i Chalmers 100 kW_{th} oxy-fuel testenhet. Svaveltrioxiden i dessa experiment skapades genom att förbränna propan och injicera SO_2 i propanet. En saltmetod visade lovande resultat i dessa mätningar. I denna metod används ett salt för att fånga H_2SO_4 i formen av sulfat. Mängden sulfat som bildats i saltet kvantifieras efter mätningen genom att lösa upp saltet och bestämma sulfatmängden i lösningen med t.ex. jonkromatografi. Saltmetoden studeras och utvecklas ytterligare i laboratoriemiljö. Olika salters - NaCl, KCl, K_2CO_3 och $CaCl_2$ – förmåga att fånga H_2SO_4, utan störning från SO_2 studerades. En syntetisk rökgas används och gasformig H_2SO_4 genererades genom förångning av en svag svavelsyralösning. Både NaCl och KCl visade sig vara lämpliga för att mäta låga koncentrationer av H_2SO_4 i rökgasmiljö. En in-situ tillämpning av saltmetoden användes för att studera närvaron av H_2SO_4 i rökgaskanalen av en sodapannan och en sulfitpannan. Mätningarna visade att under normal drift av dessa pannor förelåg ingen risk för lågtemperaturkorrosion orsakad av kondensering av H_2SO_4.

Nyckelord: Eldstadsmätning, fullskaliga mätningar, BFB-panna, Sodapanna, NH_3, HCN, HNCO, NO, SO_2, SO_3, H_2SO_4, syradaggpunkt

Publications

List of publications included in this thesis:

I.   Vainio, Emil; Brink, Anders; Hupa, Mikko; Vesala, Hannu; Kajolinna, Tuula: *Fate of Fuel Nitrogen in the Furnace of an Industrial Bubbling Fluidized Bed Boiler During Combustion of Biomass Fuel Mixtures*, Energy & Fuels, 26 (1), pp 94–101, 2012.

II. Vainio, Emil; Brink, Anders; Hupa, Mikko; Vesala, Hannu; Kajolinna, Tuula: *Fuel nitrogen reactions in a biomass fired FBC - measurements and kinetic simulations*, 21st International Conference on Fluidized Bed Combustion, Naples, Italy, June 3-6, 2012, ISBN 978-88-89677-83-4.

III. Vainio, Emil; Yrjas, Patrik; Zevenhoven, Maria; Brink, Anders; Laurén, Tor; Hupa, Mikko; Kajolinna, Tuula; Vesala, Hannu: *The fate of chlorine, sulfur, and potassium during co-combustion of bark, sludge, and solid recovered fuel in an industrial scale BFB boiler*, Fuel Processing Technology, Volume 105, pp 59-68, January 2013.

IV. Vainio, Emil; Brink, Anders; DeMartini, Nikolai; Hupa, Mikko; Vesala, Hannu; Tormonen, Kauko; Kajolinna, Tuula: *In-furnace Measurement of Sulphur and Nitrogen Species in a Recovery Boiler*, Journal of Pulp & Paper Canada (JPPS), 36 (3-4), pp 135-142, 2010.

V.   Fleig, Daniel; Vainio, Emil; Andersson, Klas; Brink, Anders; Johnsson, Filip; Hupa, Mikko: *Evaluation of SO_3 Measurement Techniques in Air and Oxy-Fuel Combustion*, Energy & Fuels, 26 (9), pp 5537–5549, 2012.

VI. Vainio, Emil; Fleig, Daniel; Brink, Anders; Andersson, Klas; Johnsson, Filip; Hupa, Mikko: *Experimental Evaluation and Field Application of a Salt Method for SO_3 Measurement in Flue Gases*, Energy & Fuels, 27 (5), pp 2767–2775, 2013.

Author contributions

Papers I and III: Emil Vainio was the main author of these papers. He was involved in the planning of the measurement campaign together with the co-authors and was involved in the in-furnace measurements. Hannu Vesala was responsible for the measurement system and Tuula Kajolinna for the FTIR. The author was responsible for the evaluation and interpretation of the data obtained from the measurements.

Paper II: Emil Vainio was the main author of this paper and conducted the simulations and evaluation of the data.

Paper IV: Emil Vainio was the main author of this paper. He was involved in the planning of the measurement campaign together with the co-authors and was involved in the in-furnace measurements. Hannu Vesala was responsible for the measurement system. Kauko Tormonen and Tuula Kajolinna were responsible for the FTIR and GC. The author was responsible for the evaluation and interpretation of the data obtained from the measurements.

Paper V: Emil Vainio was the second writer of the paper. He conducted the measurements with the salt method, acid dew point meter, and the isopropanol method, and was responsible for the evaluation and interpretation of this data. Daniel Fleig was the main author of the paper and was responsible for planning the measurement campaign.

Paper VI: Emil Vainio was the main author of this paper and was responsible for the planning of the work. He built the laboratory setup and performed the experimental work. For the field measurements he built the sampling system, performed the IC analyses, and evaluated the results.

Other publications completed during this thesis:

VII. Vainio, Emil; Brink, Anders; Vesala, Hannu; Tormonen, Kauko; Hupa, Mikko: *Extractive determination of the flue gas composition in a recovery boiler furnace*, Joint Meeting of the Scandinavian-Nordic and French Sections of the Combustion Institute, Copenhagen, Denmark, November 9-10, 2009.

VIII. Vainio, Emil; Brink, Anders; Yrjas, Patrik; Hupa, Mikko; Kajolinna, Tuula; Vesala, Hannu: *In-furnace measurements of gaseous species in a 107 MW_{th} BFB boiler*, 9th European Conference on Industrial Furnaces and Boilers, INFUB9, Estoril, Portugal, 26-29 April, 2011, ISBN 978-972-99309-6-6.

IX. Vainio, Emil; Brink, Anders; Hupa, Mikko; Vesala, Hannu; Tormonen, Kauko: *Measurement of nitrogen species in the furnace of an industrial combustor burning biomass*, General Section Meeting of the Scandinavian-Nordic Section of the Combustion Institute, Trondheim, Norway, November 28-29, 2011.

X. Vainio, Emil; Brink, Anders; Hupa, Mikko; Vesala, Hannu; Kajolinna, Tuula; *Simulation of the reduction of nitrogen species in air jets*, Finnish – Swedish Flame Days, Jyväskylä, Finland, April 17-18, 2013.

XI. Vainio, Emil; Yrjas, Patrik; Zevenhoven, Maria; Brink, Anders; Laurén, Tor; Hupa, Mikko: *The fate of chlorine, sulfur, and potassium during co-combustion of bark, sludge, and REF in a 107 MW_{th} BFB boiler*, Impacts of Fuel Quality on Power Production and the Environment, Saariselkä, Finland, August 29 - September 3, 2010.

XII. Vainio, Emil; Brink, Anders; DeMartini, Nikolai; Hupa, Mikko; Vesala, Hannu; Tormonen, Kauko; Kajolinna, Tuula: *In-furnace Measurement of Sulfur and Nitrogen Species in a Recovery Boiler*, ICRC, International Chemical Recovery Conference, Williamsburg, Virginia, USA, March 29 - April 1, 2010.

XIII. Vainio, Emil; Fleig, Daniel; Brink, Anders; Andersson, Klas; Johnsson, Filip; Hupa, Mikko: *SO₃ measurement techniques – a study in a 100 kW$_{th}$ test unit fired with a SO₂-doped propane flame*, Industry Maffliers, France, 11-13 June, 2012.

XIV. Vainio, Emil; Brink, Anders; DeMartini, Nikolai; Laurén, Tor; Hupa, Mikko: *Development of a method to measure low quantities of SO₃/H₂SO₄ in recovery boiler flue gas ducts*, 8th International Black Liquor Colloquium – Black liquor and Biomass to Bioenergy and Biofuels, Belo Horizonte, Brazil, May 19-23, 2013.

List of abbreviations

BFB	Bubbling Fluidized Bed
CFB	Circulating Fluidized Bed
CFD	Computational Fluid Dynamics
DLPI	Dekati Low Pressure Impactor
DMDS	Dimethyl Disulfide
DMS	Dimethyl Sulfide
EDX	Energy Dispersive X-ray
ESP	Electrostatic Precipitator
EU	European Union
FBC	Fluidized Bed Combustion
FTIR	Fourier Transform Infrared
Fuel-N	Fuel-bound nitrogen
GC	Gas Chromatography
IC	Ion Chromatography
ICP-MS	Inductively Coupled Plasma Mass Spectrometry
IR	Infrared
MM	Methyl Mercaptan
NO_x	$NO + NO_2$
PID	Photoionization Detector
ppmv	parts per million by volume
SEM	Scanning Electron Microscopy
SO_x	$SO_2 + SO_3$ (or H_2SO_4)
SRF	Solid Recovered Fuel
STP	Standard Temperature and Pressure (0°C and 1 atm)
tds/d	tons of dry solids per day
TFN	Total Fixed Nitrogen
TRS	Total Reduced Sulfur

Table of contents

1. INTRODUCTION

Biomass as an energy source for the production of heat and electricity has recently gained a great deal of attention. Utilizing biomass for energy production is one alternative for reducing the use of fossil fuels and increasing self-sufficiency in energy. Biomass, such as woody biomass, is also regarded as a CO_2-neutral fuel, as long as it is utilized in a sustainable maner. The European Union has set a target of obtaining 20% of its energy from renewable sources by 2020 [1]. Finland's target is to obtain at least 38% of its energy from renewable sources. Solid biomass is one of the most important energy sources for meeting these targets. As can be seen in Figure 1, energy from wood-based fuels accounted for one-fourth of Finland´s total energy consumption in the first quarter of 2013 [2]. A large share of this energy comes from by-products of the forest industry, including black liquor, bark, and sawdust. In 2011 black liquor accounted for approximately half of the electricity produced from wood-based fuels [3].
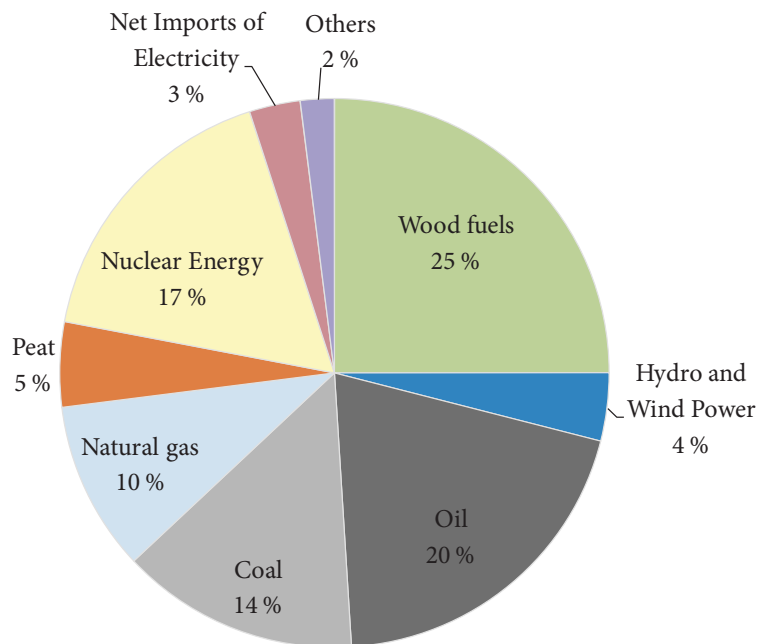
Figure 1. Share by energy source of Finland´s total energy consumption in the first quarter of 2013 [2].

Biomass combustion for the production of heat and electricity is conducted in large industrial combustors. Black liquor, which is a by-product of the pulping process, is

combusted in a recovery boiler. The black liquor contains the cooking chemicals used in the pulping process and the organic material dissolved from the wood. The cooking chemicals are recovered in the recovery boiler and the organic matter in the black liquor is combusted to produce heat and electricity. Large-scale solid biomass combustion can be conducted in, e.g., grate-fired furnaces and fluidized bed combustors.

The CO_2 emissions from biomass combustion are regarded as CO_2-neutral; however, harmful NO_X and SO_X emissions are formed. The emissions of these pollutants are regulated by emission limits. The emission limits of NO_X and SO_2 for new power plants burning biomass in the EU are shown in Table 1.

Table 1. Emission limits of NO_X and SO_2 set by the EU directive 2010/75/EU [4]. The values are expressed as mg/Nm³ of SO_2 and NO_2 in a flue gas containing 6 vol% O_2.

	50 to 100 MW$_{th}$	100 to 300 MW$_{th}$	> 300 MW$_{th}$
NO$_X$	250	200	150
SO$_2$	200	200	150

The NO_X and SO_X emissions are the main constituents of acid rain. Nitrogen oxide emissions also form harmful smog and particulate matter. Additionally, NO_X emissions lead to eutrophication of lakes and rivers. The emissions of NO_X and SO_X are typically low in modern industrial combustors; however, these emissions may rise during combustion of certain biofuels and waste fuels. Modeling is used for the prediction of the emission performance of boilers, e.g., when developing new technologies, optimizing the combustion, and when building bigger boilers. Computational fluid dynamics (CFD) has proven to be a powerful tool for this purpose. However, very little data from full-scale boiler furnaces is available for the validation of models based on CFD, and models often rely on data from laboratory experiments.

Combustion of sulfur-rich fuels may cause corrosion problems in boilers. A small part of the SO_2 formed during combustion forms SO_3. At lower temperatures in the flue gas duct, SO_3 combined with water vapor forms sulfuric acid. This may cause

severe corrosion of the plant if the material temperature in the flue gas duct is below the sulfuric acid dew point temperature. Therefore, it is crucial to determine the sulfuric acid dew point temperature in boilers in order to keep the cold end above the sulfuric acid dew point temperature and at the same time to take as much energy as possible from the flue gas. Biomass usually contains relatively high amounts of calcium and potassium, which effectively recaptures SO_X. Therefore, the risk of sulfuric acid induced corrosion in biomass combustion is normally low. However, sulfuric acid induced low temperature corrosion is often speculated to occur in recovery boilers. Alkali chlorides, which may form in biomass combustion, can also cause severe corrosion of boiler tubes. Here, the sulfur in the fuel may prevent corrosion by sulfating alkali chlorides to less corrosive alkali sulfates.

2. OBJECTIVES OF THIS WORK

The main objectives of this thesis were to:

- Gain a deeper understanding of the fate of fuel-bound nitrogen and sulfur in industrial-scale furnaces burning various biomass fuel mixtures, by conducting two big measurement campaigns: one in a bubbling fluidized bed boiler, in which different fuel mixtures were combusted, and the second in a Kraft recovery boiler.
- Gain knowledge of the role of sulfur in co-combustion of biofuels with different ash properties.
- Evaluate SO_3 measurement techniques for the measurement of low quantities of SO_3 and study the risk of sulfuric acid induced corrosion in the cold end of recovery boilers.

In Paper I, in-furnace measurements of nitrogen species in a bubbling fluidized bed boiler, burning various fuel mixtures, were conducted. These measurements were performed in order to gain information about the formation of NO_X emissions, i.e., how the nitrogen is released, what intermediate nitrogen species are present at different locations and heights in the furnace, and where the reduction to elemental nitrogen takes place in a full-scale furnace. This kind of data is essential for the validation of detailed models to describe the combustion and emission formation inside the furnace. In **Paper II** the reduction of nitrogen species to elemental

nitrogen in the BFB boiler was simulated using the Chemkin software and a detailed reaction mechanism. Additionally, different mixing approaches of the combustion gases and air jets were compared. The fate of sulfur, potassium, and chlorine was examined during the measurement campaign in the bubbling fluidized bed boiler, in **Paper III**. The main objective in this case was to gain knowledge about the role of sulfur in the combustion of biomass fuels with different ash compositions and properties. The concentrations of sulfur, potassium, and chlorine were determined in the bottom ash, ash from the bottom of the second pass ash hopper, and filter ash from the baghouse filters. Additionally, SO_2 and HCl measurements were performed in the furnace and flue gas duct.

In **Paper IV**, gaseous sulfur and nitrogen species present in a Kraft recovery boiler were studied. The measurement campaign was carried out to obtain information about the reactive nitrogen and sulfur species present at different locations in the furnace and freeboard of the boiler.

In **Paper V** different measurement techniques for SO_3 were compared in the Chalmers oxy-fuel test unit, in both oxy-fuel and air-fired conditions. The presence of gaseous sulfuric acid in the cold end of both a Kraft and a sulfite recovery boiler was studied, due to speculations about sulfuric acid-induced corrosion in the cold end of recovery boilers. For this purpose, an SO_3 measurement technique was further developed and tested, in both the Chalmers 100 kW_{th} oxy-fuel test unit and in the laboratory, in **Paper VI**.

3. BACKGROUND

3.1. Stages in Combustion of a Solid Biofuel Particle

A solid biomass particle entering a combustor undergoes four distinct combustion stages: drying, devolatilization, combustion of gases, and char burning. These stages are shown in Figure 2. Overlapping of these combustion stages may occur, when considering the combustion of a single particle [5]. When a biomass particle is introduced to a hot environment the water in the particle starts to evaporate. During the devolatilization stage, volatile gases and tars are released from the particle and are combusted in the presence of oxygen. In the char combustion stage, the char reacts with oxygen to form mainly CO and CO_2. After the combustion is completed, an inorganic ash remains.
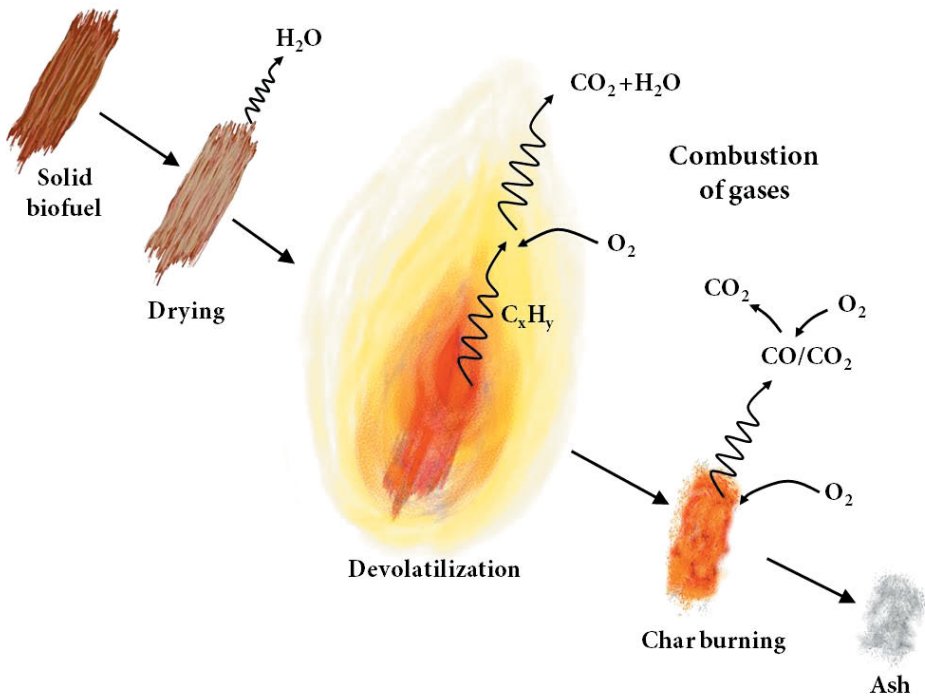
Figure 2. Stages in combustion of a solid biomass particle.

3.2. NO$_X$ Formation in Combustion and Removal from Flue Gases

Nitrogen oxide emissions (NO + NO$_2$) in combustion originate from the fuel-bound nitrogen and the N$_2$ in the combustion air. The formation of NO$_X$ emissions in combustion devices can be divided into four main mechanisms [6]:

- Thermal NO$_X$ mechanism, which was first described by Zel'dovich [7]. Thermal NO$_X$ is formed from the N$_2$ in the combustion air in the precence of O and OH radicals (Reactions 1-3). This mechanism is relevant at temperatures above 1500°C, due to the high activation energy of Reaction 1 [8].

$$O + N_2 \rightleftharpoons NO + N \qquad (1)$$
$$N + O_2 \rightleftharpoons NO + O \qquad (2)$$
$$N + OH \rightleftharpoons NO + H \qquad (3)$$
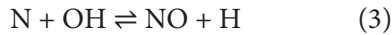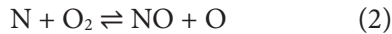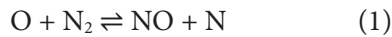
- Prompt or Fenimore NO$_X$ mechanism [9]. Prompt NO$_X$ is formed from the N$_2$ in the combustion air in the presence of hydrocarbon radicals. More recently, it has been shown that one of the main patways to prompt NO$_X$ is initiated by CH that rects with N$_2$ forming NCN [10][11]:

$$CH + N_2 \rightleftharpoons H + NCN \qquad (4)$$

- N$_2$O-intermediate mechanism [12]. In this mechanism N$_2$O is formed from N$_2$ in fuel-lean conditions in the presence of oxygen radicals :

$$O + N_2 + M \rightleftharpoons N_2O + M \qquad (5)$$

- Fuel NO$_X$, which forms from the nitrogen bound in the fuel. The nitrogen in the fuel is released as intermediate nitrogen species, mainly NH$_3$ and HCN.

The reactive nitrogen species formed by these mechanisms will undergo further reactions in the combustion process. Depending on the combustion conditions, the reactive nitrogen species formed may oxidize to become a part of the NO$_X$ emissions or reduce to N$_2$. In combustion of solid fuels, the main source of NO$_X$ emissions is from the fuel-bound nitrogen; however, some thermal NO$_X$ may also be formed [8].

Primary methods for reducing NO$_X$ emissions are based on staged combustion. In air staging the combustion air is staged to a number of air levels. Air is mixed with the combustion gases in stages; in the last stage, the final burnout of gases occurs.

The idea behind air staging is to limit the availability of O_2, O, and OH [13]. Up to 50% of NO_X reduction can be achieved with air staging [13][14].

In fuel staging, the fuel is fed at two different heights in the boiler. At the first level, the fuel is combusted with excess air. At the second level, reducing conditions are restored by feeding the secondary fuel, and a reduction of NO to N_2 is achieved. The combustion is completed with burnout air. Up to 78% reduction with staged combustion has been reported [15]. The operation of staged combustion is complex given the need for a second feed level [16].

Secondary methods for NO_X reduction include selective non-catalytic reduction (SNCR) and selective catalytic reduction (SCR). In SNCR, an NO_X reduction agent is added to the combustion, e.g., NH_3 or urea. Reduction of NO_X with NH_3 was first described by Lyon [17]. The reducing agent is injected into the furnace and reacts with NO to form N_2 and water, according to the global Reaction 6.

$$4NO + 4NH_3 + O_2 \rightarrow 4N_2 + 6H_2O \qquad (6)$$
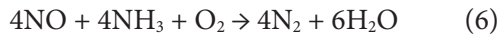
This reaction occurs in a fairly narrow temperature window, approximately 800-1200°C [18]. If the temperature is too low the NH_3 will remain un-reacted. On the other hand, if the temperature is too high the reduction agent may oxidize to NO and become a part of the NO_X emissions. The optimal temperature window is dependent on various factors, such as the concentrations of O_2, H_2, and CO [19-22]. In SCR, the temperature window is lower, approximately 200-500°C, and the reaction between the reducing agent and NO occurs over a catalyst. Ammonia or urea is mixed with the flue gas up-stream of the catalyst and reacts over a catalyst forming N_2 and water. The SCR process using NH_3 as reducing agent and platinum as catalyst was patented by the Engelhard Corporation in 1957 [23]. More than 90% of reduction can be achieved with SCR [24].

3.3. SO_X Formation in Combustion and Removal from Flue Gases

Sulfur dioxide emissions are formed from the sulfur bound in the fuel. During combustion the sulfur is released from the fuel mainly as H_2S [25]. The released H_2S is oxidized to SO_2, which is partially recaptured in the ash and partially forms the SO_2 emissions. A small part of the SO_2 oxidizes further to form sulfur trioxide (SO_3). Sulfur trioxide can be formed by two mechanisms: homogeneous gas-phase

reactions and heterogeneous reactions in the presence of a catalyst. Homogenous oxidation of SO_2 takes place by the reaction of SO_2 with oxygen radicals [26][27] or with OH radicals via $HOSO_2$ as an intermediate [28]:

$$SO_2 + O \rightleftharpoons SO_3 \qquad\qquad (7)$$
$$SO_2 + OH \rightleftharpoons HOSO_2 \qquad\qquad (8)$$
$$HOSO_2 + O_2 \rightleftharpoons SO_3 + HO_2 \qquad (9)$$

The heterogeneous reactions occur in the presence of catalytic surfaces, e.g., iron oxides in ashes or deposits in the furnace [29].

The extent of the conversion of SO_2 to SO_3 is mainly dependent on the excess air in the flue gas and the amount of catalysts in the combustion process [29][30]. Bennett [31] showed empirically that the final conversion of SO_2 to SO_3 is up to 6% in oil combustion and 1.5% in coal combustion at high excess oxygen levels. However, it is difficult to predict the amount of SO_3 formed for a given fuel. For example, in biomass combustion the ash effectively captures the formed SO_3.

To decrease the emissions of sulfur, different absorbents can be used, e.g., limestone. Both wet and dry flue gas desulfurization (FGD) are effective ways of reducing SO_2 emissions. In wet FGD, an alkaline solution is sprayed in a direction countercurrent to that of the flue gas, and the SO_2 is captured in the solution. Wet FGD can remove up to 95% of the SO_2 in a flue gas [32]. Several dry FGD systems exist. An example of dry FGD is the lime spray dry system, which has a removal efficiency of over 90% [33].

3.4. Fluidized Bed Combustion of Biomass

Fluidized bed combustion (FBC) is a well-established technology for the combustion of a wide range of fuels to produce heat and power. FBC has many advantages compared to other solid fuel combustion technologies, e.g., fuel flexibility, high combustion efficiency, and emission performance. Two main types of fluidized bed combustion exist:

- Bubbling fluidized bed (BFB)
- Circulating fluidized bed (CFB)

A schematic picture of a BFB boiler is shown in Figure 3. In BFB combustion the bed usually consists of silica sand [34], which is located in the bottom part of the furnace. The bed is kept in a fluidized state by introducing fluidizing or primary air through nozzles in the boiler bottom. The fuel is fed into the hot bed, where the main combustion takes place. The amount of fuel in the bed is only 1-3% of the total bed material [35]. The good mixing in the bed and the large thermal capacity of the bed enable the combustion of low grade fuels [36][37]. The BFB technology is suited for the combustion of a wide range of low-grade fuels, such as biofuels and sludge with high moisture content, low heating value, and high ash content. Above the bed, the un-burnt gases are combusted by introducing air in several levels. To avoid bed agglomeration in FBC, the bed temperature is kept fairly low. Typical bed temperatures are in the range of 800-900°C [36].

In CFB combustion, the primary air velocity is higher, the particle size of the bed is smaller, and the fuel particles are smaller than those in BFB combustion. This leads to the entrainment of bed material with the gas stream. The bed material is collected in cyclones and recirculated to the bottom of the furnace. Circulating fluidized bed boilers are usually chosen when boiler size is large (>100 MW$_{th}$). The main fuel combusted with the CFB technology is coal [37].
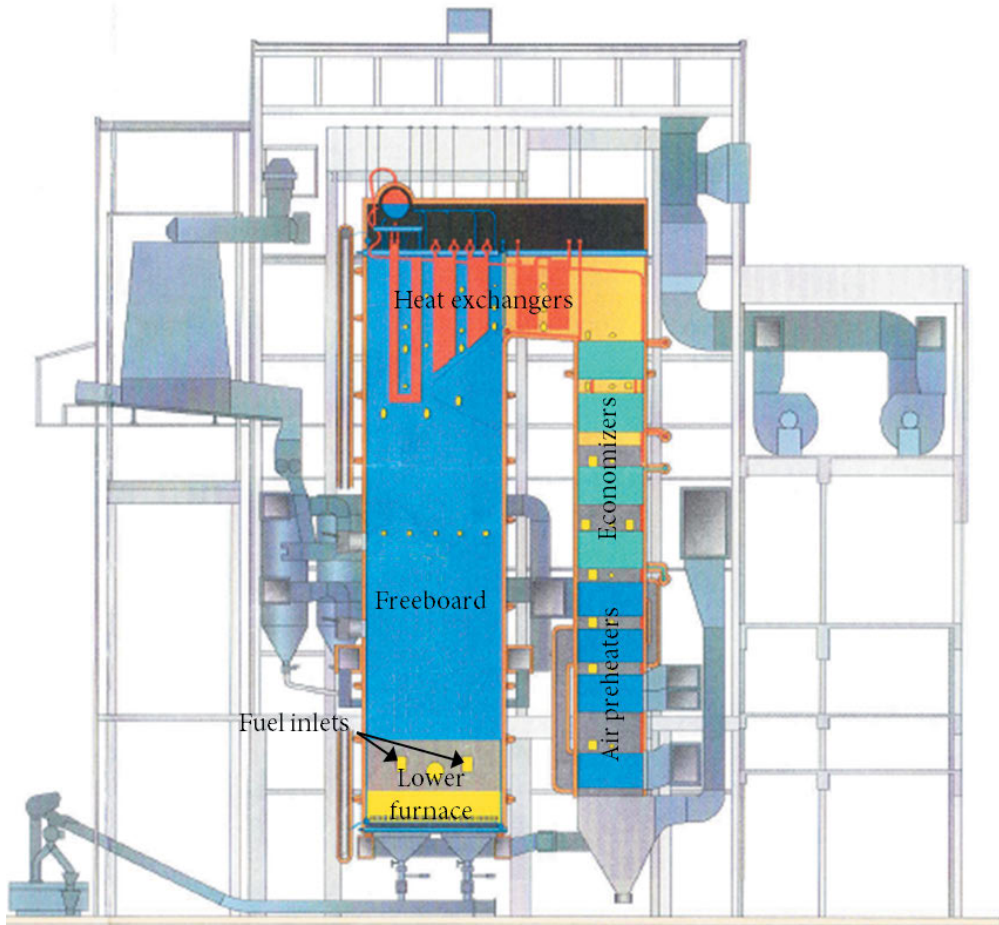
Figure 3. Bubbling fluidized bed boiler (courtesy of Valmet Power Oy).

3.4.1. NO_X Formation and Reduction in FBC

The NO_X emissions in fluidized bed combustion originate from the nitrogen bound in the fuel. The temperature in FBC is fairly low, 800-900°C, which means that thermal NO_X is not formed. In this work it is assumed that the formation of prompt NO_X and NO_X by the N_2O mechanism are negligible in FBC conditions.

The release of nitrogen and the formation of NO_X are dependent upon many factors, such as fuel composition, nitrogen content in the fuel, combustion temperature, and air staging. Woody biomass has a fairly low nitrogen content, 0.1-0.4 wt% [38][39]. However, municipal sewage sludge, as well as sludge from the pulp and paper

industry, may contain a significant amount of nitrogen [40-44]. Higher nitrogen contents than that observed in woody biomass can also be found in herbaceous biomass, such as straw and miscanthus [16][45]. The fuel-bound nitrogen in biomass is mainly released with the volatiles in fluidized bed combustion conditions [46-50]. It has been shown that a higher reduction is achieved with fuels with higher nitrogen content [15][46]. A volatile nitrogen content of above 80% has been shown for wood-based residues [47] as well as a volatile nitrogen content of 68-75% for woody biomass [46]. This means that most of the nitrogen will be released to the freeboard, and the homogeneous gas-phase reactions are the most important in reducing NO_X emissions. Only a small amount of nitrogen will remain in the char. Thus, the reduction of NO with char is not that important in FBC combustion of biomass [51]. Coal, on the other hand, has much lower amounts of volatiles than biomass. Nitrogen is retained to a larger extent in the coal char, and the the reduction of NO with the char to N_2 plays an important role in reducing NO emissions [50-52].

In woody biomass nitrogen is mainly bound to proteins, and is mainly released as NH_3, HCN, and small amounts of HNCO [53][54]. The NH_3/HCN ratio has proven to be higher for biomass fuels than for coals [47][55][56]. Furthermore, higher temperatures yield lower NH_3/HCN ratios [53][54], and the ratio also decreases with higher heating rates [55].

Figure 4 shows the main nitrogen reaction pathways during combustion of a solid biomass particle in fluidized bed combustion conditions. Most of the nitrogen is released as volatile nitrogen, which includes tar-N and gaseous intermediate nitrogen species. Information is limited on the products of tar cracking from biomass fuels. However, tar decomposition in fluidized bed pyrolysis of coal has been shown to release NH_3, HCN, and HNCO [57]. The released NH_3, HCN, and HNCO form NH_i radicals (i = 0,1,2) in the combustion process in the presence of H and OH radicals. The formed NH_i radicals can react with NO to form molecular nitrogen, and thus reduce the final NO emissions. The NH_i radicals may also become oxidized and form NO.

Some N_2O may also be formed in FBC conditions, however, N_2O is not usually present to a large extent in the flue gas during biomass FBC [46][51]. Furthermore,

most of the N_2O formed in combustion is by homogeneous oxidation of HCN [58-60] and some N_2O is formed from char-N reactions [58][60].
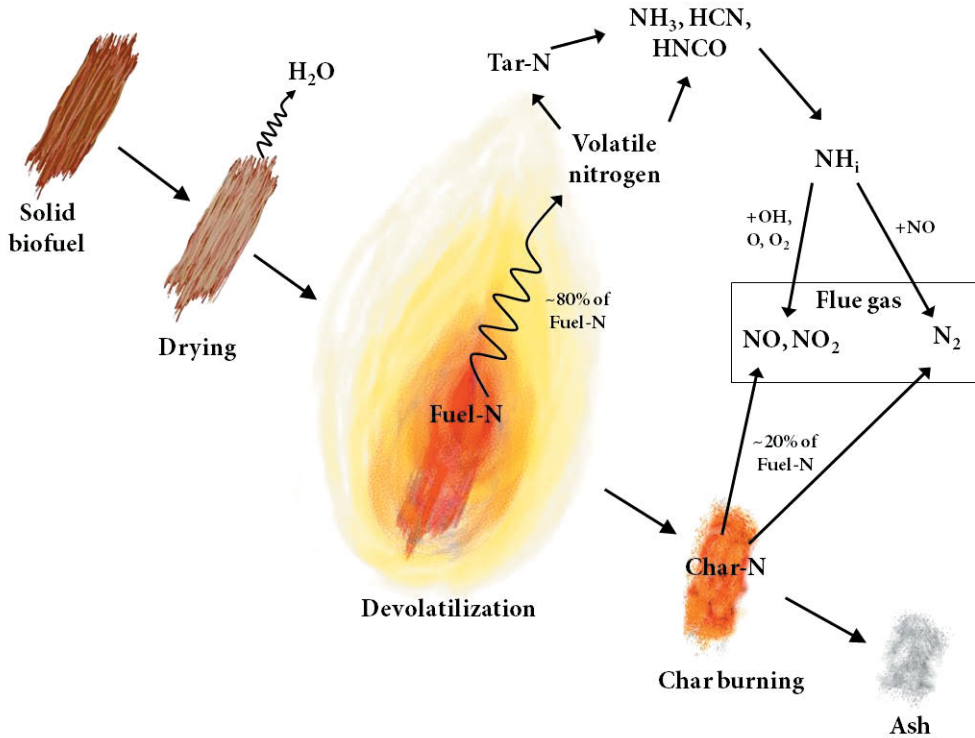
Figure 4. Release of fuel-bound nitrogen and main reaction pathways of nitrogen during biomass combustion in fluidized bed conditions.

3.4.2. SO_X Formation and Recapture in FBC

Sulfur in woody biomass is mainly present as organically-bound sulfur [61]. The sulfur in the fuel is released mainly as H_2S in combustion [25]. The released H_2S is oxidized to SO_2 and a small part of the SO_2 is further oxidized to SO_3. A part of the sulfur is recaptured in the ash and a part forms the final SO_X emissions. Biomass typically contains relatively high concentrations of potassium and calcium. These effectively recapture the formed SO_2 and SO_3 by forming K_2SO_4 and $CaSO_4$.

Alkali metals present in biomass may lead to problems related to slagging [62-65] and fouling [63-67]. This reduces the boiler efficiency and may result in unplanned shutdowns of the boiler. Alkali chlorides form if chlorine is present in biomass

combustion. Alkali chlorides have low melting temperatures [68] and may lead to severe corrosion of boiler tubes [44][67][69][70]. When alkali chlorides form in the combustion, the sulfur present in the fuel has an important role in sulfating these alkali chlorides. The sulfur present in the fuel sulfates the formed alkali chlorides, which results in a less sticky ash [71] with a lower corrosion potential [72][73]. Sulfur containing additives may be added to the combustion, if the sulfur in the fuel is not enough to sulfate all the alkali chlorides. Reaction 10 shows the homogeneous sulfation of KCl with SO_2. Glarborg and Marshall [74] and Iisa et al. [75] suggested that the sulfation of alkali chlorides is initiated by the oxidation of SO_2 to SO_3, and the formed SO_3 reacts with the alkali chlorides (Reaction 11). Further, Kassman et al. [76] showed experimentally that the sulfation of gaseous KCl is more efficient with SO_3 than with SO_2. Sulfation of condensed/solid alkali chlorides also occurs, however, the homogeneous gas-phase sulfation has proven to be faster [75].

$$4KCl(g) + 2SO_2(g) + O_2(g) + 2H_2O(g) \rightarrow 2K_2SO_4(g,c) + 4HCl(g) \qquad (10)$$

$$2KCl(g) + SO_3(g) + H_2O(g) \rightarrow K_2SO_4(g,c) + 2HCl(g) \qquad (11)$$
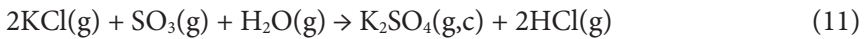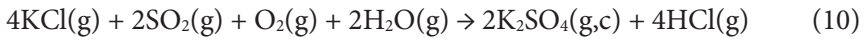
Absorbents such as limestone can be used when burning fuels with high sulfur contents in FBC. First, calcination of limestone takes place in the furnace, after which the formed CaO captures the SO_X.

3.5. Black Liquor Combustion

Black liquor is a by-product of the chemical pulping process. It contains the spent inorganic cooking chemicals and the organic material dissolved from the wood. The organic material is mainly lignin, hemicelluloses, and extractives. Black liquor is combusted in a recovery boiler. A schematic picture of a recovery boiler is shown in Figure 5. The black liquor recovery boiler has two main purposes:

- Recover the spent cooking chemicals
- Generate steam and electricity

This means that the recovery boiler has dual functions, working as a steam boiler as well as a chemical reactor [77].
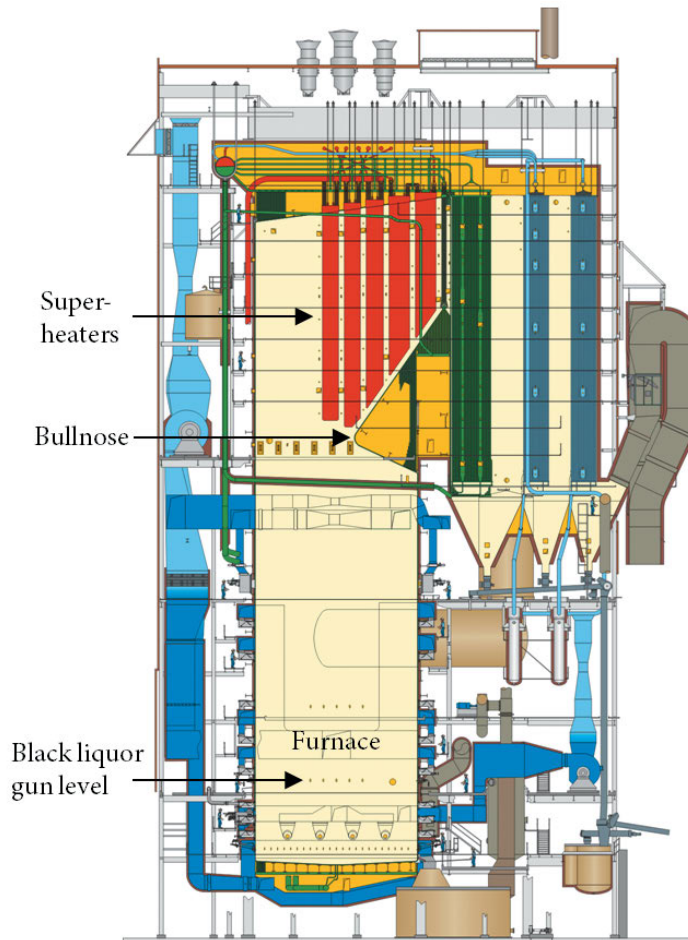
Figure 5. A schematic picture of the UPM Wisaforest recovery boiler in Jakobstad (courtesy of Andritz Oy).

In modern recovery boilers the black liquor is concentrated in evaporators to around 80% of dry solids. A typical black liquor composition is shown in Table 2. The high-dry-solids black liquor is sprayed into the recovery boiler furnace through several liquor guns, which are located about five meters above the furnace floor [78]. The combustion stages of a black liquor droplet are similar to those of biomass particles. First, drying of the droplet takes place when the black liquor is sprayed into the recovery boiler furnace. One big difference compared to solid biomass combustion is that during the devolatilization stage, the black liquor droplet swells considerably; the volume expansion of a Kraft black liquor droplet is typically 20-50 times [79][80]. The swelling properties vary from liquor to liquor [80][81]. The volatile matter is fully or partly released in-flight. The material that reaches the bed consists of the inorganic part, some volatile organic material, and char. Smaller droplets may completely burn in-flight, while bigger droplets may continue the devolatilization in the bed. The inorganic matter forms a smelt on the furnace bottom. The smelt consists of sodium carbonate (Na_2CO_3), sodium sulfide (Na_2S) and a small amount of sodium sulfate (Na_2SO_4). Here, the char has an important role in reducing the sulfate to sulfide in the smelt. The oxidation of Na_2S to Na_2SO_4 should be avoided in the smelt since Na_2S is one of the cooking chemicals. The smelt exits the recovery boiler and is transported for further treatment in the chemical recovery cycle.

Table 2. An example of the elemetal composition of a Kraft black liquor. The sample is taken before the mixing tank [77].

Element	wt% in dry solids
C	38.2
H	3.4
O	31.1
N	0.1
S	5.2
Na	19.8
K	1.9
Cl	0.1
Others (Ca, Si, Fe, Mg, Al, Mn)	0.2

3.5.1.NOₓ Formation and Reduction in Black Liquor Combustion

The nitrogen content in black liquor is typically around 0.06-0.2% [77][82][83]. This organically-bound nitrogen in the black liquor forms the NO_X emissions. About 25-30% of the fuel-bound nitrogen forms the final NO_X emissions [83][84].

Laboratory studies by Aho et al. [82][85] showed that up to 60% of the fuel-bound nitrogen is released during the pyrolysis stage as NH_3 and N_2, while Forssén et al. [83] showed that 70-80% of the fuel-bound nitrogen is released as NH_3 and N_2. However, they did not detect HCN as a pyrolysis product. A part of the released NH_3 will form NO and a part will reduce to N_2. Single particle combustion tests by DeMartini et al. [86] and Forssén et al. [83] showed that 60% of the NO formed originates from the pyrolysis stage and 40% originates from the char combustion stage. A significant amount, up to one-third of the fuel-bound nitrogen, will stay in the char and exit the recovery boiler with the smelt as cyanate [87][88]. In oxidizing conditions in the smelt bed, some of the cyanate forms NO [87][88]. Figure 6 shows the black liquor nitrogen reactions in black liquor combustion as suggested by Forssén et al. [87].
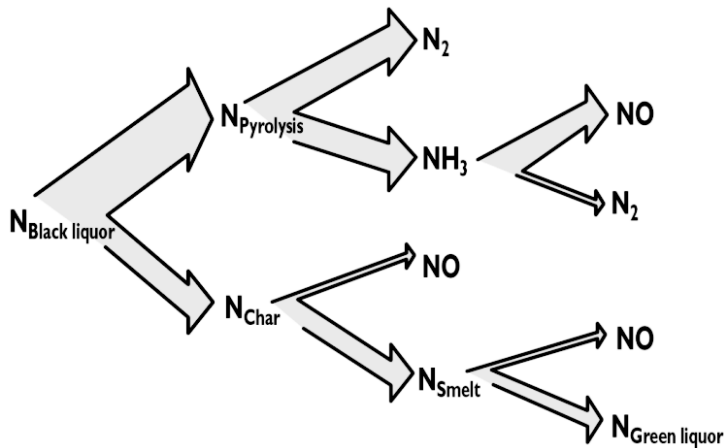
Figure 6. Fuel-bound nitrogen pathways during black liquor combustion [87].

3.5.2. Sulfur Release and Recapture in Black Liquor Combustion

The gaseous sulfur emissions from Kraft recovery boilers are mainly SO_2 and total reduced sulfur (TRS). Total reduced sulfur is mostly consisting of H_2S. Sulfur in black liquor is mainly released during the devolatilization stage. During pyrolysis, sulfur is primarily released as hydrogen sulfide (H_2S), methyl mercaptan (MM), and dimethyl sulfide (DMS) [89-91]. Some sulfur is also released during char burning in the reaction with Na_2S, CO_2, and water vapor to form H_2S and COS [92]. Additionally, when water vapor is present the formation of H_2S from the char is faster than the formation of COS [92]. Some CS_2 may also be formed during pyrolysis of black liquor [91]. Most of the sulfur is released from black liquor droplets in-flight, but also from cold spots in the bed [93]. The amount of sulfur released is highly dependent on the temperature in the furnace and the heating rate of the black liquor droplet. At higher heating rates the sulfur release is lower [94]. Several authors have shown that sulfur release peaks at a pyrolysis temperature of around 500°C [89][95][96]. Accordingly, when operating a recovery boiler at a lower temperature, more sulfur is released.

Sodium plays an important role in capturing the sulfur from the gas-phase in a recovery boiler. Most of the sodium is released as sodium vapor during char combustion, either from the bed or from droplets in-flight [93]. Tamminen et al. [97] showed that dust formed in a recovery boiler originates mainly from black liquor droplets burning in-flight, and only 5-10% of the dust originates from the bed. The release is highly temperature-dependent and occurs to a significant extent above 800°C [92].

Immediately after the formation of sodium hydroxide (NaOH) from the released sodium and the oxidation of the reduced sulfur species to SO_2, these compounds react to form sodium sulfate (Na_2SO_4), as described by the global Reaction 12 [94]. Sodium chloride vapors react with SO_2 forming Na_2SO_4 fume and HCl (Reaction 13). The sulfation of condensed NaCl is slow and does not occur at a significant level [98]. Any NaOH not consumed in Reaction 12 reacts with CO_2 to form Na_2CO_3 (Reaction 14) [94]. The sulfation of solid sodium carbonate in Reaction 15 also occurs; however, Reaction 12 is more important for the sulfur recapture in recovery boilers [94].

$$2NaOH(g) + SO_2(g) + \frac{1}{2}O_2(g) \rightarrow Na_2SO_4(g) + H_2O(g) \qquad (12)$$

$$2NaCl(g) + SO_2(g) + \frac{1}{2}O_2(g) + H_2O(g) \rightarrow Na_2SO_4(g) + 2HCl(g) \qquad (13)$$

$$2NaOH(g) + CO_2(g) \rightarrow 2NaOH(s) + CO_2(g) \rightarrow Na_2CO_3(s) + H_2O(g) \quad (14)$$

$$Na_2CO_3(s) + SO_2(g) + \frac{1}{2}O_2(g) \rightarrow Na_2SO_4(s) + CO_2(g) \qquad (15)$$
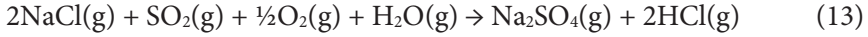
The molar ratio of S/Na_2 in the black liquor as well as the temperature in the furnace, has a great impact on the flue gas and dust chemistry. If enough sodium vapor is released all the sulfur will be recaptured by forming Na_2SO_4. The remaining sodium form mainly Na_2CO_3.

Acidic sulfates, i.e., bisulfate and pyrosulfate, cause corrosion in boiler bank tubes. Acidic sulfates may form if the S/Na_2 molar ratio is high, as in sulfite pulping, and/or the bed temperature is low. They form a sticky deposit with a low melting temperature, 185°C, which is highly corrosive [99]. This has been speculated to be formed by SO_3 reacting with Na_2SO_4 rather than with SO_2 (Reaction 16) [100].

$$Na_2SO_4(s) + SO_3(g) + H_2O(g) \rightarrow 2NaHSO_4(s) \qquad (16)$$
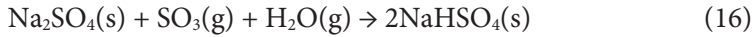
Research has shown that at higher excess air values, the fly ash acidity increases [100]. This has been explained by a higher conversion of SO_2 to SO_3 when the excess oxygen is increased, with the subsequent formation of $NaHSO_4$ [100]. However, in a Kraft recovery boiler there is enough excess sodium to capture the formed SO_3. In addition, if Na_2CO_3 and $NaHSO_4$ coexist, the sodium carbonate will neutralize the bisulfate in an aqueous solution, e.g., if water is absorbed.

3.6. Formation and Condensation of Sulfuric Acid

As the flue gas temperature drops in the convective pass (<500°C), SO_3 starts to react with water vapor to form gaseous H_2SO_4. The equilibrium conversion of SO_3 to H_2SO_4 in the temperature range of 150-500°C is shown in Figure 7.
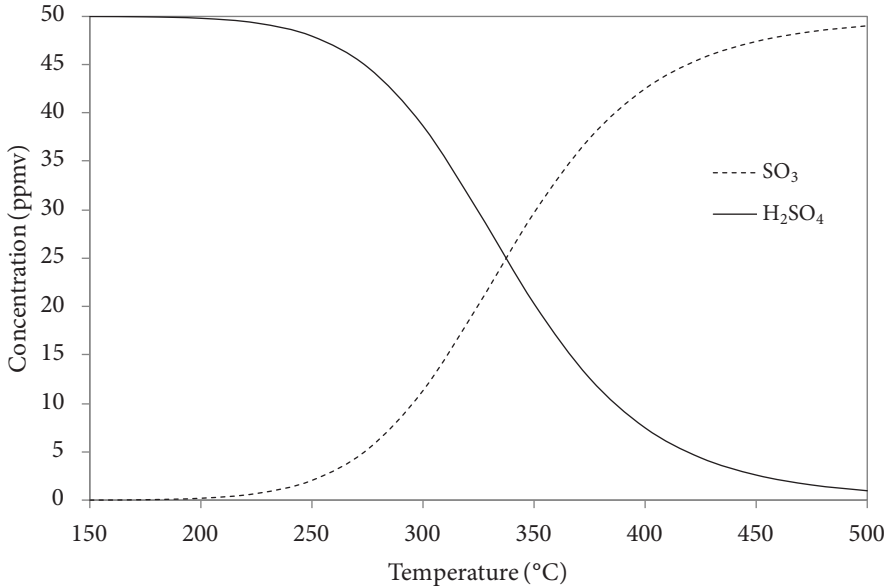
Figure 7. Equilibrium conversion of SO_3 and H_2SO_4, as a function of temperature, in a gas with 20 vol% H_2O and a $SO_3+H_2SO_4$ concentration equivalent to 50 ppmv. The calculations were conducted with the rate expression of Lovejoy et al. [102] and an initial SO_3 concentration of 50 ppmv.

The reaction between SO_3 and water vapor has been studied by many authors [101-104]. A theoretical study by Morokuma and Muguruma [101] showed that a direct reaction between one molecule of H_2O and one molecule of SO_3 does not occur, due to a too high energy barrier. Moreover, the energy barrier can be lowered by a second H_2O molecule, by forming an adduct with SO_3 ($SO_3 \cdot H_2O$). This adduct reacts with a second water molecule to form H_2SO_4 (Reaction 17). It has also been suggested that SO_3 reacts with a water dimer ($H_2O \cdot H_2O$) to form gaseous sulfuric acid and water (Reaction 18) [103].

$$SO_3 \cdot H_2O(g) + H_2O(g) \rightarrow H_2SO_4(g) + H_2O(g) \qquad (17)$$

$$SO_3(g) + H_2O \cdot H_2O(g) \rightarrow H_2SO_4(g) + H_2O(g) \qquad (18)$$
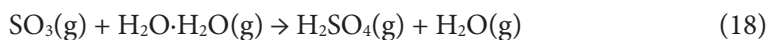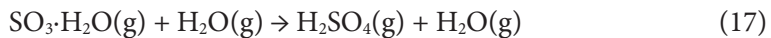
The reaction of SO_3 with water to form H_2SO_4 has a negative temperature dependence [102][103] and is second order with respect to water [101-104]. The negative temperature dependence is believed to be due to the formation of the $SO_3 \cdot H_2O$ adduct [102].

When the dew point temperature of sulfuric acid is reached, the gaseous sulfuric acid starts to form an acid mist or condenses on cold surfaces. Blue plume may form if sulfur-rich fuels are combusted and the flue gas cleaning is inadequate. Blue plume consists of H_2SO_4 aerosols that leave the flue gas stack. Severe low temperature corrosion may occur on components such as the flue gas duct, economizers, or air preheaters, if H_2SO_4 is present in the flue gas and the material temperature is below the H_2SO_4 dew point temperature [105]. Low temperature corrosion can be avoided by keeping all surfaces above the acid dew point temperature or by using acid-resistant steels. Therefore, it is important to determine the acid dew point temperature in the cold end of the flue gas duct. This can be done either by direct measurement of the acid dew point temperature or indirectly by measuring the H_2SO_4 in the flue gas and then estimating the acid dew point by correlations given by e.g. Verhoff and Banchero [106] or Bolsaitis and Elliott [107]. Generally, discussions about SO_3 measurements and SO_3 in the flue gas refer to gaseous H_2SO_4; the same applies for this work.

Figure 8 shows the sulfuric acid dew point temperature in a gas with various water vapor and sulfuric acid concentrations. The dew point temperature in the figure is calculated according to the empirical equation by Verhoff and Banchero [106]:

$T_{dew\ point} = 1000/\{2.276 - 0.0294 \times \ln(pH_2O) - 0.0858 \times \ln(pSO_3) + 0.0062 \times \ln(pH_2O) \times \ln(pSO_3)\}$,

where: $T_{dew\ point}$ is in Kelvin, p in mmHg and pSO_3 is the partial pressure of SO_3 or H_2SO_4.

The logarithmic correlation between the sulfuric acid dew point temperature and the H_2SO_4 concentration is notable. It shows that a tenfold increase in H_2SO_4 concentration corresponds to a 20°C higher acid dew point temperature.
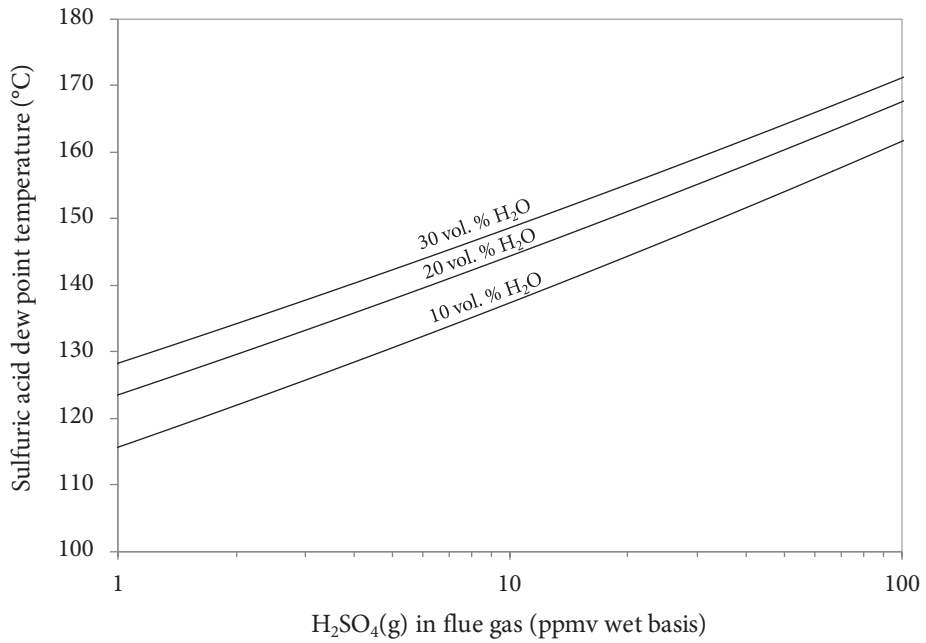
Figure 8. Sulfuric acid dew point temperature versus H_2SO_4 concentration for a flue gas with 10, 20, and 30 vol% H_2O, calculated with the empirical equation by Verhoff and Banchero [106].

4. MEASUREMENT CAMPAIGN IN A BUBBLING FLUIDIZED BED BOILER

A measurement campaign was conducted at the Rauman Voima BFB boiler. In-furnace measurements of nitrogen species were conducted, and these results are presented in **Paper I**. The measurement campaign was carried out to get information about the reactive nitrogen species present at different locations in the furnace during co-combustion of wood-based fuels and sludge. The reduction of nitrogen in this BFB boiler was also simulated and presented in **Paper II.** The fate of sulfur, potassium and chlorine during co-combustion of fuels with different ash properties was also studied in the boiler, and the results are presented in **Paper III**.

4.1. Experimental

4.1.1. Bubbling Fluidized Bed Boiler and In-Furnace Measurement Locations

The thermal capacity of the Rauman Voima BFB boiler is 107 MW. A schematic picture of the boiler is shown in Figure 9. The fuel was fed into the furnace through two fuel chutes on the left wall and two chutes on the right wall. The combustion air was divided into fluidizing air, secondary air, and tertiary air.

The gas composition was measured from the lower furnace, at the fuel inlet level, to the bullnose level. The gas composition was measured in 7 ports for a total of 14 in-furnace measurement locations. The gas was measured at every port at approximately 1 m and 2 m inside the furnace for 20 minutes of stable measurement. The measurement locations are shown in Figure 9, and are indicated with dots.
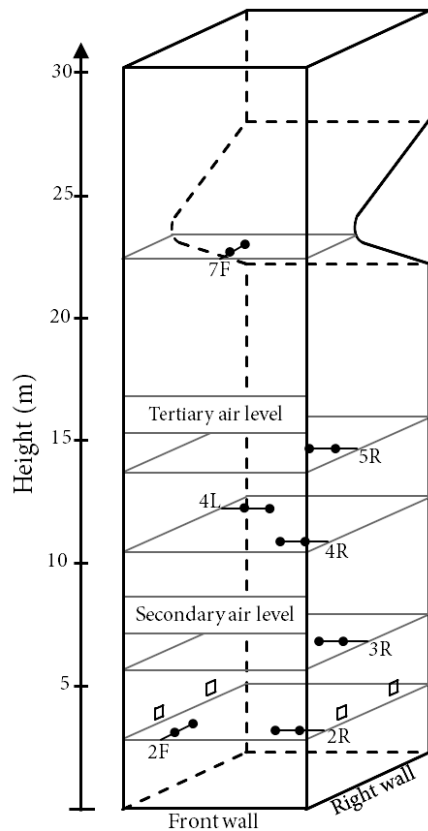
Figure 9. A schematic picture of the BFB boiler. The in-furnace measurement locations are indicated with dots.

The measurements were carried out over three days, with a different fuel blend for each day. The fuel blend and the boiler data for each measurement day are shown in Table 3. The base fuel in the trials was spruce bark. On the second day sludge was included, which consisted mainly of paper mill sludge and partially of municipal sewage sludge. On day three solid recovered fuel (SRF) was included in the fuel mix. The SRF consisted mainly of demolition wood. A photograph of each fuel blend is show in Figure 10. The thermal power of the boiler was held constant during each measurement day. The temperature in the furnace was measured with a suction pyrometer at different levels in the furnace. These measurements showed that the peak temperature in the furnace did not exceed 1100°C, thus, indicating that no thermal-NO_X was formed.

Table 3. Fuel mixture and boiler data for the three cases.

	Day 1	Day 2	Day 3
Fuel fraction (wt% wb)			
Bark	100	84	74
Sludge	-	16	16
SRF	-	-	10
Fuel feed (kg/s on wb)	14.2 ± 0.9	15.7 ± 1.1	15.3 ± 1.3
Thermal power (MW)	105 ± 6.9	103 ± 7.5	102 ± 8.5
Excess air ratio	1.3 ± 0.06	1.35 ± 0.05	1.34 ± 0.04
Temperatures			
Bed	780 ± 8	750 ± 18	800 ± 11
Mid-furnace	980 ± 56	990 ± 39	990 ± 42
Bullnose level	860 ± 21	820 ± 43	850 ± 21

Day 1	Day 2	Day 3

Figure 10. Photographs of the fuels for each measurement day.

4.1.2. Fuel and Ash Sampling and Analyses

Fuel samples were collected after the mixing silo during each measurement day. Standard fuel analyses were conducted by an external laboratory for each pure fuel as well as for the fuel mixture. Additionally, chemical fractionation was performed for the three pure fuels, i.e., bark, sludge, and SRF. Chemical fractionation was originally developed for the characterization of coal [108], and has been modified for the characterization of biomass [109]. The method has been further modified for biomass characterization and it has been used for approximately 170 fuels at Åbo Akademi University [110][111][112]. The method gives an indication of how the ash-forming elements are bound in the fuel. With the chemical fractionation technique, ash-forming matter can be distinguished according to its solubility in increasingly aggressive aqueous solvents. The solvents used are water, 1M ammonium acetate (NH$_4$Ac), and 1M hydrochloric acid (HCl). The elemental composition of the liquid fractions and the remaining solids were analyzed by an external laboratory using inductive coupled plasma with an atomic emission spectrometer (ICP-AES) and an inductive coupled plasma with a mass spectrometer (ICP-SFMS).

Table 4 shows the fuel properties of the pure fuels and fuel mixtures. All the fuels had a high volatile matter content, which means that most of the nitrogen is released during the devolatilization stage. The sludge had the highest nitrogen and sulfur content, resulting in a higher fuel nitrogen and sulfur content to the boiler.

The chemical fractionation results showed that the sludge contained high amounts of aluminosilicates, which are known to capture alkali metals in combustion [43][44][113-115]. The aluminosilicates most likely originated from kaolin from the paper mill sludge and zeolites from the municipal sewage sludge. The bark had the highest concentration of soluble potassium, which is known for being reactive in combustion. Reactive sodium was found mainly in the sludge.

Table 4. Fuel properties of the pure fuels and fuel mixtures.

	Bark	Sludge	SRF	Bark+Sludge	Bark+Sludge +SRF
Moisture content (wt%)	52.3	75.6	45.0	56.0	55.4
Ash content at 550°C (wt% db)	3.8	26.5	16.0	5.4	8.2
Volatile matter (wt% db)	75.2	61.5	72.3	73.6	72.3
Fixed carbon (wt% db)	21.0	12.0	11.7	21.0	19.5
LHV (MJ/kg db)	17.8	13.2	17.7	17.8	17.7
LHV (MJ/kg wb)	7.4	2.7	8.9		
Ultimate analysis (wt% db ash free)					
C	53.1	52.0	61.7	53.1	54.8
H	5.8	6.3	7.9	5.8	6.1
N	0.43	2.56	0.82	0.59	0.58
O	39.5	35.1	30.7	39.6	38.6
S	0.05	1.22	0.37	0.13	0.23
Cl	<0.02	0.12	0.21	<0.02	0.02
Ca/S (molar ratio)	17.3	1.1	4.0	6.5	5.5

The bottom ash, ash from the bottom of the second pass ash hopper, and filter ash from the baghouse filters were collected on each measurement day. The sampling locations are shown in Figure 11. The ash flows were higher when sludge was in the fuel mixture. Scanning electron microscopy (SEM) coupled with energy dispersive x-ray analysis (EDX) was used to analyze the ash samples. Three samples were analyzed for each co-combustion case.

Fine particles were sampled with a low-pressure impactor (DLPI) in the second pass, location D in Figure 11. The temperature in the measurement location was 165°C, and the impactor was heated to the same temperature. The impactor consisted of 13 impactor stages, collecting particles with an aerodynamic diameter ranging from 21

nm to 10.8 μm. Larger particles were removed with a cyclone to prevent the upper impactor stages from overloading. The sampling time varied between 5 and 7 minutes, and the flow rate was approximately 10 l/min (STP). The particles collected in the impactor stages were analyzed with SEM/EDX.
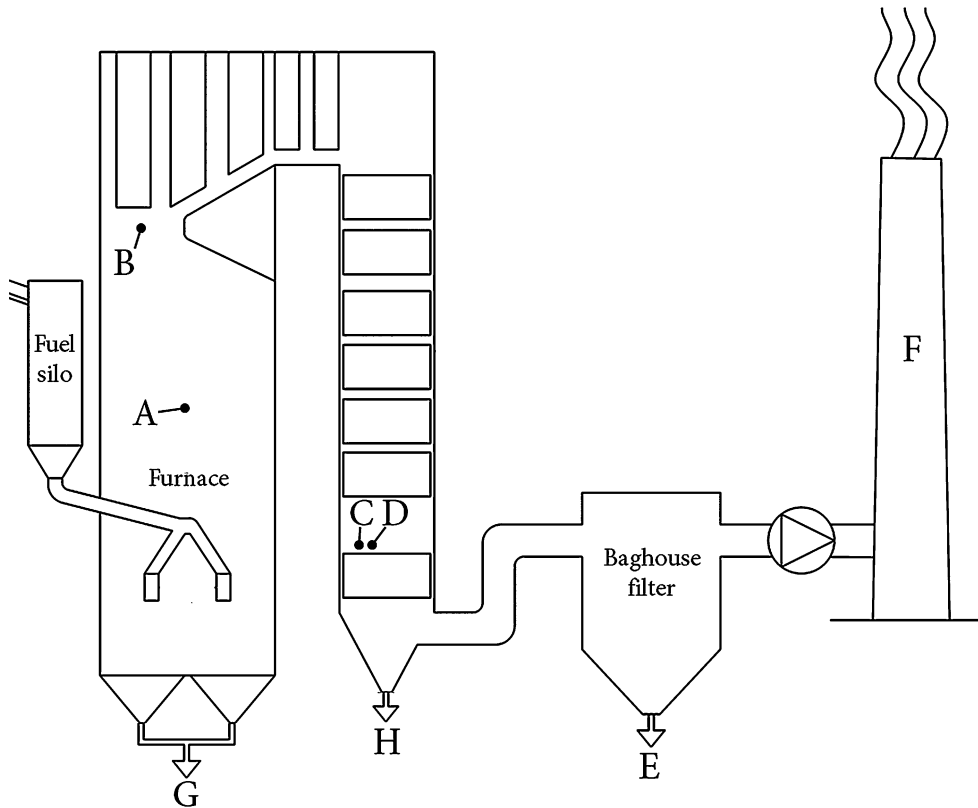
Figure 11. Measurement locations in the BFB boiler (**Paper III**): A-C. Gas measurement of SO_2 and HCl; D. Impactor measurements; E. Collection of filter ash; F. Measurement of stack gases; G. Collection of bottom ash; H. Collection of second pass ash.

4.1.3. In-Furnace Gas Measurement Technique and Analyzers

The in-furnace gas measurements were performed with an extractive quenching probe, which was connected to the analyzers. The probe is developed and built by the Technical Research Centre of Finland (VTT). The quenching of the gas sample is performed by diluting the gas with nitrogen gas in the probe tip. This method offers many advantages: the gas sample is rapidly quenched; the risk of condensing gases in the measurement equipment decrease, because the condensation temperature is lower in the diluted gas; and catalytic reactions between the probe material and the diluted gas decrease due to the lower temperature and the lower concentrations of the gases. England et al. [116] showed that the probe material may catalyze the reduction of NO to N_2 in a sampling probe if the probe and gas sample are uncooled, thus giving NO readings that are too low.

A cross-sectional picture of the probe is shown in Figure 12. The probe length is approximately four meters, which allows for measuring two meters inside the boiler. The probe consists of four coaxial pipes. The three outer pipes serve to cool the probe, which is done with pressurized air. After the quenching section in the probe tip, the gas sample is electrically heated to approximately 200°C. This is done in order to avoid condensation of gases in the in the probe. The temperature of the gas sample in the probe is monitored by three thermocouples: one located after the quenching section; one in the middle; and one in the back end of the probe. Due to the probe construction, the pipes in the probe will have different temperatures. To prevent any damage to the probe construction due to thermal expansion, two expansion springs are located in the back end of the probe. A filter was placed after the probe to remove particles from the gas sample. When using filters in the probe tip, reactions may occur between the hot gas and the hot filter cake formed on the filter [117][118].

The analyzers used in the in-furnace measurements were a portable FTIR and a $CO/CO_2/O_2$ analyzer. All the analyzers were mounted on a fixed point in the boiler. NH_3, HCN, NO, and HNCO were analyzed using the FTIR analyzer. The FTIR analyzer was of type Gasmet CX-4000, which has a sample cell volume of 0.4 l and an optical path length of 5.0 m. The sample cell was heated to 180°C. The spectral resolution was 8 cm^{-1} and the measurement cycle was 20 s with 200 scans. The

CO/CO$_2$/O$_2$ analyzer of type Modular System S710, measures CO and CO$_2$ by infrared absorption and O$_2$ is measured by paramagnetism. The relative uncertainty in the determination of NH$_3$ and HCN was ±15% and for NO ±20%. In measurement ports 2F, 2R, and 3R the uncertainty for NH$_3$ was ±20% due to the higher hydrocarbon concentrations in these ports.
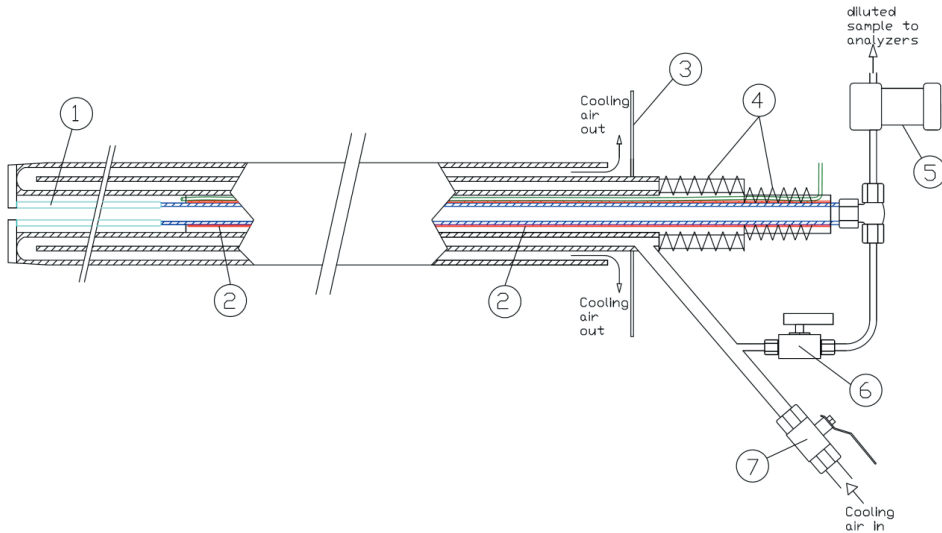
Figure 12. Cross section of the gas sampling probe. (1) Quenching section in the probe tip, (2) electrically heated center pipe, (3) steering plate for the cooling air, (4) expansion springs, (5) heated fine filter, (6) back purge valve, (7) cooling-air valve.

To determine the rate of dilution, sulfur hexafluoride (SF$_6$) was used as tracer gas. Sulfur hexafluoride is suitable for this application because it is chemically inert, it is not present in the flue gas, and it has high infrared absorption properties. However, SF$_6$ has a relatively low thermal stability; SF$_6$ starts to decompose at temperatures around 600°C, and therefore it is not suitable to mix it with the quenching gas during the measurements. Instead, the SF$_6$ gas and the quenching gas were mixed prior to the actual measurement in order to determine the baseline of SF$_6$, i.e., the concentration of SF$_6$ in the quenching gas. During the in-furnace measurements, the SF$_6$ gas was mixed with the gas sample after the probe, where the temperature of the gas is approximately 200°C. The flows of the quenching gas and the tracer gas were regulated by mass flow controllers (Environics series 2000), and these gases were led to the probe tip. A schematic picture of the gas sampling setup is shown in Figure 13.

The gas sample was transported to the analyzers in a 25 m long Teflon pipe. The line was heated to approximately 180°C, to avoid condensation of gases in the line.
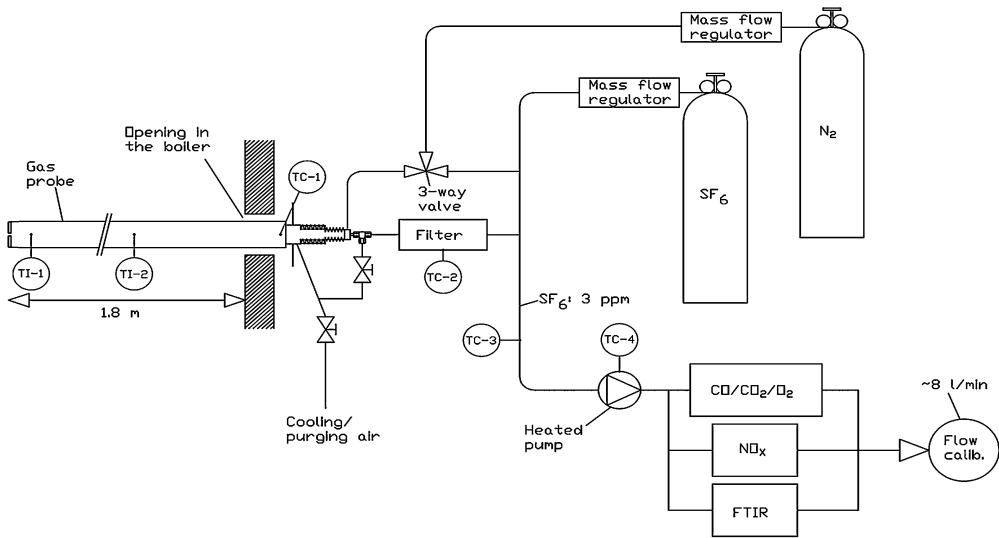
Figure 13. Setup of the measurement equipment. TI = temperature indicator, TC = temperature controller.

An example of the SF$_6$ concentration during baseline and in-furnace measurement is shown in Figure 14. The dilution factor is calculated from the SF$_6$ concentration during baseline measurement and in-furnace measurement according to the equation:

$$f = \frac{1}{\dfrac{c_{BL}^{SF_6}}{c_{M}^{SF_6}} - 1},$$

where

f is the dilution factor

$c_{BL}^{SF_6}$ is the average SF$_6$ concentration during baseline measurement

$c_{M}^{SF_6}$ is the SF$_6$ concentration during in-furnace measurement
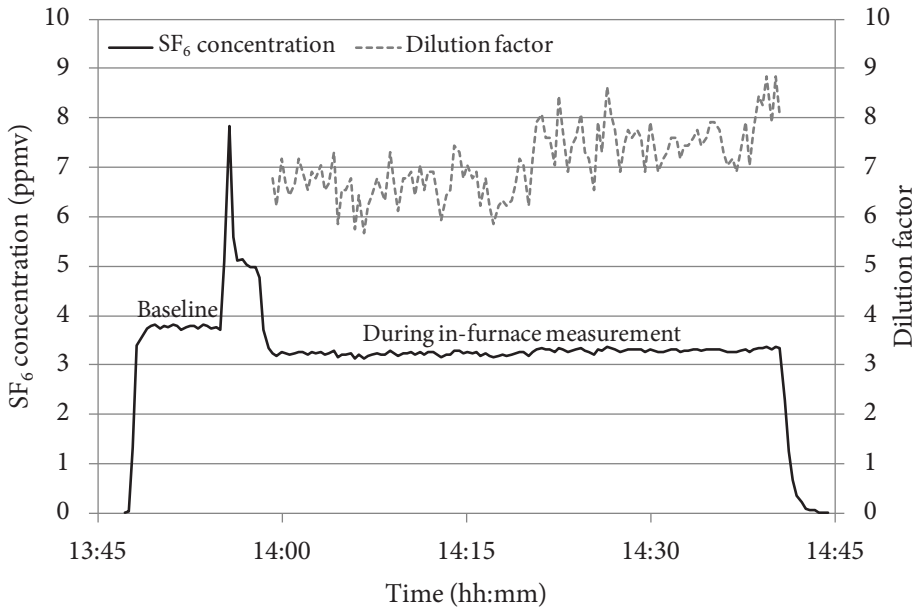
Figure 14. Sulfur hexafluoride concentration during a baseline and in-furnace measurement. The calculated dilution rate is shown by the dashed line.

The dilution factor was often slightly higher toward the end of the measurement. This may be attributed to particle accumulation in the filter, leading to a pressure drop over the filter. This leads to less gas being drawn from the furnace and, thus, a higher dilution ratio.

The gas composition was also continuously measured at the bottom of the second pass using an extractive non-diluting probe connected to the analyzers. The probe and sample line were heated to 200°C to avoid condensation of gases in the equipment. A portable FTIR analyzer (Gasmet DX-4000N) and a zirconium oxide based oxygen analyzer were used to determine the gas composition. H_2O, CO_2, CO, NO, NH_3, HCN, and N_2O were analyzed with the FTIR in the second pass.

4.1.4. Simulations of Fuel-N Reduction

The simulations of the effect of air staging on the reduction of nitrogen in the freeboard of the BFB boiler were done with the Chemkin software. The detailed Åbo Akademi University gas-phase chemical kinetic reaction scheme was used [119]. The mechanism includes 60 species in 371 elementary gas phase reactions. A combustion process can ideally be modeled by a reactor network consisting of plug flow reactors and/or well-stirred reactors [120]. A common approach in mixing of flows is to have the reactant or side flow gradually entrained in the bulk stream or main flow [121]. Another approach is to have the bulk flow gradually entrained into the reactant flow. This reversed-mixing approach has been used for modeling the SNCR process [122], re-burning [123], and ammonia chemistry [124]. The gradual dilution approach is also known as the Zwietering approach [125]. In this work, the gradual dilution approach was used for the modeling of the nitrogen reduction in the jet. The reversed-mixing approach was used, i.e., the air jet was gradually diluted by the combustion gases. This means that the air jet will be fuel-lean in the beginning, and the fuel to air ratio will change along the jet. Utilizing the opposite mixing approach, by gradually mixing the combustion air with the combustion gases, would mean that the conditions would mainly be fuel-rich. Additionally, direct mixing of the combustion gases with the air jet using plug flow reactors was used.

A reactor system consisting of plug flow reactors was set up to describe mixing of the combustion gases with the air jets. The mixing approach applied, with the gradual dilution of the air jet with the combustion gases, is shown in Figure 15. The main parameters for the reactor system, such as entrainment of the bulk gas, residence times, and velocity of the jet, were calculated with CFD. The degree of dilution of the air jets with combustion gases in the secondary and tertiary air simulations were determined to reflect the excess air ratio measured in the gas above the secondary and tertiary air levels in the BFB boiler. The measured excess air ratios above the secondary and tertiary air levels were 0.93 and 1.33, respectively. The gas composition measured two meters above the fuel inlet and approximately two meters inside the furnace was used as the input gas composition in the secondary air jet simulations. Furthermore, the gas compositions from the secondary air jet simulations were used as input in the tertiary air jet simulations.
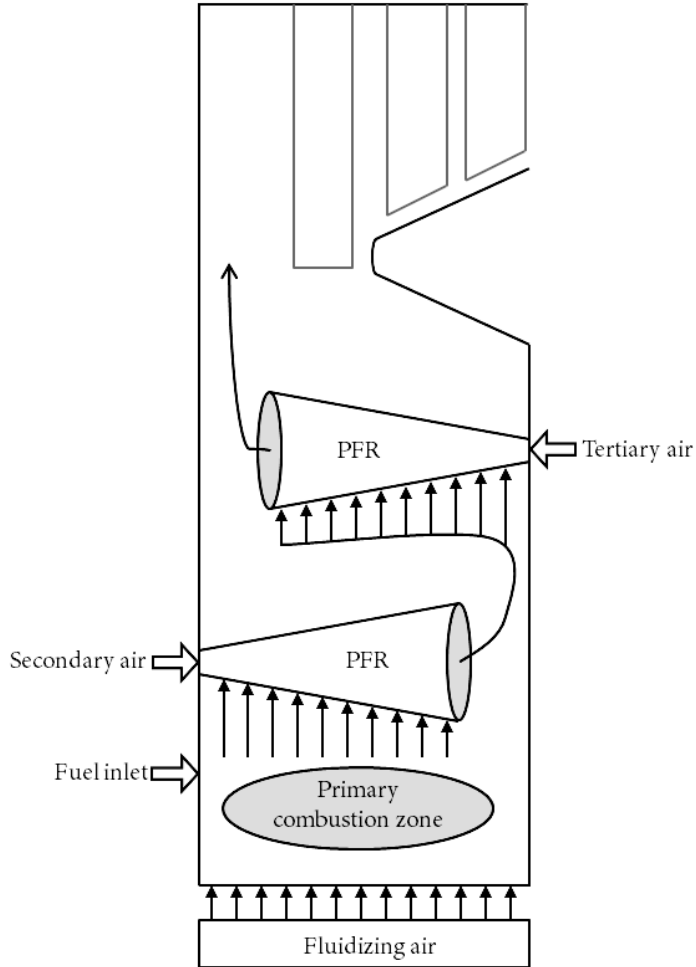
Figure 15. Illustration of the applied mixing approach in the simulations using the gradual mixing approach. The air jets are described by PFRs and the combustion gases are gradually entrained into the jets.

4.2. Results from the Bubbling Fluidized Bed Combustor

Selected results from **Papers I-III** will be presented in this chapter, starting with the in-furnace measurement result of nitrogen species. Next, the simulation results on the reduction of nitrogen species of the same boiler are shown. Last, the fate of sulfur in the furnace is presented, i.e., the results of sulfur in fine particles, in the coarser ash particles, and in the gas-phase.

4.2.1. NO_X Formation and Fuel-N Reduction in the Furnace

The concentrations of NH_3, HCN, HNCO, and NO measured during the bark, sludge, and SRF co-combustion case are shown in Figure 16. To enable comparison of the results, the values in the figure are normalized to a dry flue gas and 6 vol% O_2. The results suggest that the release of reactive nitrogen species from the fuel was mainly in the form of NH_3 and HCN; in the measurement port above the fuel chutes (3R), at 1.8 m, the average concentrations measured were 500 ppmv NH_3, 120 ppmv HCN, and 160 ppmv NO. This was the only measurement port at which HNCO could be quantified; however, the concentration of HNCO was low, roughly 1% of the overall total fixed nitrogen (TFN) species. Between the secondary and tertiary air levels, NH_3 was the main TFN species. Above the tertiary air level, most of the TFN species had oxidized to NO or reduced to N_2.

In port 3R the gas composition was very different at the two depths. The gas composition measured in port 3R is shown in more detail in Figure 17. First, the probe was inserted 1.8 m into the boiler, and the measurement continued for 20 min. In this case, the main TFN species was NH_3 and no oxygen was present; the concentration of NH_3 was about three times higher than that of HCN or NO. After 20 min of measurement, the probe was purged and the measurement continued at 1.8 m. Similar concentrations of NH_3, HCN, and NO were again observed. The gas composition was very different closer to the wall, at 0.8 m, where oxygen was also present. This oxygen might originate from the air stream arriving with the fuel and flowing along the wall. Consequently, the concentrations of TFN was different at 0.8 m than at 1.8 m; the concentrations of NO and NH_3 were roughly equal at 0.8 m. Finally, the probe was put back at 1.8 m, where reducing conditions prevailed. Again, the main TFN species was NH_3.
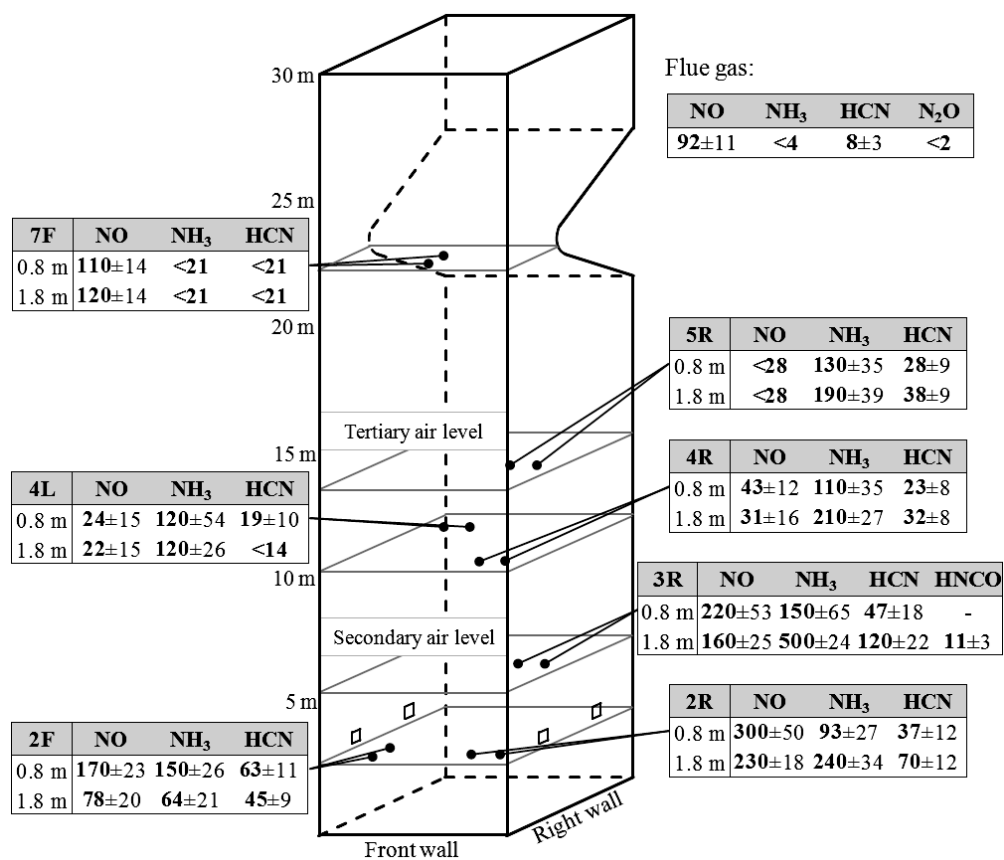
Figure 16. Average concentrations of nitrogen species measured at five levels in the furnace, 0.8 m and 1.8 m from the boiler inner wall. The values are normalized to a dry flue gas and 6 vol% O_2. The values are based on data from a 20 min measurement period. Data from **Paper I**.
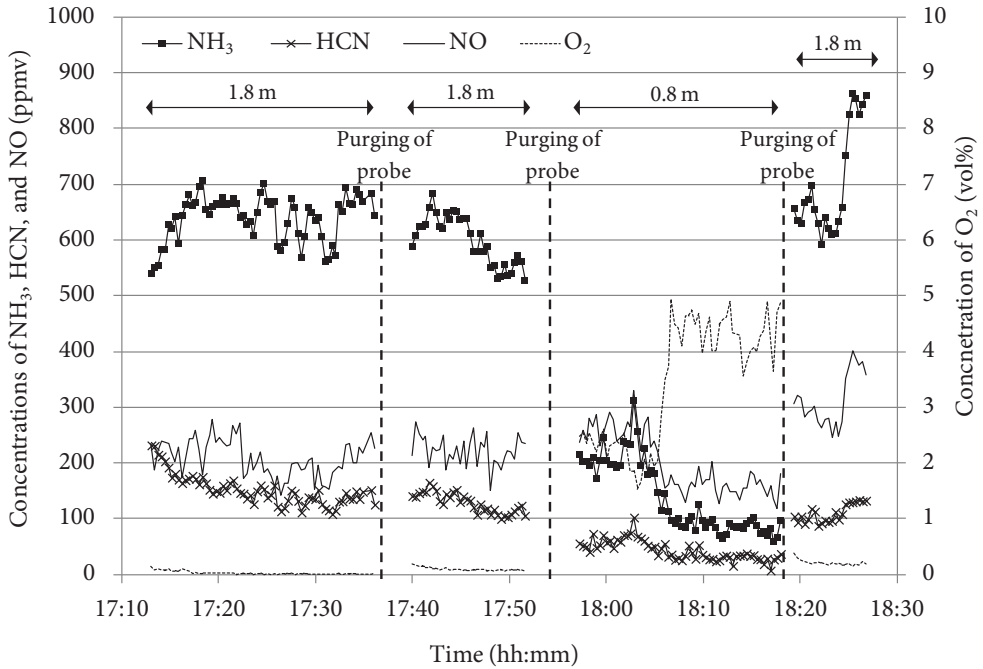
Figure 17. Concentrations of NH₃, HCN, NO, and O₂ in the measurement port above the fuel inlet (port 3R), at 1.8 m and 0.8 m from the inner wall. Figure from **Paper VIII**.

The fuel-N conversion to NO, NH₃, HCN, and HNCO along the freeboard is shown in Figure 18. The figure is based on the measurement at about 2 m inside the furnace. The conversion is calculated according to the following equation:

$$\text{Fuel-N conversio} = \frac{(^N\!/_C)_{\text{gas}}}{(^N\!/_C)_{\text{fuel}}},$$

where $(N/C)_{\text{gas}}$ is the molar ratio of the nitrogen and carbon species measured in the gas. The carbon species measured in the gas include: CO_2, CO, CH_4, C_2H_2, C_2H_4, and C_6H_6. $(N/C)_{\text{fuel}}$ is the molar ratio of the nitrogen and carbon in the fuel. Unfortunately, during the bark mono-combustion the measurements were conducted at only two heights. Figure 18 clearly shows that in the lower furnace, below the secondary air level, almost no reduction of the TFN species to N_2 occurred. When going above the secondary air level, a huge reduction in the nitrogen species to N_2 can be observed. The fuel-N conversion to TFN gases between the secondary and tertiary air levels was between 27-31% in all the combustion cases.

35

When going above the tertiary air level, a further reduction took place. The final reduction of the released fuel-N species was over 90% in all cases.
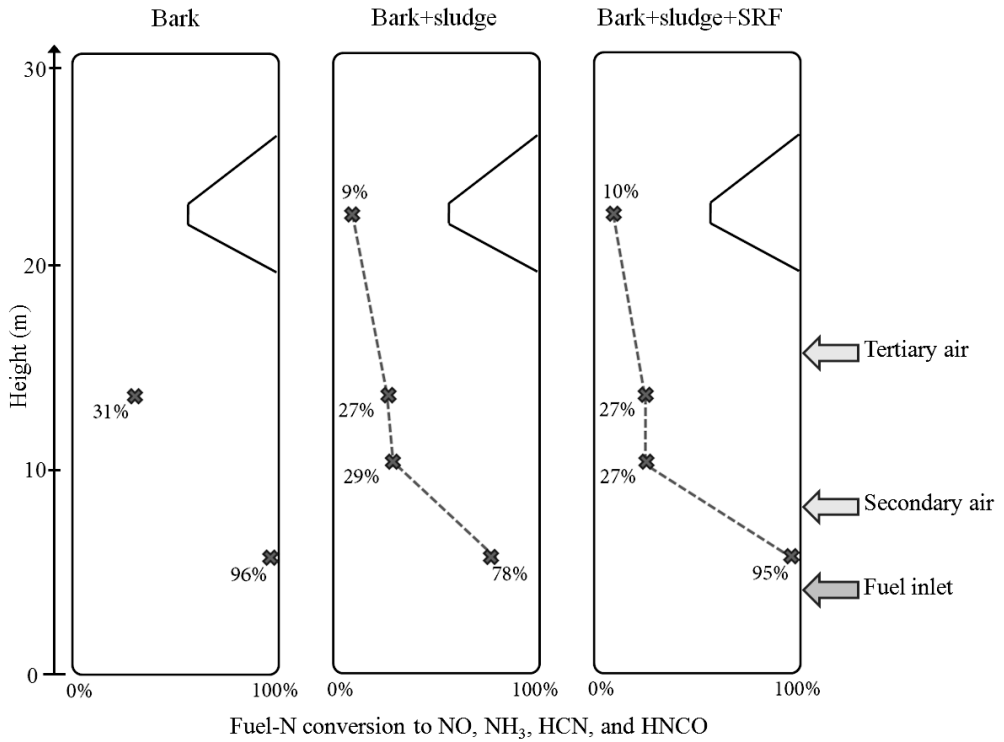
Figure 18. Fuel-N conversion to NO, NH₃, HCN, and HNCO along the freeboard in the three co-combustion cases. Figure from **Paper I**.

4.2.2. Simulation of the Reduction of Reactive Nitrogen in the Air Jets

The results from the in-furnace measurement 2 m above the fuel inlet and 1.8 inside the furnace were used as input gas in the simulation of the reduction of reactive nitrogen species in the secondary air jet. The measured gas composition is shown in Table 5.

Table 5. Input gas composition used in the simulations of the reduction in the secondary air jet. The gas composition is measured 2 m above the fuel inlet (port 3R) 1.8 m from the inner wall. Data from **Paper I**.

Gas composition 2 m above the fuel inlet	
NH_3	640 ppmv
HCN	162 ppmv
NO	216 ppmv
H_2O	31.4 vol%
N_2	57.1 vol%
CO_2	7.3 vol%
CO	2.5 vol%
CH_4	1.0 vol%
C_2H_2	0.19 vol%
C_2H_4	0.28 vol%

The result of the simulation of the reduction in the secondary air jet is shown in Figure 19. Three distinct zones can be seen in the figure when looking at the total reduction of nitrogen species to N_2. In the beginning of the jet, mixing of combustion gases into the jet takes place; however, the gases are still too cold for any reduction to occur. Hence, in the beginning only accumulation of reactive nitrogen species takes place. When the temperature in the jet rises over approximately 800°C at 0.12 s, a huge reduction of TFN gases takes place via the reaction between NH_3 and NO to form N_2. The reduction of TFN occurs as more NH_3 and HCN flows in with the combustion gases, as long as the excess air ratio is above one. Accumulation of TFN gases occur after 0.37 s when the excess air ratio is greater than one. This shows that oxygen plays an important role in forming the radicals needed in the

reduction of TFN. Total fixed nitrogen species in the end of the secondary air jet is 300 ppmv, which corresponds to a 66% reduction to N_2.
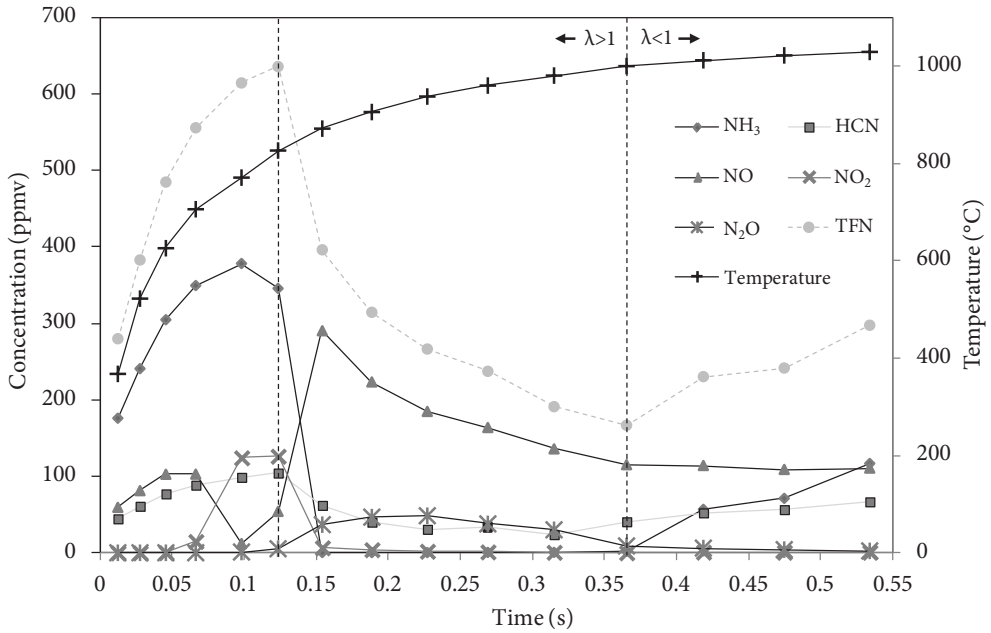
Figure 19. Simulation results of the nitrogen species in the gradual mixing of the secondary air with the combustion gases. Figure from **Paper II**.

The output gas composition from the secondary air jet simulation was used as input in the tertiary air jet simulation. The reduction of TFN in the tertiary air jet is shown in Figure 20. Again, the air jet is cold and fuel-lean in the beginning of the jet, and no reduction of TFN takes place. The TFN gases are accumulating until the temperature rises high enough for the reduction to take place. When the temperature in the jet reaches approximately 800°C a large reduction in TFN occurs. Reduction of TFN takes place as more NH_3 and HCN are mixed into the air jet. The final NO concentration is about 100 ppmv, and the reduction of TFN in the tertiary air jet simulation is 52%.
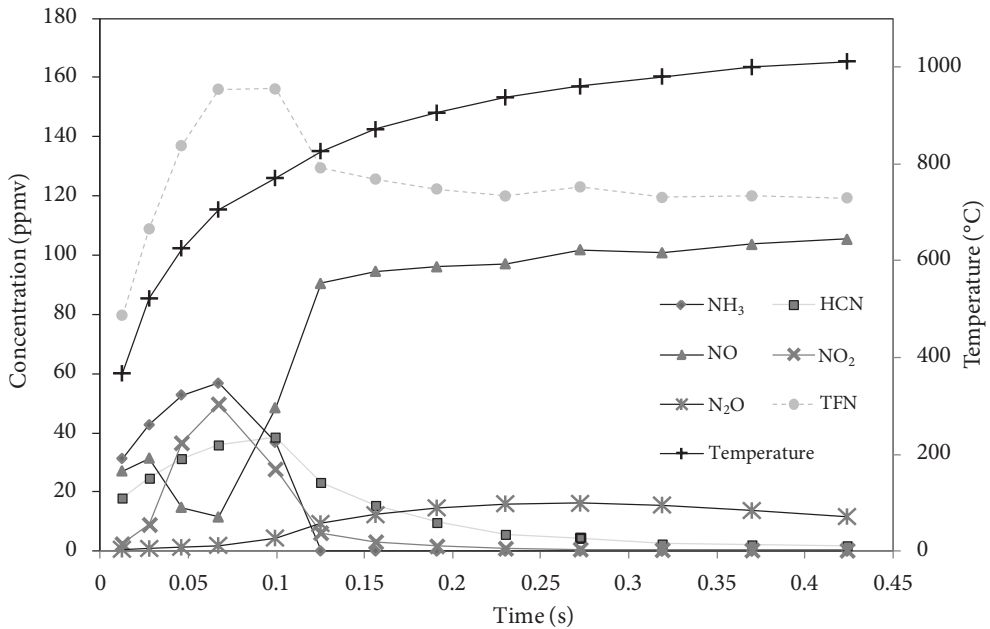
Figure 20. Simulation results of the nitrogen species in the gradual mixing of the tertiary air with the combustion gases. Figure from **Paper II**.

The measured and simulated values of nitrogen species after the secondary and tertiary air jets are shown in Figure 21. The results using both the gradual mixing approach as well as the instant mixing approach are shown. In the direct mixing approach, the combustion gases and air jet are mixed in one step. The speciation of nitrogen species after the secondary air jet is in better agreement, when using the gradual dilution approach. The NH_3 and HCN from the secondary air jet give some reduction potential for TFN in the tertiary air jet. The prediction of final NO_X emissions with the gradual mixing approach is in good agreement with the measured value. In the direct mixing approach almost no NH_3 is present after the secondary air level, and main TFN gas is NO. This leads to a poor reduction potential of TFN in the tertiary air jet. Consequently, the direct mixing approach predicts about three times higher final NO_X emissions than the measured value.
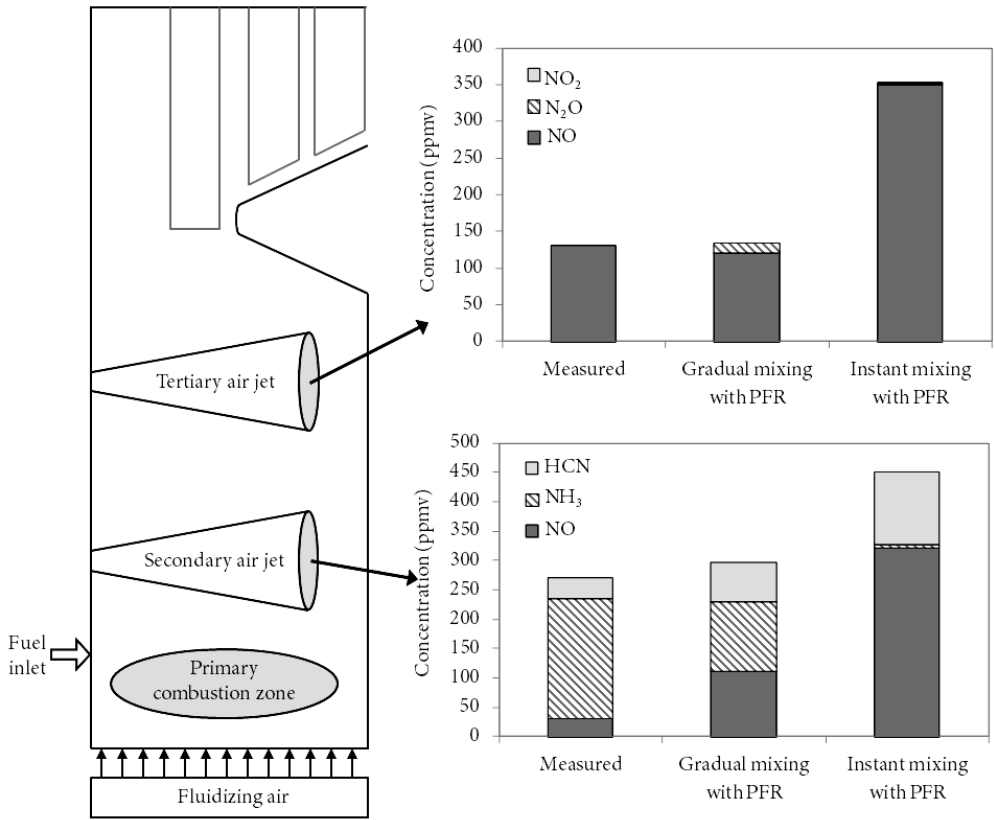
Figure 21. Measured and simulated nitrogen species after the secondary and tertiary air jets. The values are normalized to a dry flue gas with 6 vol% O_2. Figure modified from **Paper X**.

4.2.3. SO₂ Formation and Recapture

All fuel mixtures had a good sulfur-capturing potential, i.e., the Ca/S ratio was high. The ratios for the three cases were: bark 17.3, bark+sludge 6.5, and bark+sludge+SRF 5.5. Most of the sulfur was captured in the furnace, as illustrated in Figure 22. For the bark+sludge co-combustion case all sulfur was captured in the furnace. A part of the SO₂ was captured in the baghouse filter in the bark and bark+sludge+SRF cases; this is most likely due to the good contact between the flue gas and ash particles in the filter cake that is formed on the baghouse filter. Some SO₂ was present in the final flue gas only in the bark+sludge+SRF case.
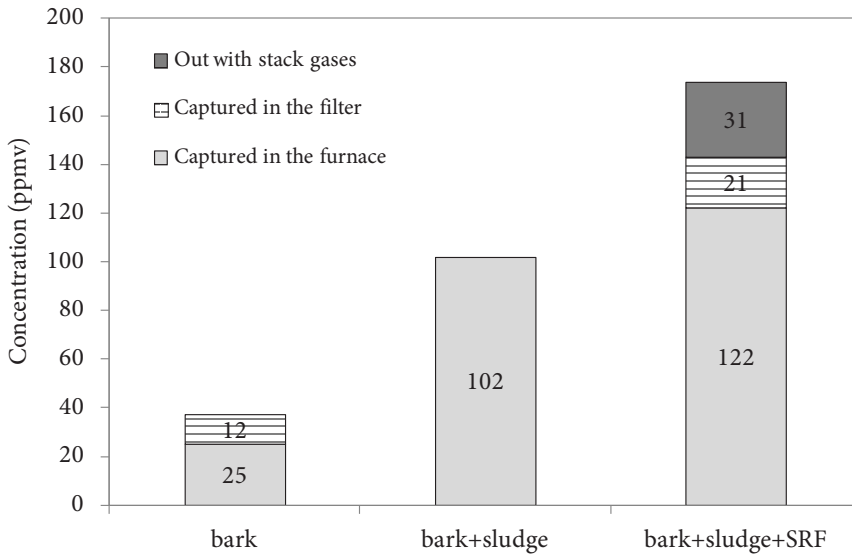
Figure 22. Fate of sulfur in the three combustion cases. Sulfur dioxide captured in the furnace and baghouse filter, and final SO₂ emissions. The values are expressed as ppmv in flue gas conditions. Data from **Paper III**.

The SO₂ concentrations at various locations in the boiler are shown in Figure 23. The measurement locations are shown in Figure 11. The sulfur dioxide is captured when going downstream with the flue gases, from measurement port A to measurement port C. This is due to the formation of primarily calcium sulfate and alkali sulfates.
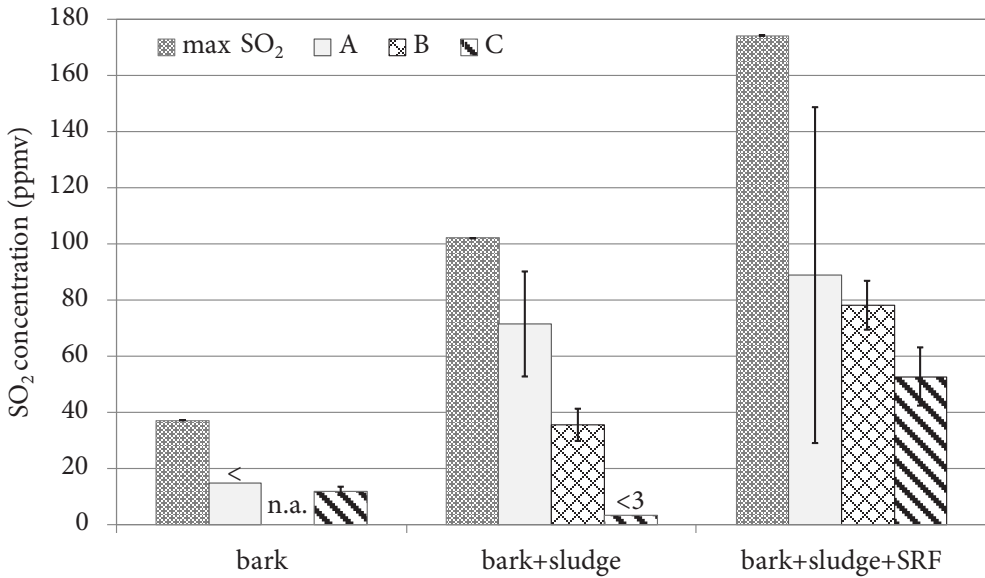
Figure 23. Sulfur dioxide concentration at various locations in the boiler and calculated maximum conversion of sulfur in the fuel to SO_2. The gases are normalized to 3.5 vol% O_2. Data from **Paper III**.

In the bark+sludge+SRF co-combustion case, some chlorine was also present in the fuel mixture. This was due to the fairly high chlorine content in the SRF. Sulfur played an important role by sulfating alkali chlorides in this case. As the SO_2 concentration drops from measurement port A downstream to measurement port C, the HCl concentration rises. This can be seen in Figure 24. This trend could be due to the sulfation of alkali chlorides, where HCl is released, in accordance with Reaction 10.
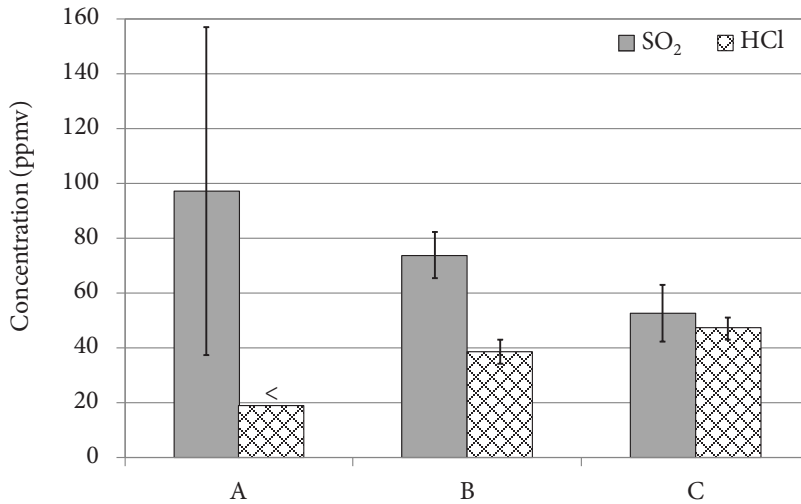
Figure 24. SO_2 and HCl concentrations in ports A to C for the bark+sludge+SRF case, normalized to 3.5 vol% oxygen. Data from **Paper III**.
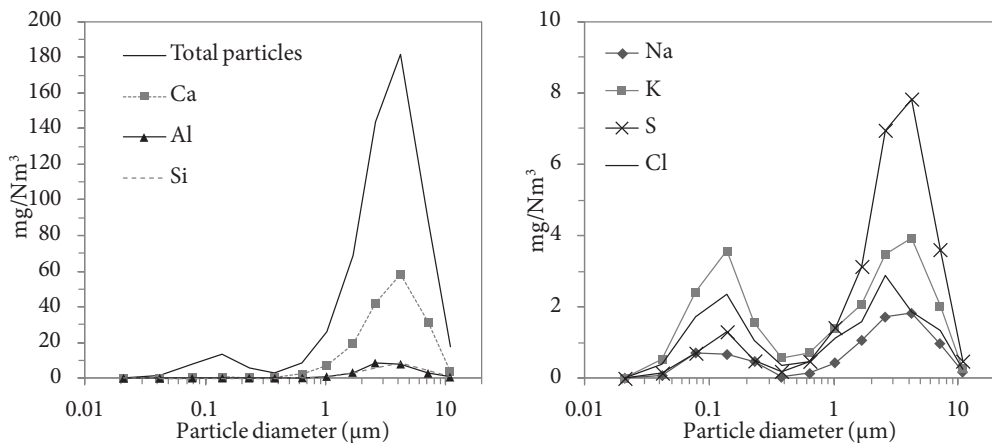
Figure 25. Particle size distributions and mass fractions of: total particles, Ca, Al, Si, Na, K, S, and Cl. The samples are taken with an impactor at 165°C at the bottom of the second pass, measurement port D, during the bark, sludge, and SRF co-combustion case. Data from **Paper III**.

The mass distribution and mass fractions of various elements in the fine particles measured in port D are shown in Figure 25. The fine particles showed a bimodal distribution. The coarser fraction consisted mainly of non-volatile elements: calcium, silica, and aluminum. The submicron particles consisted mostly of alkali sulfates and chlorides. However, the concentrations of sodium and potassium were

not enough to bind all sulfur and chlorine in the submicron particles; therefore some alkali carbonates were probably also present.

Figure 26 shows the molar flows of sulfur at various locations in the boiler during the bark+sludge+SRF co-combustion case. In ports A, B, C, and F sulfur was measured as SO_2 in the gas-phase. Sulfur dioxide is captured in the ash, when moving from measurement port A to measurement port C. The sulfur content in the fine particles (<10.8 μm) was measured in point D, before the baghouse filter. Approximately 11% of the sulfur in the fuel was found in the fine particles. The fine particles eventually ended up in the baghouse filter and became a part of the fly ash. The molar flow of fly ash was calculated by assuming that all the ash formed fly ash, because the flows of bottom ash and second pass ash were very small compared to the fly ash amount. As the figure shows, most of the sulfur was removed from the boiler with the fly ash. About 20% of the sulfur in the fuel exited with the flue gas in the form of SO_2. The ratio of sulfur input with the fuel to total sulfur output with the fly ash stream was satisfactory, about 0.9.
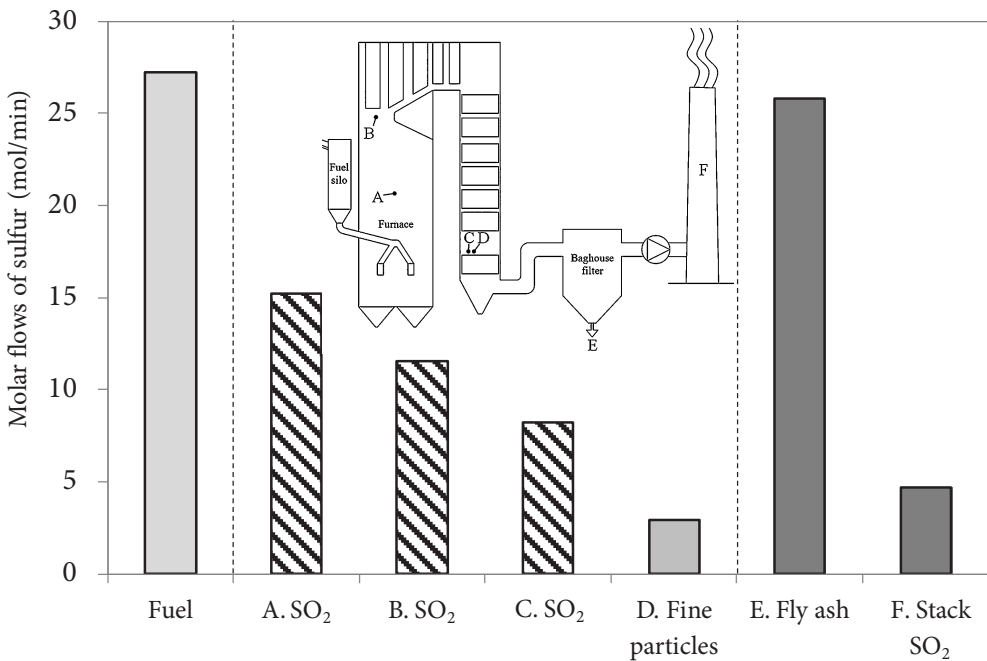
Figure 26. Molar flows of sulfur in the fuel, gas-phase at various locations, fine particles in the second pass, and fly ash for the bark+sludge+SRF co-combustion case. Data from **Paper III**.

5.   MEASUREMENT CAMPAIGN IN A KRAFT RECOVERY BOILER

A measurement campaign was conducted at the UPM Wisaforest Kraft recovery boiler in Jakobstad. In-furnace measurements of nitrogen and sulfur species were performed, and these results are presented in **Paper IV**. The measurement campaign was carried out to obtain information about the reactive nitrogen and sulfur species present at different locations in the furnace and freeboard of a Kraft recovery boiler.

5.1.   Experimental

5.1.1. Kraft Recovery Boiler and Measurement Locations

The UPM Wisaforest recovery boiler is a large modern recovery boiler, with a design capacity of 4450 tds/d (tons of dry solids per day), fired with high-dry-solids black liquor. The measurements were carried out with two different setups of the boiler. During the first two measurement days the boiler was run with a low bed, which is normal for this recovery boiler. On the third measurement day the boiler was run with a high bed. The bed at the two different operational modes is shown in Figure 27. On the third measurement day, the bed was created by lowering the black liquor temperature. Lowering the black liquor temperature leads to the formation of bigger droplets. Accordingly, less carbon conversion occurs in-flight and more carbon is accumulated on the bed. The conditions in the furnace were not very stable during the high bed operation; therefore only the results from the low bed operation are presented in this thesis.
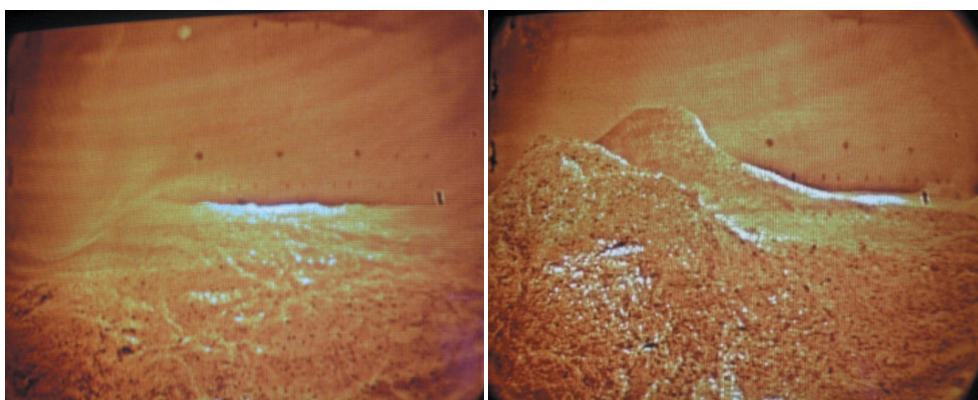
Figure 27. Pictures of the bed at the two operational modes: low bed (at left) and high bed (at right).

The black liquor was sprayed with three liquor guns from the right wall and with three liquor guns from left wall located on the third floor. The black liquor originated from approximately half from softwood pulping and half from hardwood pulping. The black liquor properties are shown in Table 6. The boiler load during the measurements was approximately 3000 tds/d, with a black liquor dry solid content of 81%. Thus, the boiler load was two-thirds of design capacity. The oil burners and odorous gas burners were not used during the measurements. The black liquor feed was kept stable at 42 kg/s, and was fed from three splash plate nozzles on the right wall and three on the left wall. A flat bed was formed on the bottom of the furnace. The combustion air was divided into three levels: primary, secondary, and tertiary air.

Table 6. Black liquor properties and elemental composition in wt% on dry basis.

Black liquor properties	
Dry solids content	81.4%
Ash	57.3 wt%
C	31.5 wt%
H	3.2 wt%
N	0.1 wt%
S	6.5wt%
Cl	0.3 wt%
Na	21.6 wt%
K	2.4 wt%
Na/S ratio	3.3
Higher heating value, dry basis	12.9 MJ/kg

5.1.2. In-Furnace Measurements and Analyzers

The in-furnace measurements were performed at four levels in the furnace, from the furnace bed to right above the tertiary air level. Figure 28 shows the measurement ports in the furnace. To allow visibility of all the measurement ports, the boiler is opened from one corner. In all ports, except for port 2, the gas composition was measured at two depths: 1 m and 2 m from the furnace inner wall. Port 2 was located

between two liquor guns, and measurements in this port took place 0.5 m inside the furnace. Figure 29 shows the probe placement, indicated with a black line, between the liquor guns. The picture is taken with an IR furnace camera facing down toward the furnace bottom.
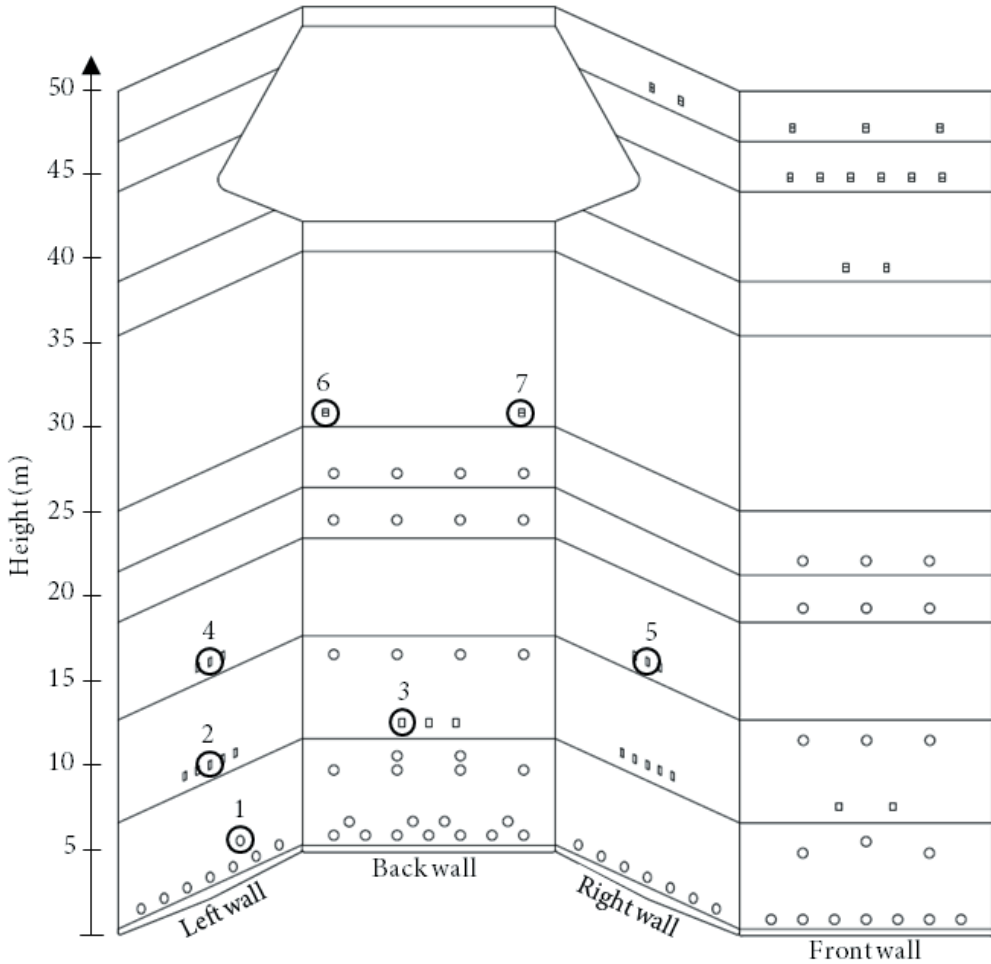
Figure 28. Measurement ports in the Kraft recovery boiler. The boiler is opened from one corner to allow visibility of all the boiler walls.
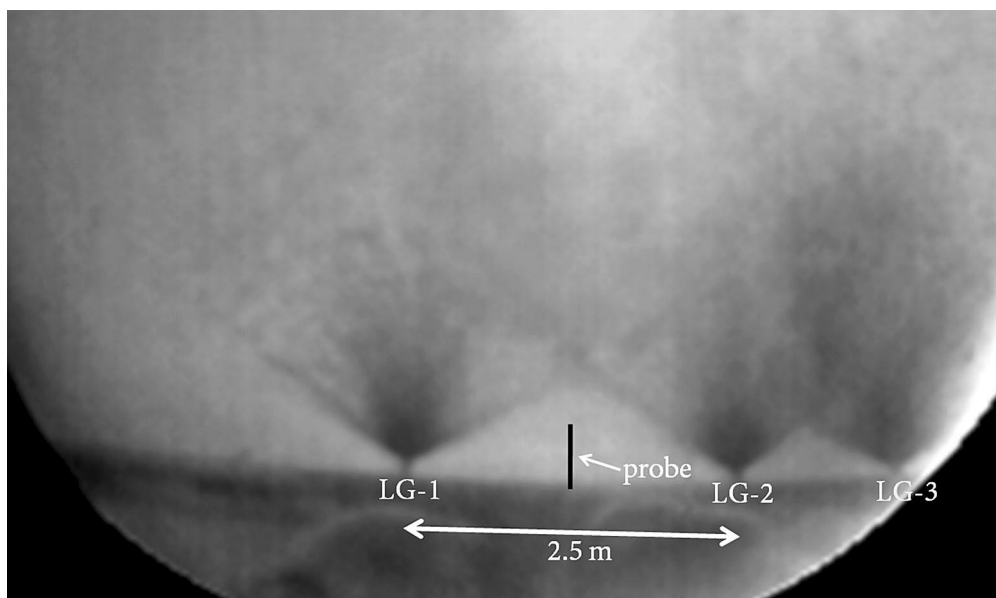
Figure 29. Probe placement between the liquor guns in measurement port 2. The probe is indicated by the black line. (LG = liquor gun)

The same type of in-furnace probe was used in the recovery boiler measurements, as in the measurement in the BFB boiler. The FTIR was also of the same type. The measurement time per port varied between 0.5 h and 2 h. Additionally, a portable gas chromatograph (Perkin Elmer Photovac Voyager) was used to measure the reduced sulfur compounds (TRS). The GC column was heated to 80°C and was connected to a photo-ionization detector (PID). The sampling with the GC was performed every five minutes during the measurement.

5.2. Results from the Kraft Recovery Boiler

The results from the measurement campaign in the recovery boiler, from **Paper IV,** are presented in this section. The in-furnace measurement data of sulfur and nitrogen species at various locations in the furnace are presented and discussed.

The results presented here focus on some selected results from the measurements, including the measurements on the black liquor spraying level, ports 2 and 3. The measurements conducted right above the tertiary air level, ports 6 and 7, are also presented. An interesting trend was observed on the left and right side on the back wall in this particular furnace; ports 6 and 7 exhibited significant differences in the main gas composition, as Figure 30 shows. In port 6, oxidizing conditions prevailed at 1 m and 2 m inside the furnace; conversely in port 7, the conditions were reducing. Consequently, this had an effect on the sulfur and nitrogen species present in these ports.
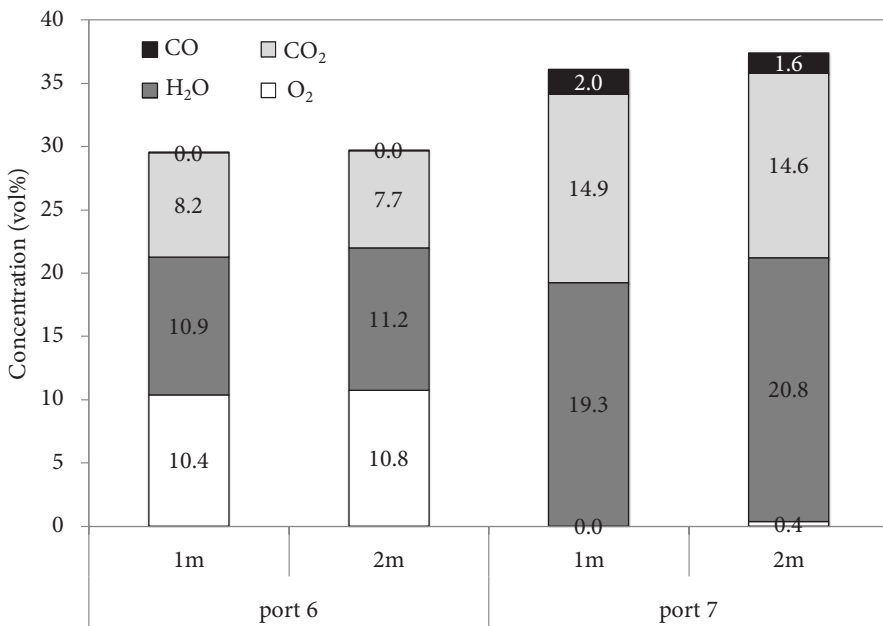
Figure 30. Main gas species measured in ports 6 and 7. These ports are located on the right and left corners of the back wall, right above the tertiary air level. Figure from **Paper IV**.

5.2.1. NO_X Formation

The nitrogen species measured at the black liquor spraying level are shown in Figure 31. In port 2, between the liquor guns, NH_3 and NO were the main nitrogen species; however, some HCN was also present. Port 3 was located on the back wall where no liquor guns were placed. At this location mainly NH_3 and HCN were present. Whether the HCN found on the black liquor spraying level comes from the volatiles, or whether it is a product of NO re-burning with hydrocarbons, is unknown. However, earlier laboratory studies of black liquor pyrolysis have not found HCN as a primary pyrolysis product [85]. Therefore, the HCN found in these measurements is believed to form via re-burning of NO.
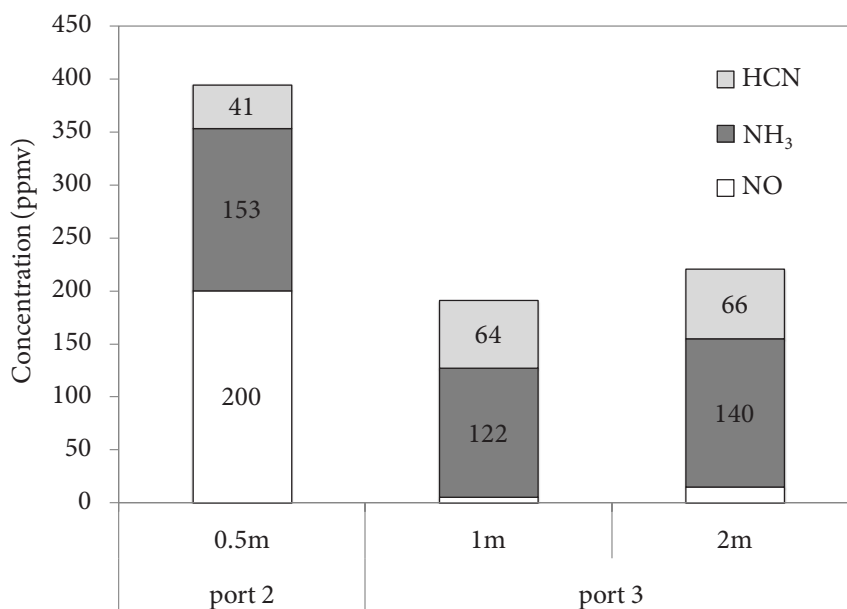
Figure 31. Nitrogen species, in wet gases, measured at the black liquor spraying level, ports 2 and 3. Data from **Paper IV**.

Above the tertiary air level, in ports 6 and 7, the conditions were very different. The nitrogen species measured in these ports are shown in Figure 32. In port 6 the conditions were oxidizing, and NO was the main nitrogen species. In port 7 the conditions were reducing, and the main nitrogen species was NH_3. However, in the flue gas, only NO was detected; it measured 67 ppmv at 3.5 vol O_2 in wet gases. This corresponds to 25% of the nitrogen bound in the black liquor. Furthermore,

approximately 30% of the nitrogen in the black liquor exited the smelt in the form of cyanate.
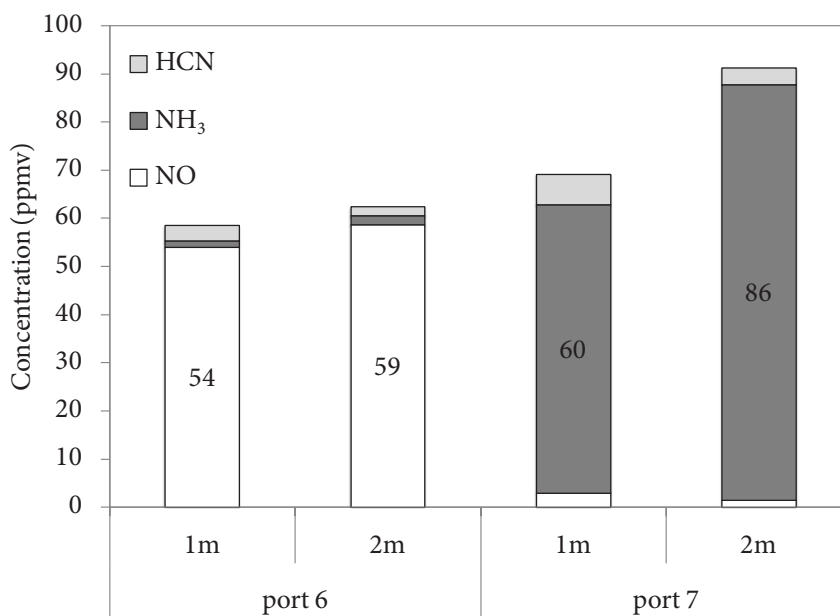
Figure 32. Nitrogen species, in wet gases, above the tertiary air level in ports 6 and 7. These ports were located on the back wall in the right and left corners. Figure from **Paper IV**.

5.2.2. Summary of Nitrogen Reactions in a Kraft Recovery Boiler

Figure 33 shows a summary of the fuel-bound nitrogen reactions in a Kraft recovery boiler. The figure is based on the in-furnace measurements of the current work and studies found in the literature. During the devolatilization stage, 60-80% of the fuel-bound nitrogen is released as NH_3 and N_2 [82][83][85][86]; however, no significant amounts of HCN have been found to be released [85]. During char oxidation, N_2 and NO are formed, however, most of the char nitrogen forms cyanate [88]. A small part of the cyanate may form NO and N_2 in smelt reactions [87][88]. Furthermore, most of the cyanate exits the boiler in the smelt, and accounts for about one-third of the black liquor nitrogen [86]. The HCN found at the black liquor spraying level in the in-furnace measurements in the present work is believed to form in the reaction between NO and hydrocarbon radicals found at the black liquor spraying level.

Nitrogen oxide flowing from the lower furnace and forming at the black liquor spraying level reacts with the hydrocarbons, which are released during the devolatilization stage, forming HCN. Depending on the amount of excess oxygen higher up in the furnace, the reactive nitrogen will be in the form of NH_3 or NO. After the final burnout, the the NO and NH_3 are partially reduced to N_2 and partially form the final NO_X emissions.
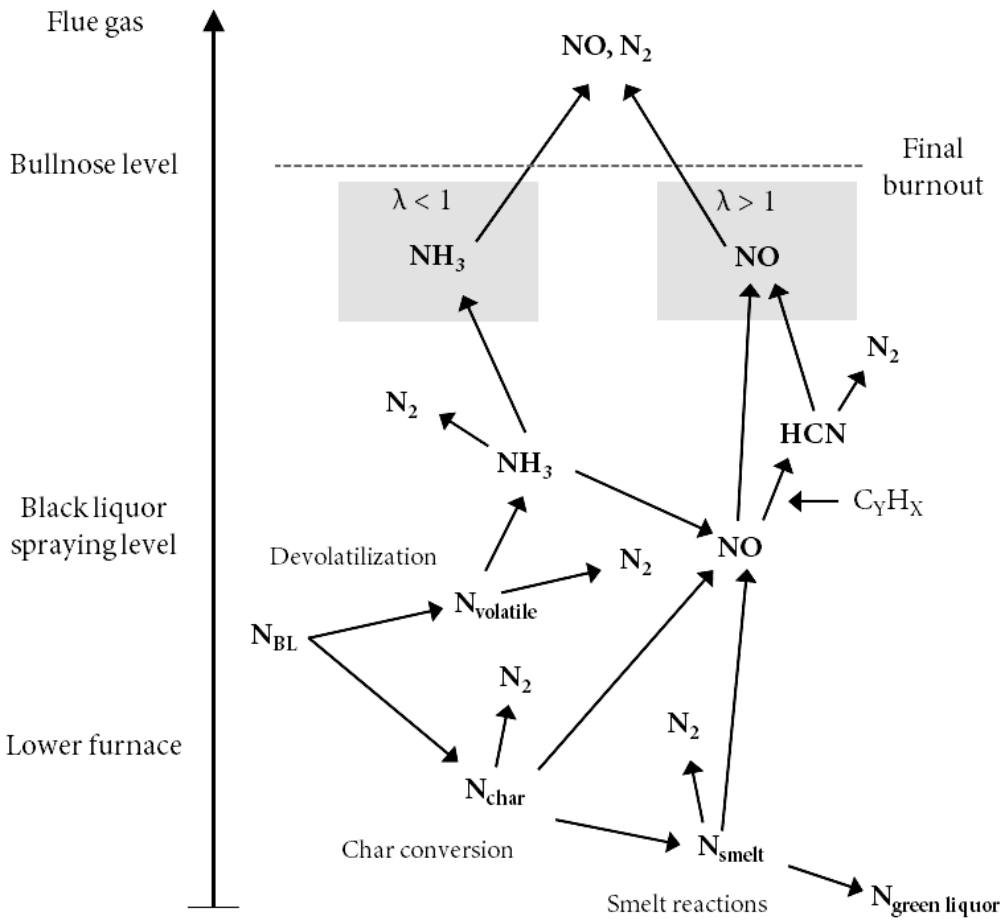
Figure 33. Main fuel-bound nitrogen pathways in the recovery boiler studied, based on this work and the literature.

5.2.3. SO_2 Formation and Recapture

The highest concentrations of sulfur species were measured between the liquor guns. The main sulfur species measured were H_2S, methyl mercaptan, dimethyl sulfide, and SO_2. The concentrations of H_2S and methyl mercaptan were high, around 4000 ppmv each. The distribution of the sulfur gases were in good agreement with the study of pyrolysis gases from black liquor by McKeuogh et al. [89]. Small amounts of CS_2 and COS were also measured between the liquor guns. These have also been shown to be released to a minor extent during pyrolysis of Kraft black liquor by Sricharoenchaikul et al. [91].
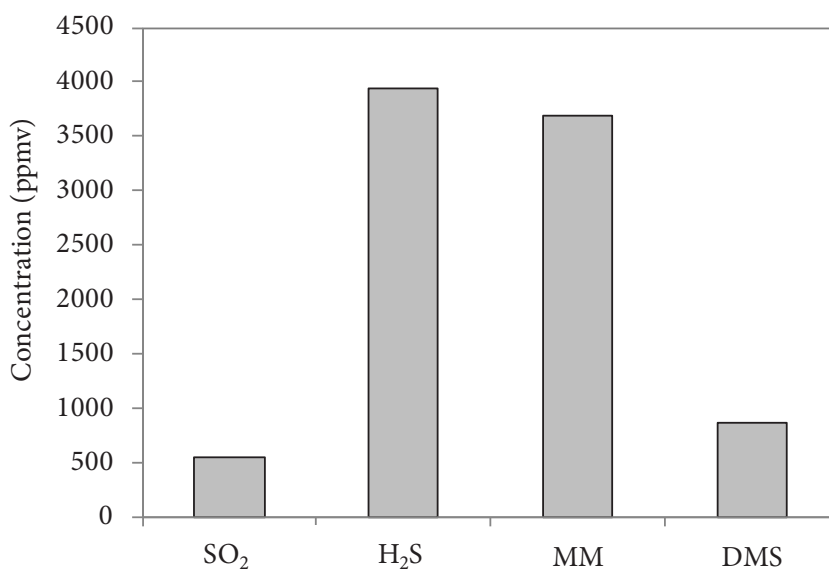
Figure 34. Main sulfur species measured between the liquor guns (port 2). MM = methyl mercaptan and DMS = dimethyl sulfide. Data from **Paper IV**.

The sulfur species measured in ports 6 and 7 are shown in Figure 35. On the oxidizing side, port 6, all sulfur had been captured to form mainly $Na_2SO_4(s,l)$. On the reducing side, SO_2 and H_2S coexisted. This was attributed to the lack of oxygen. Furthermore, the lack of oxygen implies that the sulfur species had not been captured by sodium. However, no TRS gases were detected in the flue gas, and the concentration of SO_2 was below 3 ppmv.
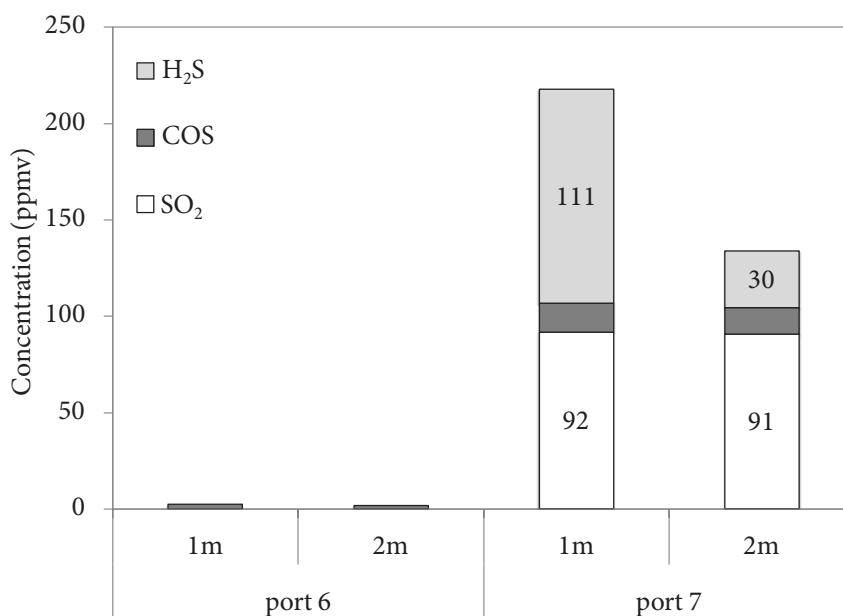
Figure 35. Sulfur species, in wet gases, above the tertiary air level in ports 6 and 7. These ports were located on the back wall in the right and left corners. Figure from **Paper IV**.

5.2.4. Summary of Sulfur Reactions in a Kraft Recovery Boiler

Figure 36 shows the sulfur release and recapture in a modern Kraft recovery boiler furnace burning high dry solids black liquor. The figure is based on the results from the in-furnace measurements presented in this work and on studies found in the literature. Sulfur is mainly released during the devolatilization stage, mostly as H_2S and MM [89][90]. The concentrations of the released H_2S and MM are about equal. Some DMS, DMDS, COS and CS_2 are also formed during the devolatilization stage [89][91]. Hydrogen sulfide is also formed by thermal decomposition of the gaseous organic sulfur compounds [89]. The highest release during pyrolysis occurs at about 500°C [89][95][96]. The sulfur is mainly released during in-flight burning [93][97], but also some sulfur is released from cold spots in the bed [93]. Some sulfur is released during char burning and in smelt reactions by forming H_2S and some COS from Na_2S [92]. Mainly H_2S is formed during the char combustion and smelt

reactions when water vapor is present [92]. Most of the sulfur leaves the boiler as Na_2S in the smelt.

The released sulfur forms SO_2 in the presence of oxygen. This SO_2 will react with Na, NaOH, and Na_2CO_3 in the presence of oxygen to form Na_2SO_4 [94]. If the conditions are sub-stochiometric, H_2S and SO_2 may coexist as high as above the tertiary air level. Eventually, virtually all the gaseous sulfur species will be captured and become a part of the fly ash.
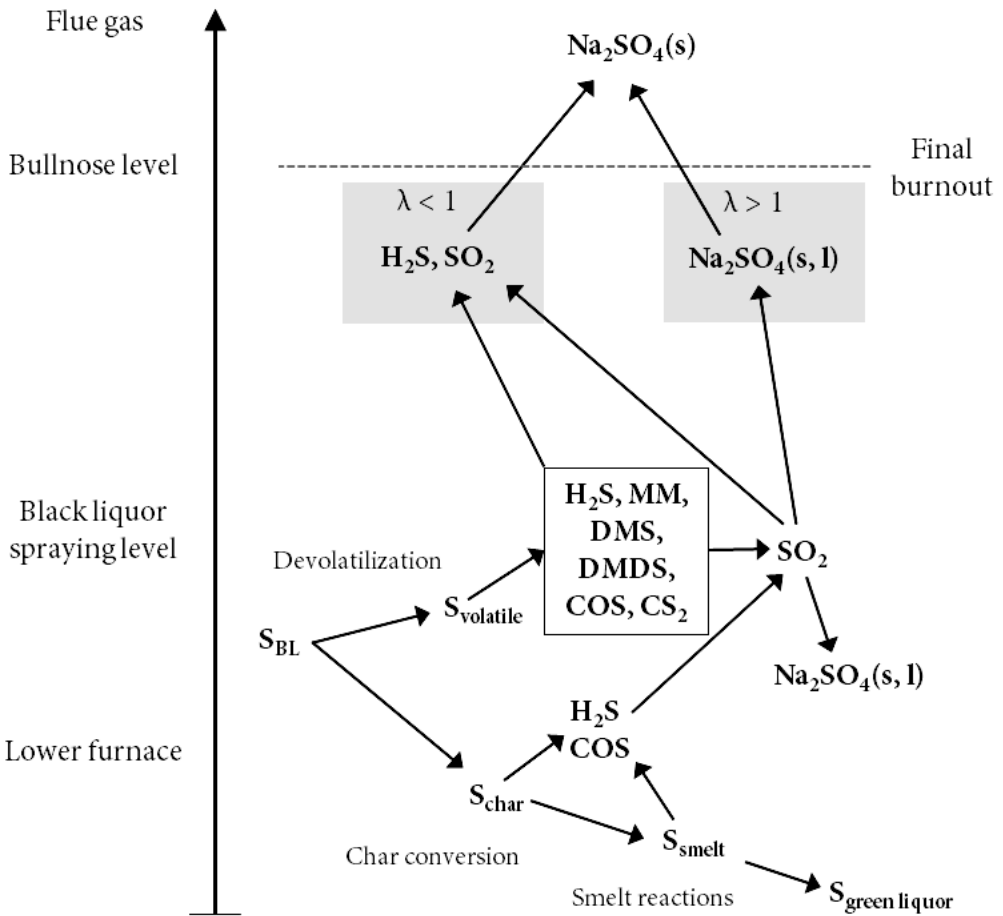
Figure 36. Main sulfur pathways in the Kraft recovery boiler studied. The figure is based on this work and the literature. MM = methyl mercaptan, DMS = dimethyl sulfide, DMDS = dimethyl disulfide.

6. EVALUATION AND DEVELOPMENT OF SO$_3$ MEASUREMENT TECHNIQUES AND MEASUREMENTS IN INDUSTRIAL BOILERS

In **Paper V**, various measurement techniques for SO$_3$ were compared in the Chalmers oxy-fuel test unit, for both oxy-fuel and air-fired conditions. In **Paper VI** a salt method for SO$_3$ measurements was further studied in controlled laboratory conditions. Additionally, an in-situ implementation of the salt method for the measurement of SO$_3$ in flue gases was used in full-scale measurements in both a Kraft and a sulfite recovery boiler. This was done in order to determine the risk of sulfuric acid-induced corrosion in the cold end of these boilers. Discussions of SO$_3$ measurements and measurement techniques generally refer to gaseous H$_2$SO$_4$. The same applies for this work.

6.1. Experimental

6.1.1. Chalmers 100 kW$_{th}$ Oxy-fuel Test Unit

In **Paper V** various SO$_3$ measurement techniques were compared in the Chalmers 100 kW$_{th}$ oxy-fuel test unit. A schematic picture of the Chalmers oxy fuel test unit is shown in Figure 37. Propane was used as fuel during the measurement campaign, and the fuel was doped with SO$_2$ to generate SO$_3$ in the furnace. The measurements were performed in both air-fired conditions and oxy-fuel conditions. The flue gas composition for the two cases in the test unit is shown in Table 7. The SO$_2$ concentration in a dry flue gas was set to 1000 ppmv in the air-fired case and 3000 ppmv in the oxy-fuel case. Most of the measurements were done in port M8, shown in Figure 37. More details of the Chalmers test unit can be found in the article by Andersson et al. [126].

Table 7. Experimental data for tests in the Chalmers oxy-fuel unit.

Test Case	O$_2$ in oxidizer (vol%, d.b.)	Flue gas composition on wet basis			
		O$_2$ (vol%)	SO$_2$ (ppmv)	H$_2$O (vol%)	CO$_2$ (vol%)
Air	21	5.39	890	12	8.6
Oxy-fuel	30	5.39	2440	18.7	~71
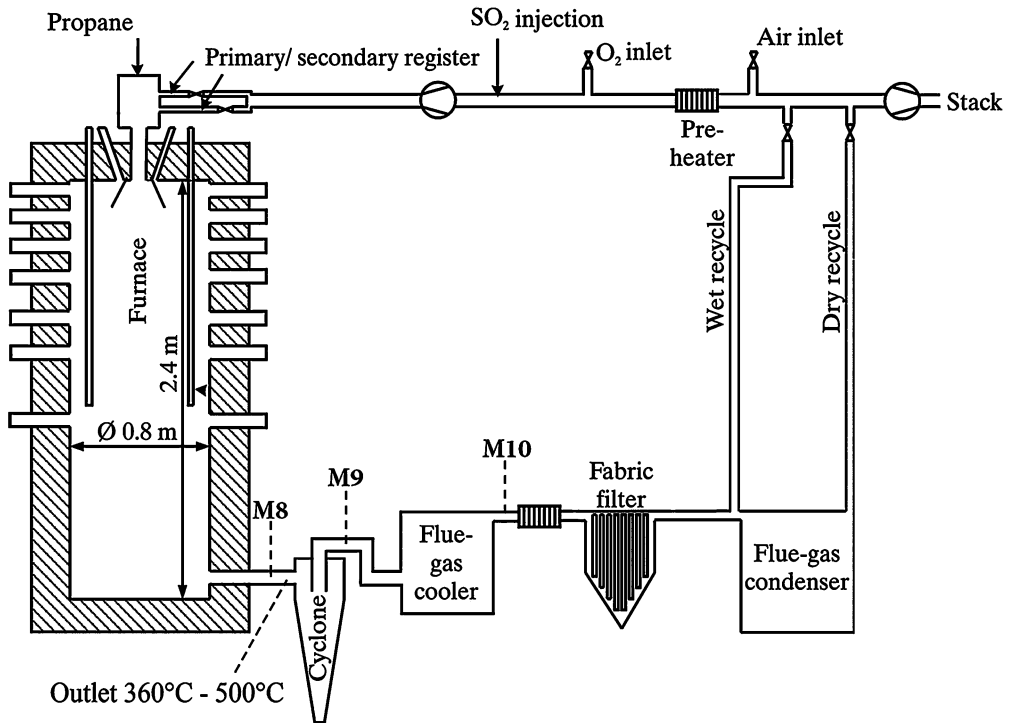
Figure 37. Chalmers 100kW$_{th}$ oxy-fuel test unit.

The furnace wall temperature was logged with 14 thermocouples, and an average furnace wall temperature was determined. Figure 38 shows the average furnace wall temperature during one measurement day. The temperature was not stable during the measurements, because the furnace was shut down overnight. The increasing trend in the furnace temperature had an effect on the conversion of SO$_2$ to SO$_3$ in the furnace; thus, the temperature in the furnace was taken into account when comparing the results. The effect of the furnace temperature has also been reported by Crumley and Fletcher [127]. They observed a higher conversion of SO$_2$ to SO$_3$ at higher flame temperatures.
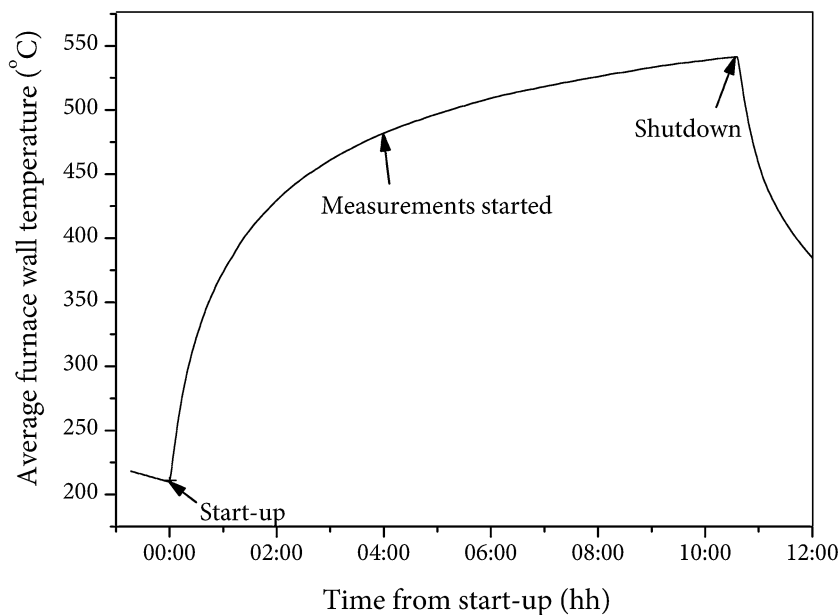
Figure 38. Typical average furnace wall temperature in the Chalmers oxy-fuel unit, calculated from the data obtained from 14 thermocouples in the wall.

6.1.2. SO₃ Measurement Techniques

The SO_3 measurement techniques evaluated were:

1. Controlled condensation method (British Standard BS 1756-4:1977)
2. Isopropanol absorption bottle method (based on EPA Method 8)
3. Salt method
4. Continuous indirect measurement using FTIR
5. Acid dew-point monitor

In methods 1-4 the flue gas was drawn from the outlet of the furnace with an oil-heated probe. The probe was heated to 200°C and had a quartz glass center pipe. A flue gas flow of 1 l/min (STP) was extracted during the measurements, and the measurement time was 30 min.

Controlled Condensation Method

The controlled condensation method is a standard method based on condensing sulfuric acid in a cooling coil, and it has been recommended by many authors [128-130]. The controlled condensation method used here is based on the British standard BS 1756-4:1977. The gases are extracted from the flue gas duct and are cooled between the water and the sulfuric acid dew point temperatures. The cooler used in this study is schematically illustrated in Figure 39. The condensate is collected and analyzed for sulfate ions. An ICS-90 Ion Chromatography system from DIONEX was used to analyze the sulfate in the condensate.
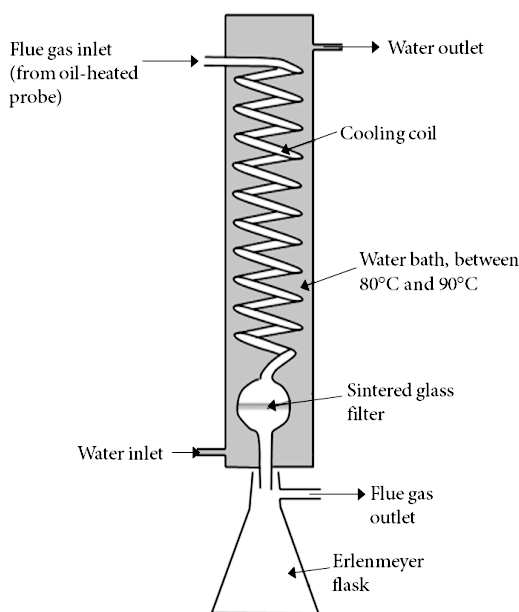
Figure 39. Schematic of the cooler applied in the controlled condensation method.

Isopropanol Absorption Bottle Method

The isopropanol method used in this work is based on the EPA Method 8 [131], with some modifications. The measurement setup used is shown in Figure 40. The flue gas is first led through one impinger bottle, filled with 100 ml of 80 vol% isopropanol. The SO_3 in the flue gas is captured in this bottle, forming sulfate. In addition, two impinger bottles with 100 ml of 3 vol% hydrogen peroxide (H_2O_2) were used in order to determine the SO_2 concentration in the flue gas. The impinger bottles were placed in an ice-water bath. After the measurements the sulfate amount

in the isopropanol and hydrogen peroxide solutions were analyzed for sulfate ions, corresponding to the amount of SO$_3$ and SO$_2$ in the flue gas. The determination of the sulfate concentration was performed by titration with barium perchlorate, using thorin as an indicator, until a color change from yellow to light red was observed.
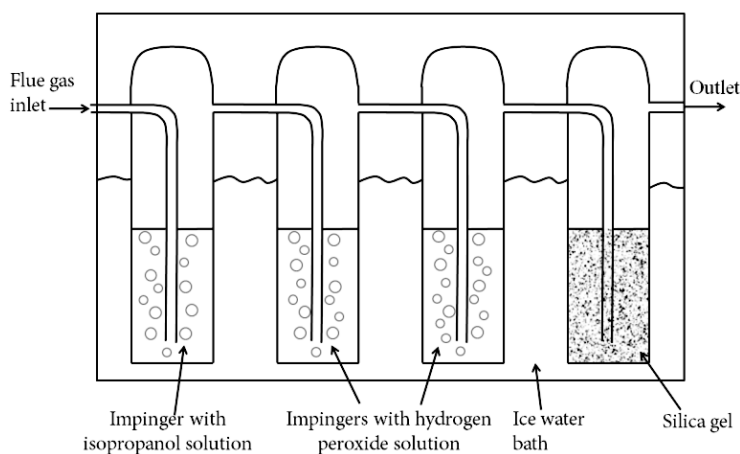
Figure 40. Measurement setup of the isopropanol bottle method for the simultaneous determination of SO$_3$ and SO$_2$.

A laboratory study of the isopropanol method was conducted before the measurement campaign in Chalmers. A gas containing 760 ppmv SO$_2$ in N$_2$ was bubbled through both impinger bottles with 100 ml of 80 vol% and 100 vol% isopropanol. Although the isopropanol solution was purged with N$_2$ after the experiments, a large amount, up to 8%, of the SO$_2$ was captured in the isopropanol. This SO$_2$ was oxidized to sulfate, thus leading to positive measurement bias. The oxidation of SO$_2$ in the isopropanol solution has been pointed out by many authors [128][129][132]. Koebel and Elsener [132] also noticed this effect; they did not recommend analyzing the solution with ion chromatography, since it normally takes too long to get the sample to a laboratory. Cooper and Ferm [128] bubbled air through the bottles after the measurement to force any SO$_2$ from the isopropanol solution. However, Koebel and Elsener [132] observed that this is difficult to achieve in practice. Therefore, the method was modified for this work by keeping the measurement time as short as possible and by bubbling argon through the solution to force any SO$_2$ from the solution. Further, the sulfate analyses were made directly after the measurement, in order to avoid oxidation of SO$_2$ in the isopropanol solution.

Salt Method

The principle of the salt method is to capture gaseous H$_2$SO$_4$ in a salt, forming sulfates of that particular salt. The salt method was first described by Kel´man [133] in the early 1950s. Kel´man used NaCl as salt to capture H$_2$SO$_4$ from flue gases. However, the salt method has not been commonly-used and is a largely unknown method. The salt method using NaCl has been evaluated by Cooper et al. [128][134][135]. They made an attempt to test the salt method using NaCl in the laboratory with known H$_2$SO$_4$ concentrations. However, they encountered problems with condensation of sulfuric acid in the equipment and verification of the true H$_2$SO$_4$ concentration [134][135]. The conclusion was that the method has great potential, but it needs to be studied further.

In the salt method the flue gas is led through a salt plug of NaCl. The salt is heated above the sulfuric acid dew point temperature. If the flue gas contains any H$_2$SO$_4$, it is captured in the salt by forming sulfate. Gaseous H$_2$SO$_4$ reacts with solid NaCl, forming sodium bisulfate (NaHSO$_4$) (Reaction 19) or sodium sulfate (Na$_2$SO$_4$) (Reaction 20). Furthermore, H$_2$SO$_4$ may react with the formed Na$_2$SO$_4$ in Reaction 20 to form NaHSO$_4$ (Reaction 21).

$$NaCl(s) + H_2SO_4(g) \rightarrow NaHSO_4(s) + HCl(g) \qquad (19)$$

$$2NaCl(s) + H_2SO_4(g) \rightarrow Na_2SO_4(s) + 2HCl(g) \qquad (20)$$

$$Na_2SO_4(s) + H_2SO_4(g) \rightarrow 2NaHSO_4(s) \qquad (21)$$
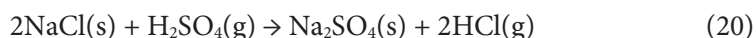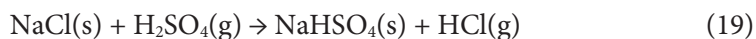
After the measurement, the salt is dissolved in deionized distilled water and the amount of sulfate in the solution is analyzed. The concentration of H$_2$SO$_4$ in the flue gas can be calculated when the amount of flue gas drawn through the salt and the amount of sulfate found in the salt are known.

The salts studied included NaCl, KCl, and CaCO$_3$. In all experiments 1.0 g (on a dry basis) of ultrapure salt (purity 99.999%) was packed into a Teflon tube, as illustrated in Figure 41. The salt tube was heated well above the acid dew point temperature to 200°C. The amount of sulfate formed in the salt was analyzed by dissolving the salt in deionized distilled water and analyzing the solution with ion chromatography (ICS-90 Ion Chromatography system from DIONEX).
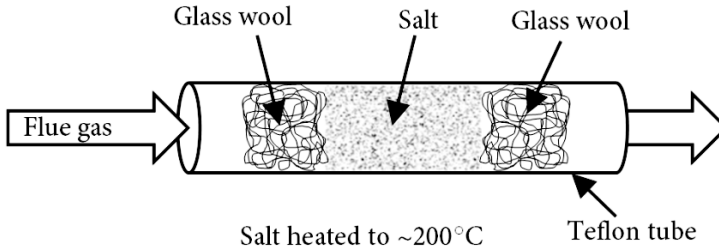
Figure 41. Schematic picture of the salt tube used in **Paper V** and **Paper VI**.

The measurement setup is shown in Figure 42. The SO$_2$ concentration was simultaneously determined by capturing it in 3 vol% of H$_2$O$_2$ in two impinger bottles placed in an ice water bath. The sulfate formed in the H$_2$O$_2$ solution was analyzed by barium-thorin titration.
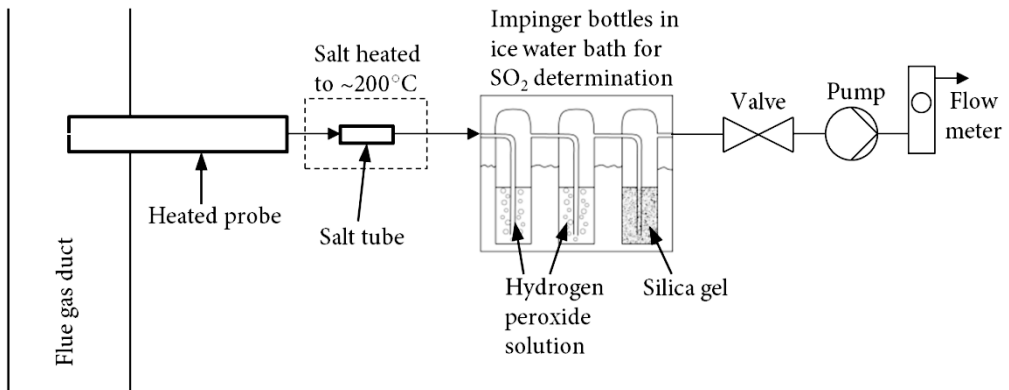
Figure 42. Measurement setup for the salt method used in the Chalmers measurements.

Continuous Indirect Measurement Using an FTIR Analyzer

An attempt was also made to continuously measure SO$_3$ indirectly with an FTIR analyzer. In the sulfation of NaCl and KCl with H$_2$SO$_4$ or SO$_3$, HCl is released. This HCl was measured with an FTIR; the measurement setup is shown in Figure 43. In this method the HCl in the flue gas must be measured in parallel to be able to determine the difference between HCl in the flue gas and HCl released from the salt. In the present work, the flue gas did not contain any HCl.
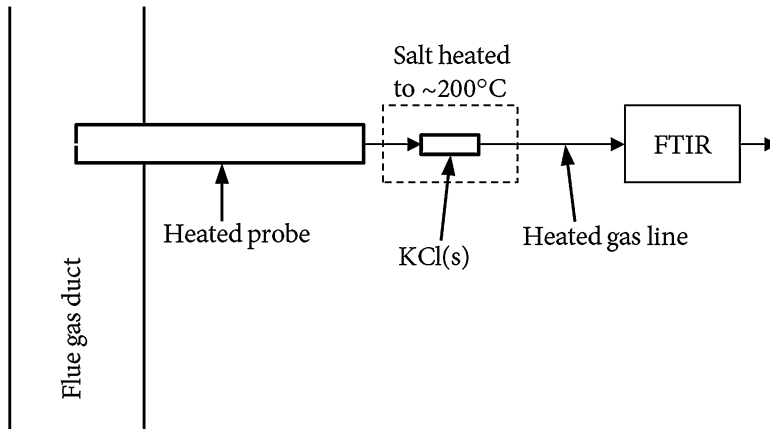
Figure 43. Measurement setup of the continuous indirect measurement of SO$_3$ via HCl.

An expired patent [136] used this same idea. In the patent, NaCl was used to capture SO$_3$ and form HCl. Direct measurement of H$_2$SO$_4$ by FTIR has also been reported; however, problems with calibration and reactions of H$_2$SO$_4$ in the measurement equipment have been encountered [134].

Acid Dew Point Monitor

An acid dew point monitor from Land Instruments, of type ADM 220, was used in the measurements. The acid dew point meter detects the acid dew point by condensing the sulfuric acid on a probe tip. An electrode is located in the probe tip, which detects a current when liquid is condensed on the tip. The probe tip temperature is controlled by cooling it with pressurized air. The probe is inserted into the flue gas channel and heated to the flue gas temperature. The tip temperature is then slowly decreased; as soon as the sulfuric acid is condensed on the tip, a current reading can be observed. According to Land [137], this current reading should be 100 µA. Stuart [138], on the other hand, recommends a current reading of 50 µA. However, readings as high as these were not observed during the measurements, and a current reading of 1 µA was used.

6.1.3. Laboratory Study of the Salt Method

In **Paper VI** different salts´ ability to capture H$_2$SO$_4$ and the selectivity towards H$_2$SO$_4$ in a gas containing both SO$_2$ and H$_2$SO$_4$ were studied. The salts tested were NaCl, KCl, K$_2$CO$_3$, and CaCl$_2$. Sodium chloride was tested based on its use in previous studies [128][133-135]. However, the salt method using NaCl has not been fully verified in controlled conditions. Potassium chloride was tested with the application of using it in a recovery boiler environment that contains a high amount of Na$_2$SO$_4$ that may lead to a positive measurement bias. In this case, the contamination from Na$_2$SO$_4$ could be determined by measuring the amount of sodium found in the salt. Potassium carbonate was chosen, based on the potential to measure H$_2$SO$_4$ and HCl simultaneously by the formation of K$_2$SO$_4$ and KCl. Calcium chloride was examined with the continuous measurement technique in mind. Calcium chloride does not form bisulfate when reacting with the salt, thus the ratio of captured H$_2$SO$_4$ to formed HCl is always 1:2. The released HCl in the sulfation could be measured and converted to H$_2$SO$_4$ concentration. In all experiments 1.0 g of ultrapure salt (on a dry basis) was used. The salts were packed into Teflon tubes as illustrated in Figure 41.

The setup used in the laboratory study is shown in Figure 44. The gas flows of SO$_2$, CO$_2$, O$_2$, and N$_2$ were controlled by Bronkhorst EL-FLOW® flow controllers. The gases were preheated to 200°C before being led to the mixing chamber. Sulfuric acid and water vapor were generated by evaporating a weak sulfuric acid solution (0.0185M). The H$_2$SO$_4$ solution was pumped into the mixing chamber with a syringe pump (Perfusor compact S by Braun), and the solution was evaporated in the mixing chamber. The mixing chamber was located in a tube furnace, which temperature was set to 250°C. The gases were led from the mixing chamber to the salt tube in a Teflon pipe. The second tube furnace was heated to 200°C. Only inert materials were used for the parts where the hot gas was in contact; the mixing chamber was made of glass and the rest of Teflon. An impinger bottle filled with water was located after the second tube furnace in order to collect any H$_2$SO$_4$ not reacted with the salt.

The gas flow through the salt was ~1 l/min (STP) and the measurement time was 30 min. The amount of sulfate formed in the salt was analyzed by dissolving the salt in deionized distilled water and analyzing the solution with ion chromatography. In the laboratory study a Metrosep anion Dual 2 column and a 732 IC detector by

Metrohm were used to determine the sulfate amount in the solutions. To prove the repeatability of the IC analysis, three injections per sample were made. The detection limit corresponding to H$_2$SO$_4$ in a flue gas was determined to be ~0.1 ppmv.
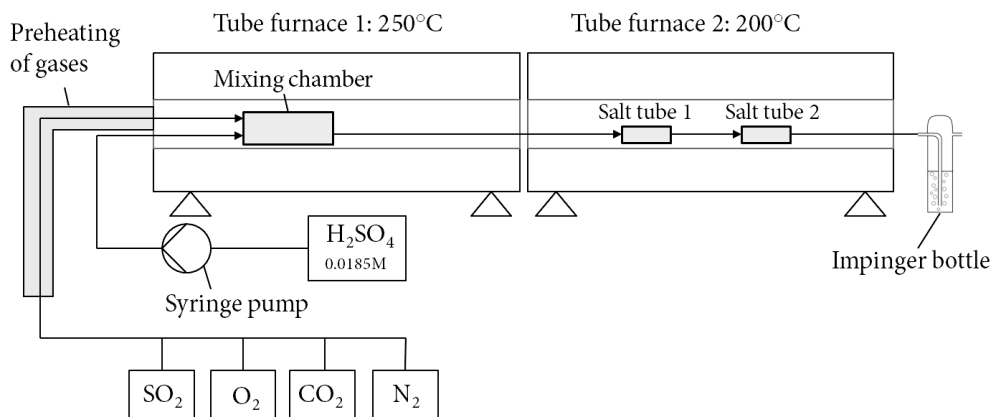
Figure 44. Experimental setup in the laboratory study in **Paper VI**.

The salt method was tested with three different gas compositions. These are shown in Table 8. The concentrations of H$_2$O, CO$_2$, O$_2$, and N$_2$ were the same for all cases and reflect a typical flue gas composition. In the first case, two serial salt tubes were used for testing the salts´ ability to capture H$_2$SO$_4$. In the second case, the salts´ interference from SO$_2$ was studied. In the third case, the selectivity toward H$_2$SO$_4$ was studied in a gas containing both SO$_2$ and H$_2$SO$_4$.

Table 8. Gas composition in the laboratory study for the three cases.

	Case 1	Case 2	Case 3
H$_2$SO$_4$ (ppmv)	50	-	50
SO$_2$ (ppmv)	-	500	500
H$_2$O (vol%)	15	15	15
CO$_2$ (vol%)	14	14	14
O$_2$ (vol%)	4	4	4
N$_2$ (vol%)	67	67	67

6.1.4. Full-Scale Measurements in a Kraft and Sulfite Recovery Boiler

Many recovery boilers suffer from low temperature corrosion. While the reason for this is often unknown, sulfuric acid-induced corrosion is often speculated. An in-situ implementation of the salt method was used to examine whether H_2SO_4 is present in the flue gas duct of a Kraft recovery boiler and a sulfite recovery boiler. The measurements were conducted downstream of the electrostatic precipitator (ESP) in the Kraft recovery boiler. The sulfite recovery boiler was equipped with an ESP for particulate removal and a scrubber for SO_2 removal, and the measurements were conducted between the ESP and the scrubber.

In addition, a measurement campaign was conducted during the start-up procedure of the Kraft recovery boiler. The H_2SO_4 concentration was measured at the bullnose level and at the economizer tubes during this start-up procedure. The measurement locations and the temperature in the measurement points are shown in Figure 45. Heavy fuel oil was burned during the start-up procedure, and the potential of forming SO_3 during this procedure was investigated.
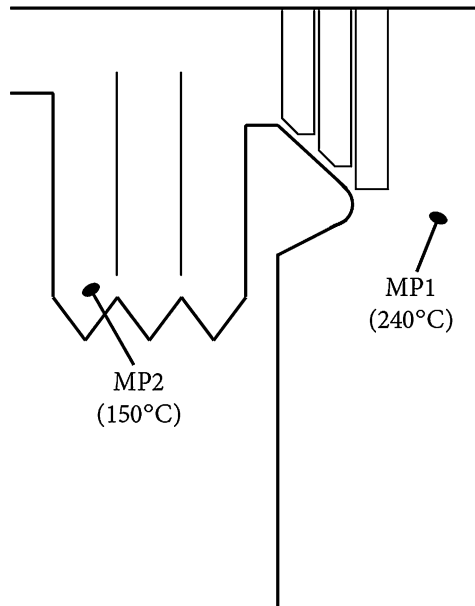
Figure 45. Measurement locations in the Kraft recovery boiler during the start-up procedure.

An in-situ implementation of the salt method was used in these full-scale measurements. The measurement setup is shown in Figure 46. Salt tubes containing 1.0 g of KCl were prepared in the laboratory prior to the measurements. The tube dimensions used were the same as those in the laboratory study. The salt tube was placed in the probe tip of a two-meter-long probe, as illustrated in Figure 46. A particle filter of quartz wool was placed upstream of the salt tube. A fresh particle filter was used in every measurement. The sulfate amounts in both the quartz filter and the salt tube were measured in order to evaluate any H$_2$SO$_4$ captured in the quartz particle filter. Accumulation of fly ash in the particle filter may lead to that a part of the H$_2$SO$_4$ is captured in the filter, leading to too low H$_2$SO$_4$ values [139][140]. The probe tip was facing in the opposite direction of the flue´s flow to minimize particle intake in the filter. A thermocouple was placed next to the salt, and after the salt temperature had reached the flue gas temperature, the measurement started. The flow through the salt was 1 l/min (STP) and the measurement time was approximately 20 minutes.
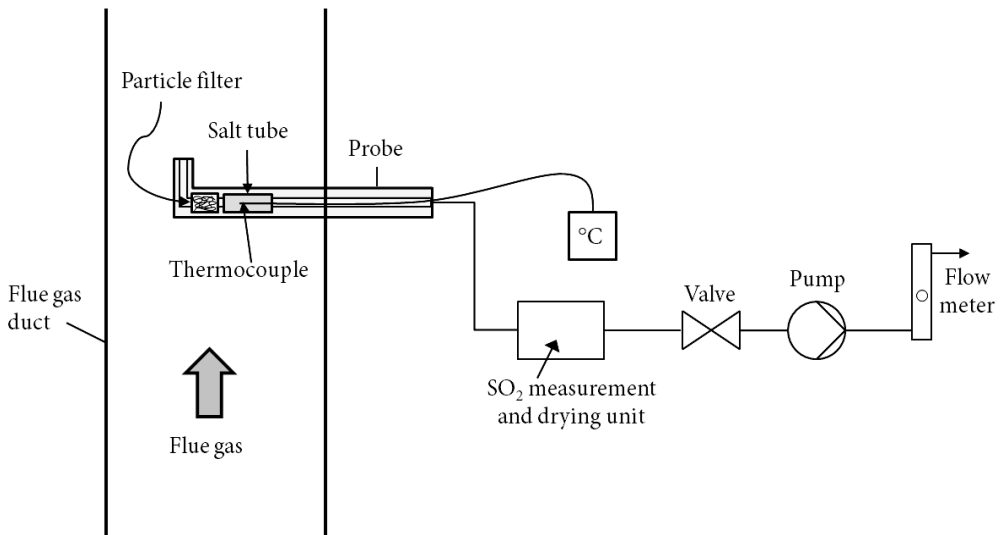
Figure 46. In-situ measurement setup in the recovery boiler measurements.

6.2.   Results - SO$_3$ Measurement Techniques and Measurements

In **Paper V,** various SO$_3$ measurement techniques were compared in the Chalmers oxy-fuel test unit, in both oxy-fuel and air-fired conditions. In **Paper VI,** the salt method, using four salts, was further studied and evaluated in controlled laboratory conditions. In addition, an in-situ implementation of the salt method was used in full-scale measurements in both a Kraft and a sulfite recovery boiler. This was done in order to determine the risk of sulfuric acid-induced corrosion in the cold end of these boilers.

6.2.1. Comparison of SO$_3$ Measurement Techniques in the Chalmers 100 kW$_{th}$ Test Unit

The SO$_3$ concentrations measured at the outlet of the Chalmers oxy-fuel test unit, measurement port M8, with the controlled condensation method and with the salt method, using NaCl, KCl, and K$_2$CO$_3$, are shown in Figure 47. The values obtained during the air-fired case (a) and oxy-fuel case (b) are plotted as a function of time from start-up of each measurement. The average furnace temperature is also plotted. The figure clearly shows that as the temperature in the furnace rises, the SO$_3$ formation increases. Thus, the average furnace wall temperature must be taken into account when comparing the results.

The salt method using KCl and NaCl gave similar results compared to the controlled condensation method, when the rising trend in the SO$_3$ concentration is taken into account. In the oxy-fuel case, with a higher SO$_2$ concentration in the feed gas, the rising trend was even more apparent. In this case, the SO$_3$ concentration increased from 37 ppmv after 4 h from start-up to 96 ppmv after 14 h from start-up. The measured SO$_3$ concentration was overpredicted when using K$_2$CO$_3$ in the salt method. This was believed to be due to the reaction between SO$_2$ and K$_2$CO$_3$, leading to a false reading of SO$_3$. This was confirmed in the laboratory study discussed in **Paper VI**, which showed that a part of the SO$_2$ is also captured in K$_2$CO$_3$, thus leading to a false reading.
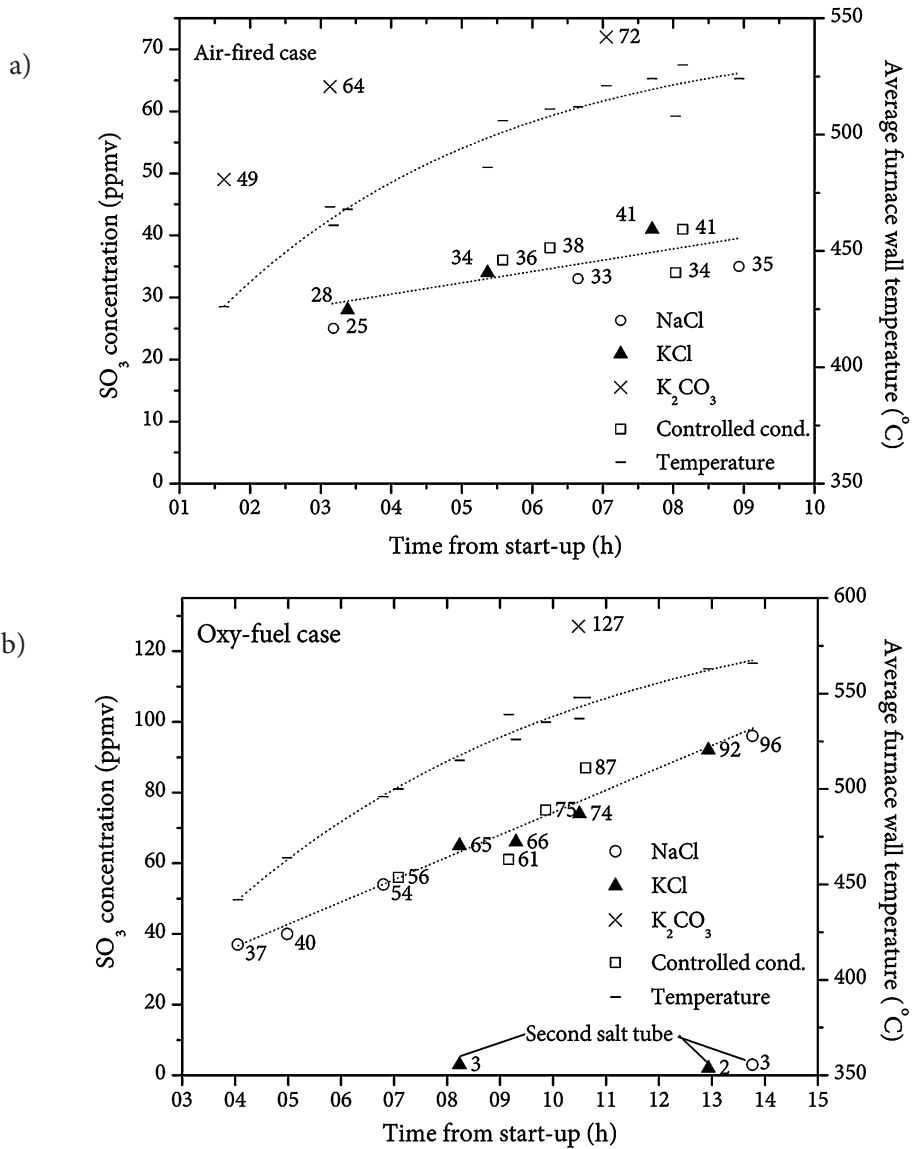
Figure 47. Comparison of the measured SO_3 concentration, on a wet basis, using the controlled condensation method and the salt method for (a) the air-fired case and (b) the oxy-fuel case. Salts used include NaCl, KCl, and K_2CO_3. The measurements are conducted at the outlet of the furnace, port M8. The average temperature of the furnace wall is also plotted. Data from **Paper V**.

A second salt tube was used in some of the trials with the salt method, using KCl and NaCl, to determine whether one salt tube is enough to capture all SO_3 or whether SO_2 is interfering with the measurement. In the oxy-fuel case, 2-3 ppmv sulfur, as

SO$_3$ or SO$_2$, was captured. Whether this was a SO$_3$ slip from the first salt tube or a reaction between SO$_2$ and the salt was unclear. This was studied further in the laboratory study of the salt method in **Paper VI**.

Isopropanol Method

The results obtained with the isopropanol method for the air-fired and oxy-fuel cases are shown in Table 9. Measured SO$_3$ values using the isopropanol method were similar to those observed for the controlled condensation and salt methods (using KCl and NaCl). However, a large amount of SO$_2$ was captured in the isopropanol solution in the first measurement. If this SO$_2$ is oxidized to sulfate in the solution, it will lead to significant errors in the SO$_3$ values. Oxidation of SO$_2$ may occur in situations such as during transportation of the samples to a laboratory. The SO$_2$ captured in the isopropanol was determined by measuring the SO$_2$ after the isopropanol solution and by comparing this value to the SO$_2$ found in the flue gas. The oxidation of SO$_2$ in the isopropanol was also observed after titration, when the color changed back from light red to yellow, indicating that sulfate was formed in the solution. As a result, argon was bubbled through the isopropanol solution in order to force out any SO$_2$ from the solution; however, significant amounts of SO$_2$ still remained in the isopropanol solution. Therefore, the isopropanol method cannot be recommended.

Table 9. Measurement data obtained with the isopropanol method. Data from **Paper V**.

Case	Average furn. wall temp.	SO$_3$ (ppmv)	Sampling time	Purging with argon	SO$_2$ measured (in H$_2$O$_2$ solution) (ppmv)	SO$_2$ captured in the isopropanol (ppmv)
Air	541°C	45	30 min	-	350	540
Air	544°C	34	20 min	10 min 1.5 l/min	570	320
Oxy-fuel	520°C	49	20 min	15 min 1.5 l/min	2160	280

Acid Dew Point Meter

While the instructions for the acid dew point meter claimed that the acid dew point is reached at a current reading of 100 µA, this current reading was not achieved in this work; thus a current reading of 1 µA was used instead. Measuring at 1 µA should result in an acid dew point temperature higher than the actual acid dew point temperature. However, the calculated SO$_3$ concentration for the measured acid dew point resulted in too low concentrations in measurement port M9. The correlations of both Verhoff and Banchero [106], as well as the data from Bolsatis and Elliott [107], were used. Furthermore, the measured dew points seemed to be more accurate at flue gas temperatures just above the acid dew-point temperature, than at higher flue gas temperatures. Higher acid dew point temperatures were measured after the flue gas cooler (port M10) than before it (port M8), although, a large part of the H$_2$SO$_4$ condensed in the cooler and in fact the acid dew point temperature should be lower in M10.

6.2.2. Continuous Indirect Measurement of SO$_3$ with an FTIR

The indirect continuous measurement of SO$_3$ by measuring the release of HCl in the sulfation of KCl is shown in Figure 48; it shows the measured HCl and the calculated SO$_3$ concentration. Converting the HCl concentration to SO$_3$ concentration was estimated by the formation of bisulfate and sulfate when SO$_3$ reacts with KCl. The difference between these two lies in the stoichiometries; in bisulfate formation the SO$_3$ to HCl ratio is 1:1, whereas in sulfate formation the SO$_3$ to HCl ratio is 1:2. A blank test conducted with no SO$_3$ in the flue gas, showed an HCl concentration of approximately 20 ppmv downstream of the KCl tube. This 20 ppmv of HCl was subtracted from the total HCl concentration when the SO$_3$ concentration was determined. The SO$_3$ concentration before the indirect measurements was 35 ppmv, measured with the salt method using NaCl. This correlates with the bisulfate curve in Figure 48. Hiroshi et al. [136] studied the same principle with NaCl as salt in the temperature range of 200-400°C. They claimed that at 200°C approximately half of the SO$_3$ was captured and formed HCl, and that the temperature must be maintained between 300-400°C in the salt in order to capture all SO$_3$. However, the lower HCl release at 200°C may be due to the formation of NaHSO$_4$ instead of Na$_2$SO$_4$.

The oscillation in the HCl concentration was synchronized with the temperature of the salt tube. The temperature in the salt tube varied between 180°C and 220°C, due to temperature regulation in the heating tape. The temperature and HCl oscillations imply that the reaction between SO_3 and KCl was switching between formation of bisulfate and sulfate. At 10:30 h from start-up, the SO_2 was switched off and the HCl concentration dropped; however, the oscillation continued. This may be due to the reactions between $KHSO_4$ and KCl that form K_2SO_4 and HCl. The indirect continuous measurement of SO_3 showed great potential. However, more work is needed to identify the uncertainties in the method and the stoichiometry of the reactions at different temperatures.
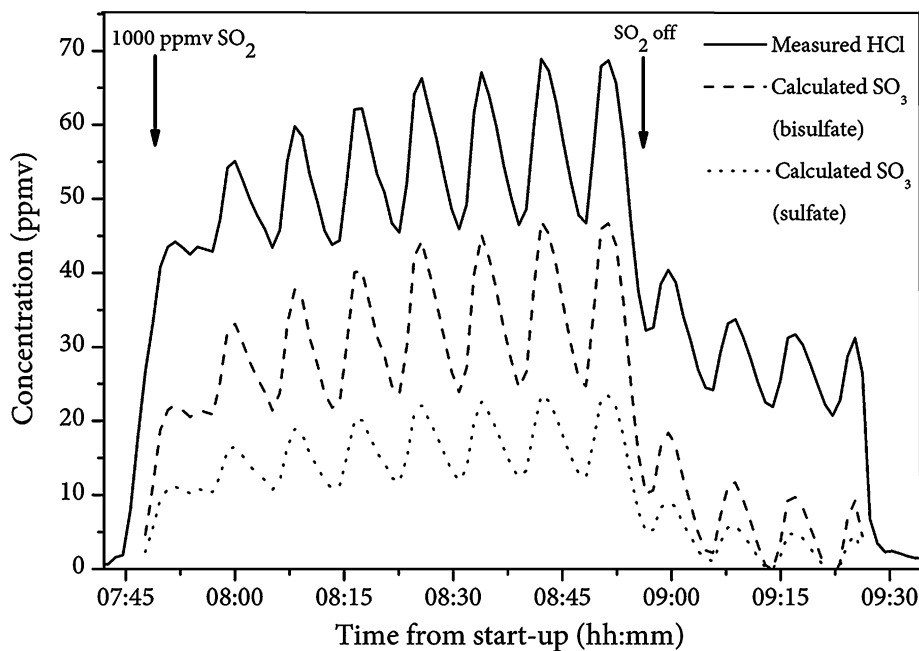
Figure 48. The measured HCl concentration downstream of the KCl salt tube and the calculated SO_3 concentration from the HCl measurement, reacting to both potassium bisulfate and sulfate. Figure from **Paper VI**.

6.2.3. Laboratory Study of the Salt Method Using Various Salts

The laboratory study was conducted with gaseous H_2SO_4 instead of SO_3. This was motivated by the rapid reaction of water and SO_3 to form H_2SO_4. The equilibrium conversion and the time to reach equilibrium for relevant flue gas conditions are shown in Figure 49 a and b. The Chemkin software was used in the calculations, which were conducted with the rate expression of Lovejoy et al. [102] and an initial SO_3 concentration of 50 ppmv. As the figures show, equilibrium is reached in a fraction of a second, with the main gas being H_2SO_4. Thus, when referring to SO_3 measurement techniques, it is in fact gaseous H_2SO_4 that is measured.
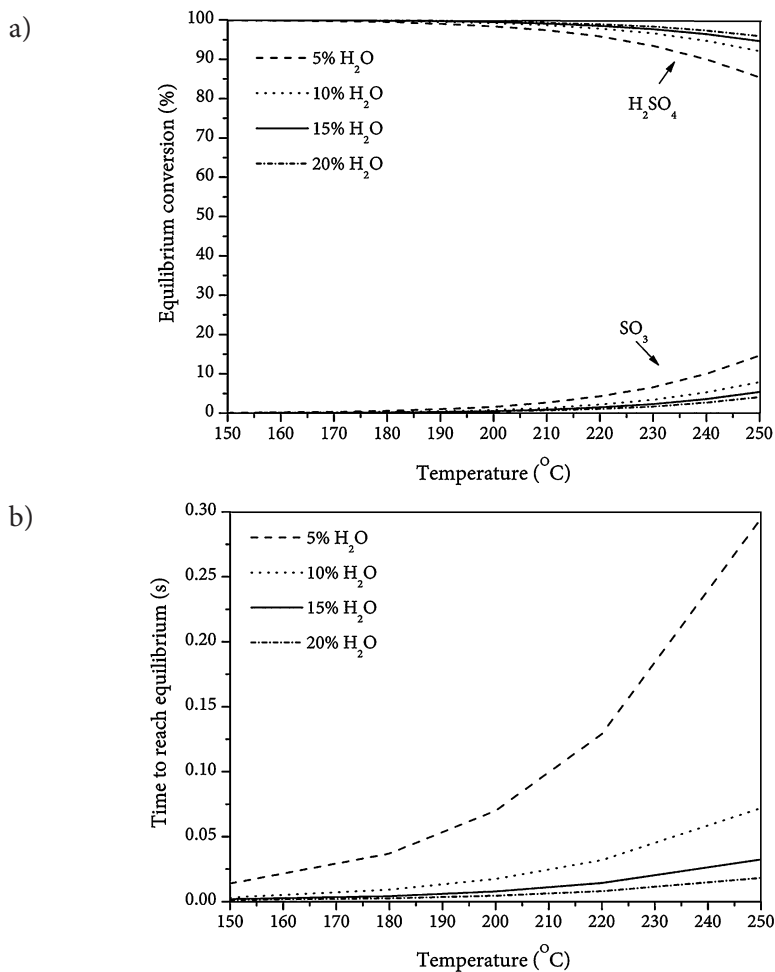
Figure 49. a) Equilibrium concentrations of SO_3 and H_2SO_4, and b) the time required for the SO_3-H_2SO_4 system to reach equilibrium, as a function of temperature and H_2O concentrations of 5, 10, 15, and 20 vol%. Figures from **Paper VI.**

The abilities of the salts to capture H$_2$SO$_4$ in a synthetic flue gas containing 50 ppmv H$_2$SO$_4$ (Case 1) are shown in Figure 50; it illustrates that all of the salts were able to capture all of the H$_2$SO$_4$. No sulfur was found in the second salt tube or in the impinger bottle. The H$_2$SO$_4$ concentration was stable, as evidenced by the small standard deviation. Furthermore, no condensation of H$_2$SO$_4$ was observed in the measurement system.
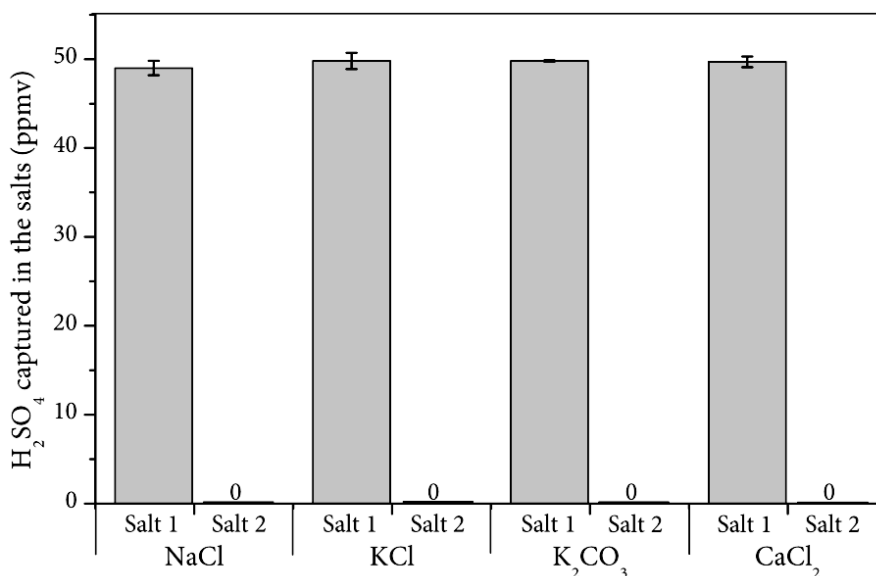
Figure 50. Average H$_2$SO$_4$ concentration measured with the various salts in a synthetic flue gas containing 50 ppmv H$_2$SO$_4$ in the absence of SO$_2$ (Case 1). The standard deviation is determined from a minimum of three measurements and three IC analyses of each measurement. Figure from **Paper VI.**

The results from Case 2 are shown in Figure 51. Here, the synthetic flue gas contained 500 ppmv SO$_2$ but no H$_2$SO$_4$. Both NaCl and KCl performed well with respect to SO$_2$ capture. Only 0.2% of the SO$_2$ was captured in these salts, which is equivalent to 1 ppmv SO$_2$ in the feed gas. A considerable amount (about 20%) of SO$_2$ was captured in the K$_2$CO$_3$ salt tube, equivalent to 100 ppmv SO$_2$ in the feed gas. Calcium chloride captured about 4%, which is equivalent to 20 ppmv SO$_2$ in the feed gas. Matsuda et al. [141] also showed a higher degree of sulfation of CaCl$_2$ by SO$_2$ compared to sulfation of NaCl and KCl, in the temperature range of 350-750°C. Boonsongsup et al. [142] showed slow reaction rates for sulfation of NaCl by SO$_2$, in the temperature range of 400-600°C. Furthermore, Sengeløv et al. [143] studied the

sulfation of KCl with SO$_2$ in the temperature range of 400-750°C and noticed a slow sulfation rate at temperatures below 600°C. However, at temperatures above 600°C the sulfation increased considerably.
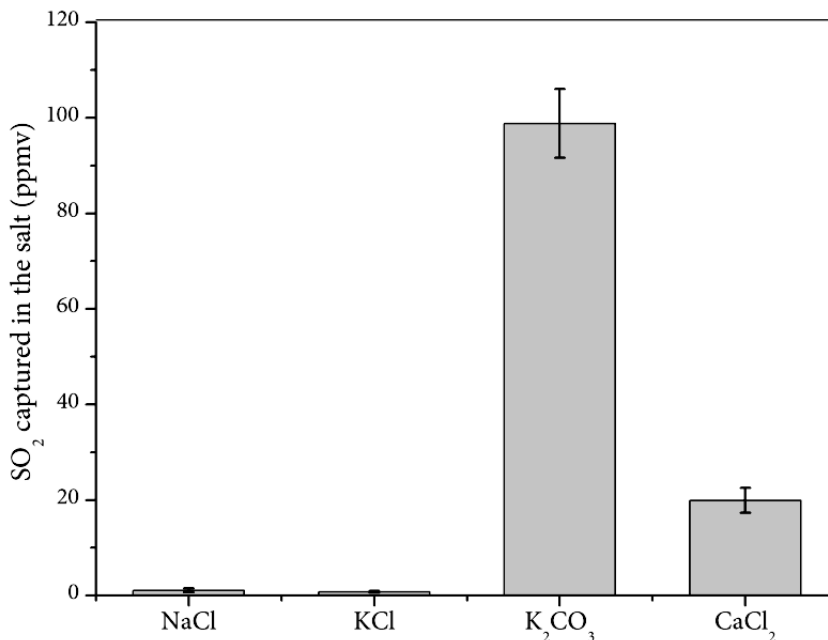
Figure 51. Average SO$_2$ captured in the salts, presented as ppmv concentration in the synthetic feed gas. The SO$_2$ concentration in the synthetic flue gas was 500 ppmv and no H$_2$SO$_4$ was present (Case 2). The standard deviation is determined from a minimum of three measurements and three IC analyses of each measurement. Figure from **Paper VI.**

The selectivity of the salts toward H$_2$SO$_4$ capture in a gas containing both SO$_2$ and H$_2$SO$_4$ was studied in Case 3. As expected, both NaCl and KCl showed high selectivity toward H$_2$SO$_4$, as illustrated in Figure 52. A large amount of SO$_2$ was captured in K$_2$CO$_3$; thus, K$_2$CO$_3$ cannot be used to determine H$_2$SO$_4$ in a gas containing SO$_2$. Surprisingly, SO$_2$ did not seem to react with CaCl$_2$ in this case, although a considerable amount of SO$_2$ was captured when only SO$_2$ was present in Case 2. The reason for this is unknown and, therefore, only KCl and NaCl can be recommended for the measurement of gaseous H$_2$SO$_4$ in flue gas conditions.
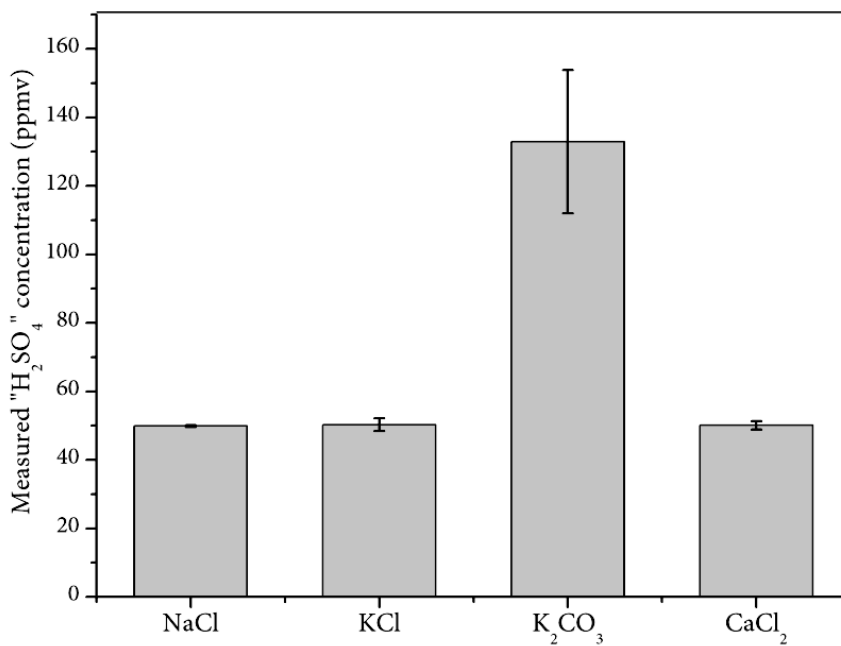
Figure 52. "H₂SO₄" concentration measured in a synthetic flue gas containing 50 ppmv H₂SO₄ and 500 ppmv SO₂ (Case 3). The standard deviation is determined from a minimum of three measurements and three IC analyses of each measurement. Figure from **Paper VI.**

6.2.4. SO$_3$/H$_2$SO$_4$ Measurements in the Cold End of a Kraft and Sulfite Recovery Boiler

Neither H$_2$SO$_4$ nor SO$_2$ was detected in the flue gas during normal operation in the Kraft recovery boiler flue gas duct; thus, no risk of sulfuric acid-induced corrosion existed. In the sulfite recovery boiler, the SO$_2$ concentration before the scrubber was high and varied between 1000 and 1400 ppmv in a dry gas. The results are shown in Table 10. The flue gas temperature was on average 152°C. The high SO$_2$ concentration could indicate that some H$_2$SO$_4$ is also present in the cold end; however, the H$_2$SO$_4$ concentration was less than 1 ppmv. The low H$_2$SO$_4$ is most likely due to the reaction of H$_2$SO$_4$ with the fly ash forming sulfates and bisulfate.

Table 10. Sulfur dioxide and H$_2$SO$_4$ measured in a Kraft and sulfite recovery boiler. Data from **Paper XIV**.

	SO$_2$ (ppmv, dry)	H$_2$SO$_4$ (ppmv, dry)
Kraft recovery boiler	<2	0
Sulfite recovery boiler	1000-1400	<1

The H$_2$SO$_4$ concentration was also measured during the start-up of a Kraft recovery boiler. Heavy fuel oil was combusted during the start-up. The conditions were challenging, due to a heavily-sooting flame and a highly-diluted flue gas. The excess O$_2$ in the flue gas measured 19.5 vol%, leading to expectations of low H$_2$SO$_4$ concentrations. Sulfur dioxide in the flue gas was 36-38 ppmv on a wet basis during the measurements. The sulfur content in the quartz particle filter was analyzed, in order to determine whether any H$_2$SO$_4$ was captured in the quartz filter. The sulfur concentration measured in the quartz particle filter and in the KCl salt tube is shown in Figure 53. While some H$_2$SO$_4$ was measured, the concentrations were low due to the highly-diluted flue gas. No significant amount of sulfur was found in the particle filter. The 1.4 ppmv H$_2$SO$_4$ measured in MP1, located below the superheater tubes, corresponds to a 4% conversion of SO$_2$ to H$_2$SO$_4$. This is in line with the empirical conversion at high O$_2$ concentration reported by Bennett [31].
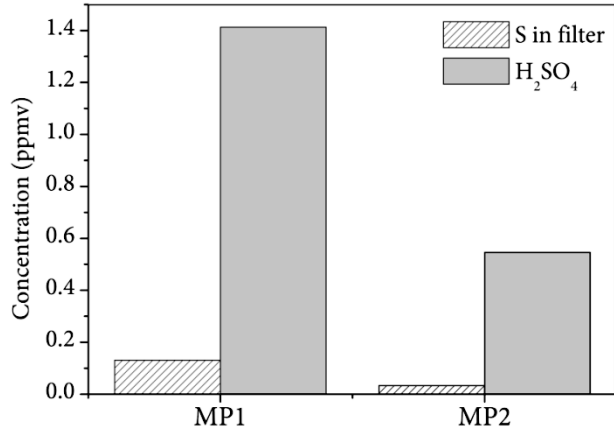
Figure 53. Measured H$_2$SO$_4$ concentration in the flue gas and the amount of sulfur found in the particle filter, presented in ppmv in wet flue gases. MP1 was located just below the superheaters and MP2 was located close to the economizer tubes. Figure from **Paper VI**.

7.   CONCLUSIONS

The fate of fuel-bound nitrogen and sulfur was studied in industrial boilers combusting biomass fuels. In-furnace measurements were conducted in a BFB boiler fired with various biomass fuel mixtures and in a Kraft recovery boiler. The reduction of reactive nitrogen in the BFB boiler was also studied with the Chemkin software using a detailed reaction mechanism. Sulfur trioxide measurement techniques were evaluated in the Chalmers oxy-fuel unit, and a salt method was further studied in the laboratory. An in-situ implementation of the salt method was used in field measurements, in both a sulfite and a Kraft recovery boiler, to study the risk of sulfuric acid induced corrosion in the flue gas duct of these boilers.

The full-scale measurement campaign in the BFB boiler gave new insights into nitrogen species in the furnace and freeboard, during co-combustion of different biofuel mixtures. The in-furnace measurements of nitrogen species showed that NO, NH_3, HCN, and HNCO coexist in the lower furnace. The main intermediate nitrogen species measured 2 m above the fuel inlet was NH_3, which accounted for over 60% of the TFN species. Some HNCO was also quantified at this measurement location, and accounted for 1% of the total nitrogen species measured. No significant reduction of TFN to N_2 was observed in the lower furnace; above the fuel inlet the fuel-N conversion to NO, NH_3, and HCN was equivalent to 78-96% for all the co-combustion cases. A drastic reduction of the TFN species was observed when moving above the secondary air level; the fuel-N conversion to NO, NH_3, and HCN was 27-31% for all of those co-combustion cases. The main TFN species between the secondary and tertiary air levels was NH_3, however, no significant reduction was seen between the two air levels. A further reduction occurred when going above the tertiary air level. The final reduction of fuel-N to N_2 was over 90%, although only air staging was applied to minimize the emissions of NO_X.

The significant reduction observed over the secondary and tertiary air levels in the in-furnace measurements was modeled by using the Chemkin software. A reactor system consisting of plug flow reactors was used to describe the mixing effect of the combustion gases with the air jet. CFD calculations were performed to obtain reactor parameters such as gas entrainment and jet velocity. The gas composition measured above the fuel inlet was used as input in the modeling. The mixing effect was shown to have a big impact on the results. Gradual dilution of the air jet with the

combustion gases in the simulations showed a good agreement with the measured values of TFN species at the secondary air level and the final NO levels. Direct mixing of combustion gases and combustion air, on the other hand, yielded final NO levels that were three times higher than the measured value.

The biofuels combusted in the BFB boiler all had high SO_2 capturing potential, i.e., high Ca/S ratios; therefore, low SO_2 emissions were observed for all cases. When bark, sludge, and SRF were co-combusted, some SO_2 was also present in the flue gases. The sulfur in the fuel played an important role in sulfating alkali chlorides, as observed when chlorine was in the fuel mixture, when SRF was co-fired. Most of the chlorine was found as gaseous HCl in the measurements, which implies that sulfation of alkali chlorides occurred. This was seen in the furnace measurements as a rise in the HCl concentration and a decrease in SO_2 when moving up in the freeboard. However, a complete sulfation did not occur and some alkali chlorides were found in the sub-micron particles. Additional capture of SO_2 and HCl was observed in the baghouse filter. This work showed the benefits of co-combustion of fuels with different ash properties. Despite the high sulfur content and low heating value of sludge, the ash components in the sludge, such as sulfur and aluminosilicates, play an important role. The sulfur has the positive effect of sulfating alkali chlorides when chlorine is present in combustion.

The measurement campaign at the Kraft recovery boiler resulted in valuable data regarding the nitrogen and sulfur species in the furnace. The main nitrogen species at reducing conditions was NH_3. Considerable amounts of HCN were measured at the black liquor spraying level. This HCN is believed to be formed via re-burning of NO, since HCN has not been found as a pyrolysis species in earlier laboratory studies. The measurements between the liquor guns showed that the main sulfur intermediates were H_2S and methyl mercaptan. This is consistent with laboratory studies of pyrolysis gases in the literature. An interesting trend was observed on the right and left sides of the back wall; reducing conditions prevailed on the right side, whereas on the left side the conditions were oxidizing. On the oxidizing side all the sulfur had been captured to form Na_2SO_4, and NO was the main TFN species. However, on the reducing side both SO_2 and H_2S coexisted and had not yet been captured in the ash. In addition, NH_3 was the main TFN species on the reducing

side. In the flue gases, the only TFN species measured was NO and the concentrations of SO_2 and TRS species were virtually zero.

In the evaluation of SO_3 measurement techniques at the Chalmers oxy-fuel unit, the controlled condensation and salt method, using KCl and NaCl, proved to be reliable in both oxy-fuel and air-fired conditions. The salt method was further studied in the laboratory by using different salts to capture H_2SO_4. Both KCl and NaCl proved to be suitable for the measurement of H_2SO_4, without a significant interference from SO_2. Using K_2CO_3 as the salt resulted in a large interference from SO_2. Calcium chloride also captured some SO_2 in a synthetic flue gas without H_2SO_4. Surprisingly, when both SO_2 and H_2SO_4 were present, SO_2 did not seem to interfere with the H_2SO_4 measurement for $CaCl_2$. Because the reason for this is unknown, only KCl and NaCl in the salt method are to be preferred. Continuous indirect measurement of H_2SO_4 by measuring the HCl release (with an FTIR) in the sulfation of KCl with H_2SO_4 was also examined. The method showed great potential, however, this method needs further development, i.e., it is not clear to what extent sulfate or bisulfate is formed in the sulfation.

An in-situ implementation of the salt method using KCl was used in field measurements, in which the presence of sulfuric acid in the flue gas in both a Kraft and a sulfite recovery boiler was studied. The in-situ method proved to be an easy method to use in field measurements, since the salt tubes can be made in advance in the laboratory and are easy to store after the measurement. Further, no heated probe or heaters for the salt are required when using the in-situ implementation. These measurements showed that corrosion due to sulfuric acid condensation during normal operation did not occur. The SO_2 level before the scrubber in the sulfite recovery boiler was above 1000 ppmv; however, no H_2SO_4 was detected in the flue gas. This implies that all the H_2SO_4 formed in the combustion had reacted with the ash particles to form sulfates.

8. REFERENCES

[1] EC 2009a - Renewable Energies Directive, 2009/28/EC of 23 April 2009.

[2] Official Statistics of Finland (OSF): Energy supply and consumption [e-publication]. ISSN=1799-7976. 1st Quarter 2013. Helsinki: Statistics Finland [referred: 25.6.2013]. Access method: http://www.tilastokeskus.fi/til/ehk/2013/01/ehk_2013_01_2013-06-20_tie_001_en.html.

[3] Official Statistics of Finland (OSF): Production of electricity and heat [e-publication]. ISSN=1798-5099. 2011. Helsinki: Statistics Finland [referred: 25.6.2013]. Access method: http://tilastokeskus.fi/til/salatuo/2011/salatuo_2011_2012-10-16_tie_001_en.html.

[4] Directive 2010/75/EU of the European Parliament and of the Council, 24 November 2010 on industrial emissions (integrated pollution prevention and control)

[5] Saastamoinen J., Richard J.: *Drying, Pyrolysis and Combustion of Biomass Particles*, Research in Thermochemical Biomass Conversion, 1988, ISBN 978-94-009-2737-7, pp 221-235.

[6] Miller J., Bowman C.: *Mechanism and modeling of nitrogen chemistry in combustion*, Prog. Energy Combust. Sci., 1989, 15(4), pp 287-338.

[7] Zel'dovich Y. B.: *The oxidation of nitrogen in combustion and explosions*. Acta Physicochem USSR, 1946, 21, pp 577–628.

[8] Glarborg P., Jensen A. D., Johnsson J. E.: *Fuel nitrogen conversion in solid fuel fired systems*. Progress in Energy and Combustion Science, 2003, 29(2) pp 89-113.

[9] Fenimore C. P.: *Formation of nitric oxide in premixed hydrocarbon flames*, Symposium (International) on Combustion, 1971, 13(1), pp 373–380.

[10] Moskaleva L. V., Lin M. C.: *The spin-conserved reaction $CH + N_2 \rightarrow H + NCN$: A major pathway to prompt NO studied by quantum/statistical theory calculations and kinetic modeling of rate constant*. Proc Combust Inst, 2000, 28(2), pp 2393–2401.

[11] Vasudevan V., Hanson R. K., Bowman C. T., Golden D. M., Davidson D. F.: *Shock Tube Study of the Reaction of CH with N_2: Overall Rate and Branching Ratio*, J. Phys. Chem. A, 2007, 111(46), pp 11818-11830.

[12] Malte P. C., Pratt D. T.: *The Role of Energy-Releasing Kinetics in NO_X Formation: Fuel-Lean, Jet-Stirred CO-Air Combustion*, Combustion Science and Technology, 1974, 9(5-6), pp 221-231.

[13] Coda Zabetta E., Hupa M., Saviharju K.: *Reducing NO_X Emissions Using Fuel Staging, Air Staging, and Selective Noncatalytic Reduction in Synergy*, Ind. Eng. Chem. Res., 2005, 44(13), pp 4552-4561

[14] Obernberger I.: *Decentralized biomass combustion: state of the art and future development*, Biomass and Bioenergy, 1998, 14(1), pp 33–56.

[15] Salzmann R., Nussbaumer T.: *Fuel Staging for NO_X Reduction in Biomass Combustion: Experiments and Modeling*, Energy & Fuels 2001, 15(3), pp 575-582.

[16] Nussbaumer T.: *Combustion and co-combustion of biomass: fundamentals, technologies, and primary measures for emission reduction*, Energy & Fuels, 2003, 17(6), pp 1510–1521.

[17] Lyon R. K.: *Method for the reduction of the concentration of NO in combustion effluents using N_3*, U.S. Patent 3900554, 1975.

[18] Javed M. T., Irfan N., Gibbs B.M.: *Control of combustion-generated nitrogen oxides by selective non-catalytic reduction*, Journal of Environmental Management, 2007, 83(3), pp 251–289.

[19] Lyon R. K.: *The NH_3 -NO-O_2 Reaction*, Int. Journal of Chem. Kinetics, 1976, 8(2), pp 315-318.

[20] Lyon R. K., Hardy J. E.: D*iscovery and development of the thermal $DeNO_X$ process*, Ind. Eng. Chem. Fundamen., 1986, 25(1), pp 19–24.

[21] Kasuya F., Glarborg P., Johnsson J. E., Dam-Johansen K.: *The thermal $DeNO_X$ process: Influence of Partial Pressures and Temperature*, Chemical Engineering Science, 1995, 50(9), pp 1455-1466.

[22] Tayyeb Javed M., Nimmo W., Gibbs B.M.: *Experimental and modeling study of the effect of CO and H_2 on the urea $DeNO_X$ process in a 150 kW laboratory reactor*, Chemosphere, 2008, 70(6), pp 1059–1067.

[23] Andersen H. C., Cohn J. G. E., Steele D. R.: *Method of selectively removing oxides of nitrogen from oxygen-containing gases*, Engelhard Ind Inc, U.S. patent 2975025, 1957.

[24] Radojevic M.: *Reduction of nitrogen oxides in flue gases*, Environmental Pollution, 1998 102(1), S1, pp 685-689.

[25] Porbatzki D., Stemmler M., Műller S.: *Release of inorganic trace elements during gasification of wood, straw, and miscanthus*, Biomass and Bioenergy, 2011, 35(1), pp S79-S86.

[26] Glarborg P., Kubel D., Dam-Johansen K., Chiang H.-M., Bozzelli J. W.: *Impact of SO_2 and NO on CO oxidation under post-flame conditions*, International Journal of Chemical Kinetics, 1996, 28(10), pp 773–790.

[27] Srivastava R. K., Miller C. A., Erickson C, Jambhekar R.: *Emissions of sulfur trioxide from coal-fired power plants*, J Air Waste Manag Assoc., 2004, 54(6), pp 750-762.

[28] Hindiyarti L., Glarborg P., Marshall P.: *Reactions of SO_3 with the O/H Radical Pool under Combustion Conditions*. J. Phys. Chem. A, 2007, 111(19), pp 3984-3991.

[29] Marier P., Dibbs H. P.: *The catalytic conversion of SO_2 to SO_3 by fly ash and the capture of SO_2 and SO_3 by CaO and MgO*, Thermochimica Acta, 1974, 8(1–2), pp 155–165.

[30] Jørgensen T. L., Livbjerg H., Glarborg P.: *Homogeneous and heterogeneously catalyzed oxidation of SO_2*, Chem. Eng. Sci., 2007, 62(16), pp 4496–4499.

[31] Bennett R. P.: *Chemical reduction of sulfur trioxide and particulates from heavy oils*, Preprints of Papers - American Chemical Society, Division of Fuel Chemistry, 1976, 21(1), pp 35-42.

[32] Srivastava R. K., Jozewicz W., Singer C.: *SO_2 scrubbing technologies: A review,* Environmental Progress, 2001, 20(4), pp 219–228.

[33] Srivastava R. K., Jozewicz W.: *Flue Gas Desulfurization: The State of the Art,* Journal of the Air & Waste Management Association, 2001, 51(12), pp 1676-1688.

[34] Khan A. A., de Jong W., Jansens P. J., Spliethoff H.: *Biomass combustion in fluidized bed boilers: Potential problems and remedies*. Fuel Process. Technol. 2009, 90(1), pp 21–50.

[35] Basu B.: *Combustion and gasification in fluidized beds*. Taylor and Francis Group, LLC., 2006, ISBN 0-8493-3396-2.

[36] Oka S. N.: *Fluidized Bed Combustion*, Marcel Dekker, Inc. New York, USA, 2004, ISBN: 0-8247-4699-6.

[37] Koornneef J., Junginger M., Faaij A.: *Development of fluidized bed combustion - An overview of trends, performance and cost*, Progress in Energy and Combustion Science, 2007, 33(1), pp 19–55.

[38] Demirbas A.: *Combustion characteristics of different biomass fuels*, Progress in Energy and Combustion Science, 2004, 30(2) pp 219–230.

[39] Zevenhoven M., Yrjas P., Skrifvars B.-J., Hupa M.: *Characterization of Ash-Forming Matter in Various Solid Fuels by Selective Leaching and Its Implications for Fluidized-Bed Combustion*, Energy & Fuels, 2012, 26(10), pp 6366–6386.

[40] Åmand L-E, Leckner B: *Co-combustion of sewage sludge with wood/coal in a circulating fluidized bed boiler - a study of gaseous emissions*, 42nd International Energy Agency - Fluidized Bed Conversion (IEA-FBC) meeting, May 10-11, 2001, Sidney, Nova Scotia, Canada.

[41] Leckner B., Åmand L.-E., Lücke K., Werther J.: *Gaseous emissions from co-combustion of sewage sludge and coal/wood in a fluidized bed*, Fuel, 2004, 83(4-5), pp 477–486.

[42] Louhimo J. T.: *Combustion of pulp and papermill sludges and biomass in BFB*, in Proceedings of the 12th International Conference on Fluidized Bed Combustion (ed. L. Rubow), 1993, Volume 1, ASME, New York, pp. 249–264.

[43] Pettersson A., Elled A.-L., Möller A, Steenari B-M., Åmand L-E.: *The Impact of Zeolites During Co-Combustion of Municipal Sewage Sludge with Alkali and Chlorine Rich Fuels*, Proceedings of the 20th International Conference on Fluidized Bed Combustion, 2010, Part 7, pp 902-909.

[44] Aho M., Yrjas P., Taipale R., Hupa M., Silvennoinen J.: *Reduction of superheater corrosion by co-firing risky biomass with sewage sludge*, Fuel, 2010, 89(9), pp 2376-2386.

[45] Spliethoff H., Hein K. R. G.: *Effect of co-combustion of biomass on emissions in pulverized fuel furnaces*, Fuel Processing Technology, 1998, 54(1-3), pp 189–205.

[46] Winter F., Wartha C., Hofbauer H.: *NO and N_2O formation during the combustion of wood, straw, malt waste and peat*, Bioresource Technology, 1999, 70(1), pp 39-49.

[47] Abelha P., Gulyurtlu I., Cabrita I.: *Release of nitrogen precursors from coal and biomass residues in a bubbling fluidized bed*, Energy & Fuels, 2008, 22(1), pp 363–371.

[48] Konttinen J., Hupa M., Kallio S., Winter F., Samuelsson J.: *NO formation tendency characterization for biomass fuels*, Proceedings of the 18th International Conference on Fluidized Bed Combustion, 2005, pp 225-235.

[49] Di Nola G., de Jong W., Spliethoff H.: *TG-FTIR characterization of coal and biomass single fuels and blends under slow heating rate conditions: Partitioning of the fuel-bound nitrogen*, Fuel Processing Technology 2010, 91(1), pp 103–115.

[50] Khan A. A., de Jong W., Jansens P. J., Spliethoff H.: *Biomass combustion in fluidized bed boilers: Potential problems and remedies*, Fuel Processing Technology, 2009, 90(1) pp 21-50.

[51] Leckner B., Karlsson M.: *Emissions from circulating fluidized bed combustion of mixtures of wood and coal*, Proceedings of the 12th International Conference on Fluidized Bed Combustion, 1993, pp 109-115.

[52] Johnsson J. E., *Formation and reduction of nitrogen oxides in fluidized-bed combustion*, Fuel, 1994, 73(9), pp 1398-1415

[53] Hansson K.-M., Åmand L.-E., Habermann A., Winter F.: *Pyrolysis of poly-L-leucine under combustion-like conditions*, Fuel, 2003, 82(6), pp 653-660.

[54] Hansson K.-M., Samuelsson J., Tullin C., Åmand L.-E.: *Formation of HNCO, HCN, and NH_3 from the pyrolysis of bark and nitrogen-containing model compounds*, Combustion and Flame, 2004, 137(3), pp 265–277.

[55] Leppälahti J.: *Formation of NH₃ and HCN in slow-heating-rate inert pyrolysis of peat, coal and bark,* Fuel, 1995, 74(9), pp 1363-1368.

[56] Stubenberger G., Scharler R., Zahirović S., Obernberger I.: *Experimental investigation of nitrogen species release from different solid biomass fuels as a basis for release models*, Fuel, 2008, 87(6), pp 793–806.

[57] Ledesma E. B., Li C.-Z., Nelson P. F., Mackie J. C.: *Release of HCN, NH₃ and HNCO from the thermal gas-phase cracking of coal pyrolysis tars*, Energy & Fuels, 1998, 12(3), pp 536–541.

[58] Åmand L.-E., Leckner B.: *Formation of N₂O in a Circulating Fluidized-Bed Combustor*, Energy & Fuels ,1993, 7(6), pp 1097-1107.

[59] Kilpinen P., Hupa M.: Homogeneous N₂O chemistry at fluidized bed combustion conditions: A kinetic modeling study, Combustion and Flame, 1991, 85(1-2), pp 94–104.

[60] Winter F., Wartha C., Löffler G., Hofbauer H.: *The NO and N₂O formation mechanism during devolatilization and char combustion under fluidized-bed conditions*, Symposium (International) on Combustion, 1996, 26(2), pp 3325–3334.

[61] Werkelin, J.: *Ash-forming elements and their chemical forms in woody biomass fuels*, Academic Dissertation, 2008, Åbo Akademi University, Turku, Finland, ISBN: 978-952-12-2125-5.

[62] Gilbe C., Öhman M., Lindström E., Boström D., Backman R., Samuelsson R., Burvall J.: *Slagging Characteristics during Residential Combustion of Biomass Pellets*, Energy & Fuels, 2008, 22(5), pp 3536-3543.

[63] Baxter L. L., Miles T. R., Miles Jr. T. R., Jenkins B. M., Milne T., Dayton D., Bryers R. W., Oden L. L.: *The behavior of inorganic material in biomass-fired power boilers: Field and laboratory experiences*, Fuel Process. Technol. 1998, 54(1-3), pp 47–78.

[64] Miles T. R., Miles Jr. T. R., Baxter L. L., Bryers R. W., Jenkins B. M., Oden L. L.: *Alkali Deposits Found in Biomass Power Plants: A Preliminary Investigation of Their Extent and Nature*, Vol. I, SAND96-8225, Vol. 2 and NRELrTP-433-8142 (1996).

[65] Jenkins B. M., Baxter L. L., Miles Jr. T.R., Miles T. R.: *Combustion properties of biomass*, Fuel Processing Technology, 1998, 54(1-3), pp 17–46.

[66] Theis M., Skrifvars B.-J., Zevenhoven M., Hupa M., Tran H.: *Fouling tendency of ash resulting from burning mixtures of biofuels. Part 3. Influence of probe surface temperature*, Fuel, 2006, 85(14-15), pp 2002-2011.

[67] Coda Zabetta, E., Barišić V., Peltola K., Hotta A.: *Foster Wheeler Experience with Biomass and Waste in CFBs*, 33rd Clearwater Conference Clearwater, June 1-5, 2008, Florida U.S.A.

[68] Hupa M., Backman R., Skrifvars B.-J., Hyöty P.: *The Influence of Chlorides on the Fireside Behavior in the Recovery Boiler*, Tappi J., 1990, 73(6), pp 153-158.

[69] Salmenoja K., Mäkelä K.: *Corrosion in fluidized bed boilers burning potassium and chlorine containing fuels*, Tappi J., 1999, 82(6).

[70] Davidsson K., Åmand L.-E., Leckner B., Kovacevik B., Svane M., Hagström M., Pettersson J. B. C., Pettersson J., Asteman H., Svensson J.-E., Johansson L.-G.: *Potassium, Chlorine, and Sulfur in Ash, Particles, Deposits, and Corrosion during Wood Combustion in a Circulating Fluidized-Bed Boiler*, Energy & Fuels, 2007, 21(1), pp 71-81.

[71] Theis M., Skrifvars B.-J., Zevenhoven M., Hupa M., Tran H.: *Fouling tendency of ash resulting from burning mixtures of biofuels. Part 2: Deposit chemistry*, Fuel, 2006, 85(14-15), pp 1992-2001.

[72] Pettersson J., Folkeson N., Johansson L.-G., Svensson J.-E.: *The Effects of KCl, K_2SO_4 and K_2CO_3 on the High Temperature Corrosion of a 304-Type Austenitic Stainless Steel*, Oxid Met, 2011, 76(1-2), pp 93–109.

[73] Paneru M., Stein-Brzozowska G., Maier J., Scheffknecht G.: *Corrosion mechanism of alloy 310 austenetic steel beneath NaCl deposit under varying SO_2 concentrations in an oxy-fuel combustion atmosphere*, Energy & Fuels, 2013, 27(10), pp 5699-5705.

[74] Glarborg P., Marshall P.: *Mechanism and modeling of the formation of gaseous alkali sulfates*, Combustion and Flame, 2005, 141(1-2), pp 22–39.

[75] Iisa K., Lu Y., Salmenoja K.: *Sulfation of Potassium Chloride at Combustion Conditions*, Energy & Fuels, 1999, 13(6), pp 1184-1190.

[76] Kassman H., Bäfver L., Åmand L.-E.: *The importance of SO_2 and SO_3 for sulphation of gaseous KCl – An experimental investigation in a biomass fired CFB boiler*, Combustion and Flame, 2010, 157(9), pp 1649–1657.

[77] Hupa M.: *Recovery boiler chemistry – the picture becomes sharper*, Paperi ja puu – Paper and timber, 1993, 75(5), pp 310–319.

[78] Adams T. N.: *General Characteristics of Kraft Black Liquor Recovery boilers*, Chapter 1 in Kraft Recovery Boilers, 1997, TAPPI Press, Atlanta, ISBN 0-9625985-9-3.

[79] Frederick J., Hupa M.: *Black liquor Droplet Burning Process*, Chapter 5 in Kraft Recovery Boilers, 1997, TAPPI Press, Atlanta, ISBN 0-9625985-9-3.

[80] Whitty K., Backman R., Forssén M., Hupa M., Rainio J., Sorvari V.: *Liquor-to-liquor differences in combustion and gasification processes: Pyrolysis behaviour and char reactivity*, Journal of Pulp and Paper Science, 1997, 23(3).

[81] Hupa M., Solin P., Hyöty P.: *Combustion behavior of black liquor droplets*, J. Pulp Paper Sci., 1987, 13(2), pp J67–J72.

[82] Aho K., Hupa M., Nikkanen S.: *Fuel nitrogen release during black liquor pyrolysis; Part 2: Comparisons between different liquors*, Tappi J., 1994, 77(8), pp 182-188.

[83] Forssén M., Hupa M., Hellström P.: *Liquor-to-liquor differences in combustion and gasification processes: Nitrogen oxide formation tendency*, Tappi J., 1999, 82(3), pp 221-227.

[84] Tamminen T., Forssén M., Hupa M.: *Dust and flue gas chemistry during rapid changes in the operation of black liquor recovery boilers: Part 3 – Gaseous emissions*, Tappi J., 2002, 1(7) pp 25-29.

[85] Aho K., Hupa M., Vakkilainen E.: *Fuel nitrogen release during black liquor pyrolysis; Part 1: Laboratory measurements at different conditions*, Tappi J., 1994, 77(5), pp 121-127.

[86] DeMartini N., Forssén M., Niemelä K., Samuelsson Å., Hupa M.: *Release of nitrogen species from the recovery processes of three kraft pulp mills*, Tappi J., 2004, 3(10).

[87] Forssén M., Hupa M., Pettersson R., Martin D.: *Nitrogen oxide formation during black liquor char combustion and gasification*, Journal of Pulp and Paper Science, 1997, 23(9), pp J439-J446.

[88] Kymäläinen M., Forssén M., Jansson M., Hupa M.: *The Fate of Nitrogen in the Chemical Recovery Process in a Kraft Pulp Mill. Part III: The Effect of Some Process Variables*, Jornal of Pulp and Paper Science, 2002, 28(5).

[89] McKeough P. J., Kurkela M., Arpiainen V., Mikkanen P., Kauppinen E., Jokiniemi J.: *The Release of Carbon, Sodium and Sulphur During Rapid Pyrolysis of Black Liquor*, TAPPI International Chemical Recovery Conf., 1995, Toronto, Canada, pp A217-A226.

[90] Feuerstein D.L., Thomas J.F., Brink D.L.: *Malodorous Products from the Combustion of Kraft Black Liquor. I. Pyrolysis and Combustion Aspects*, Tappi J., 1967, 50(6), pp 258-262.

[91] Sricharoenchaikul V., Frederick, W. J., Grace T. M.: Sulphur Species Transformations During Pyrolysis of Kraft Black Liquor, Journal of Pulp and Paper Science, 1997, 23(8), pp J394-J400.

[92] Frederick W. J., Iisa K., Wag, K., Reis, V. V., Boonsongsup L., Forssen M., Hupa M.: *Sodium and sulfur release and recapture during black liquor burning*, 1995, DOI 10.2172/254341.

[93] Borg A., Teder A., Warnqvist B.: *Inside a Kraft recovery furnace – studies of the origins of sulfur and sodium emissions*, Tappi, 1974, 57(1), pp 126-129.

[94] McKeough P. J., Vakkilainen E. K.*: Effects of black liquor composition and furnace conditions on recovery boiler fume chemistry*, International Chemical Recovery Conference, 1998, pp 487-594.

[95] Björkvik T.: *Measurement of sulphur release from black liquor droplets in a single particle reactor*, Master Thesis, 2010, Åbo Akademi.

[96] Harper F. D.: *Sulfur Release During the Pyrolysis of Kraft Black Liquor*, Doctor's Dissertation, The Institute of Paper Science and Technology Atlanta, Georgia, June, 1989.

[97] Tamminen T., Laurén T., Janka K., Hupa, M.: *Dust and flue gas chemistry during rapid changes in the operation of black liquor recovery boilers: Part 1 – Dustformation*, Tappi J., 2002, 1(5), pp 27-32.

[98] Henriksson, M., Warnqvist, B.: *Kinetics of formation of HCl(g) by the reaction between NaCl(s) and SO₂, O₂, and H₂O(g)*, Ind. Eng. Chem. Des. Dev., 1979, 18(2), pp 249-254.

[99] Poon W., Barham D., Tran H.: *Formation of acidic sulphates in kraft recovery boilers*, Tappi J., 76(7): 187-193 (1993).

[100] Backman R., Hupa M., Hyöty P.: *Corrosion relating to acidic sulfates in Kraft and sodium sulfite recovery boilers*, Tappi J., 1984, 67(12), pp 60-64.

[101] Morokuma K., Muguruma C.: *Ab Initio Molecular Orbital Study of the Mechanism of the Gas Phase Reaction SO₃+H₂O : Importance of the Second Water Molecule*, J. Am. Chem. Soc., 1994, 116(22), pp 10316-10317.

[102] Lovejoy E. R., Hanson D. R., Huey L. G.: *Kinetics and Products of the Gas-Phase Reaction of SO₃ with Water*, J. Phys. Chem., 1996, 100(51), pp 19911–19916.

[103] Jayne J. T., Pöschl U., Chen, Y.-N., Dai D., Molina L. T., Worsnop D. R., Kolb C. E., Molina M. J.: *Pressure and temperature dependence of the gas-phase reaction of SO₃ with H₂O and the heterogeneous reaction of SO₃ with H₂O/H₂SO₄ surfaces*, J. Phys. Chem. A., 1997,101(51), pp 10000-10011.

[104] Kolb C. E., Jayne J. T., Worsnop D. R., Molina M. J., Meads R. F., Viggiano A. A.: *Gas phase reaction of sulfur trioxide with water vapor*, J. Am. Chem. Soc., 1994, 116(22), pp 10314–10315.

[105] Mobin M., Malik A. U., Al-Hajri M.: *Investigations on the Failure of Economizer Tubes in a High-Pressure Boiler*, J Fail. Anal. and Preven., 2008, 8(1), pp 69–74.

[106] Verhoff F. H., Banchero J. T.: *Predicting Dew Points of Flue Gases*, Chemical Engineering Progress, 1974, 70, pp 71-72.

[107] Bolsaitis P., Elliott J. F.: *Thermodynamic activities and equilibrium partial pressures for aqueous sulfuric acid solutions*, J. Chem. Eng. Data, 1990, 35(1), pp 69–85.

[108] Benson S.A., Holm P.L.: *Comparison of inorganic constituents in three low rank coals*, Industrial & Engineering Chemistry Product Research and Development, 1985, 24(1), pp 145–149.

[109] http://www.trmiles.com/alkali/Alkali_Report.pdf

[110] Zevenhoven M., Yrjas P., Backaman R., Skrifvars B.-J., Hupa M.: *The Åbo Akademi database-fuel characterization*, paper nr. FBC2005-78093, Proceedings of the 18th International Conference on Fluidized Bed Combustion, May 22–25 2005, Toronto, Ontario, Canada.

[111] Zevenhoven M.: *Ash-forming Matter in Biomass Fuels*, Academic Dissertation, 2001, Åbo Akademi University, Turku, Finland, ISBN: 952-12-0813-9.

[112] Zevenhoven M., Yrjas P., Hupa M.: *Understanding the behavior of biomass fuels - Characterization techniques advance…*, Proc of the 35th International technical conference on clean coal and fuel systems, June 2010, Clearwater, FL, USA.

[113] Åmand L.-E., Leckner B., Eskilsson D., Tullin C.: *Deposits on heat transfer tubes during co-combustion of biofuels and sewage sludge*, Fuel, 2006, 85(10-11), pp 1313–1322.

[114] Aho M., Silvennoinen J.: *Preventing chlorine deposition on heat transfer surfaces with aluminium–silicon rich biomass residue and additive*, Fuel, 2004, 83(10), pp 1299–1305.

[115] Yrjas P., Aho M., Zevenhoven M., Taipale R., Silvennoinen J., Hupa M.: *Co-firing of sewage sludge with bark in a bench-scale bubbling fluidized BED - a study of deposits and emissions*, Proceedings of the 20th International Conference on Fluidized Bed Combustion, Part 7, 2010, pp 922–929.

[116] England C., Houseman J., Teixeira D. P.: *Sampling Nitric Oxide from Combustion Gases*, Combustion and Flame, 1973, 20, pp 439–442.

[117] Karlsson M., Åmand L.-E., *FTIR Analysis of Ammonia and Ethene in a Fluidized Bed Combustion Chamber*, Third Nordic Conference on SO_X and NO_X from Heat and Power Generation, March 13-14, 1996, Lyngby, Denmark.

[118] Kassman H., Åmand L.-E., *Secondary effects in sampling ammonia in the combustion chamber of a cfb boiler*, 42nd International Energy Agency – Fluidized Bed Conversion (IEA-FBC), May 10-11, 2001, Sidney, Nova Scotia, Canada.

[119] Coda Zabetta E., Hupa M.: *A Detailed Kinetic Mechanism with Methanol for Simulating Biomass Combustion and N-Pollutants. Combustion and Flame*, 2008 152(1-2), pp 14-27.

[120] Swithenbank J., Poll I., Vincent M.W., Wright D.D.: *Combustion design fundamentals*, Symposium (International) on Combustion, 1973, 14(1), pp. 627-638.

[121] Oliva M., Alzueta M. U., Millera A., Bilbao R.: *An Approach to the Analysis of Mixing in Reactive Systems*, Chem. Eng. Technol., 2002, 25(4), pp 417-419.

[122] Røjel H., Jensen A., Glarborg P., and Dam-Johansen K.: *Mixing Effects in the Selective Noncatalytic Reduction of NO*, Ind. Eng. Chem. Res., 2000, 39(9), pp 3221–3232.

[123] Alzueta M., Bilbao R., Millera A.: *Modeling Low-Temperature Gas Reburning. NO_X Reduction Potential and Effects of Mixing*, Energy & Fuels, 1998, 12(2), pp 329-338.

[124] Zieba M., Brink A., Schuster A., Hupa M., Scheffknecht G.: *Ammonia chemistry in a flameless jet*, Combustion and Flame, 2009, 156(10), pp 1950–1956.

[125] Zwietering Th. N.: *The degree of mixing in continuous flow systems*, Chemical Engineering Science, 1959, 11(1), pp 1–15.

[126] Andersson K., Normann F., Johnsson F., Leckner B.: *NO Emission during Oxy-Fuel Combustion of Lignite*, Ind. Eng. Chem. Res., 2008, 47(6), pp 1835-1845.

[127] Crumley P. H., Fletcher A. W.: *The formation of sulphur trioxide in flue gases*, J. Inst. Fuel, 1956, 29, pp 322–327.

[128] Cooper D., Ferm M.: *Jämförelse av mätmetoder för bestämning av SO_3 koncentrationer i rökgaser*. Värmeforsk and Institutet för Vatten- och Luftvårdsforskning (IVL) Göteborg, 1994, Värmeforsk report 494.

[129] Jaworowski R. J., Mack S. S.: *Evaluation of Methods for Measurement of SO₃/H₂SO₄ in Flue Gas*, J. Air Pollut. Control Assoc., 1979, 29(1), pp 43-46.

[130] Gustavsson L., Nyquist G.: *Värmeforsks Mäthandbok*, 2005, Värmeforsk Service AB.

[131] US Environmental Protection Agency, EPA Method 8: *Determination of Sulfuric Acid and Sulfur Dioxide from Stationary Sources.*

[132] Koebel M., Elsener M.: *Schwefeltrioxidbestimmung in Abgasen nach der Isopropanolmethode – Eine kritische Betrachtung*, Gefahrstoffe – Reinhaltung der Luft, 1997, 57, pp 193-199.

[133] Kel´man F. N., Zavodskaya Lab., 1952, 11, pp 1316-1318.

[134] Cooper D., Andersson C.: *Bestämning av SO₃ i Rökgaser med NaCl-metoden en Jämförelse av Olika Metoder*, Värmeforsk Report 616; Institutet för Vatten och Luftvårdsforskning (IVL): Göteborg 1997.

[135] Cooper D.: *Optimization of a NaCl Adsorbent Tube Method for SO₃ Measurements in Combustion Flue Gases*, Report B-1177; Institutet för Vatten och Luftvårdsforskning (IVL): Göteborg, 1995.

[136] Patent: Hiroshi, O; Shigeaki, M.; Yoshiaki, O. JP59197859 (A*): Continuous measuring method of concentration of sulfur trioxide in waste*, 1984.

[137] Land T.: *The theory of acid deposition and its application to the dew-point meter*, J. Inst. Fuel, 1977, 50, pp 68-75.

[138] Stuart D. D.: *Continuous Measurements of Acid Dewpoint and Sulfur Trioxide in Stack Gases*, 101st Air and Waste Management Association annual conference and exhibition, 24th – 27th June, 2008, Portland.

[139] Maddalone R. F., Newton S. F., Rhudy R. G., Statnick R. M.: *Laboratory and Field Evaluation of the Controlled Condensation System for SO₃ Measurements in Flue Gas Streams*, Journal of the Air Pollution Control Association, 1979, 29(6), pp 626-631.

[140] Cao Y., Zhou H., Jiang W., Chen C.-W., Pan W.-P.: *Studies of the Fate of Sulfur Trioxide in Coal-Fired Utility Boilers Based on Modified Selected Condensation Methods*, Environmental Science Technology, 2010, 44(9), pp 3429-3434.

[141] Matsuda H., Ozawa S., Naruse K., Ito K., Kojima Y., Yanase T.: *Kinetics of HCl emission from inorganic chlorides in simulated municipal wastes incineration conditions*, Chemical Engineering Science, 2005, 60(2), pp 545–552.

[142] Boonsongsup L., Iisa K., Frederick W. J., Jr.: *Kinetics of the sulfation of NaCl at combustion conditions*, Ind. Eng. Chem. Res., 1997, 36(10), pp 4212–4216.

[143] Sengeløv L. W., Hansen T. B., Bartolomé C., Wu H., Pedersen K. H., Frandsen F. J., Jensen A. D., Glarborg P.: *Sulfation of Condensed Potassium Chloride by SO_2*, Energy & Fuels, 2013, 27(6), pp 3283–3289.

RECENT REPORTS FROM THE COMBUSTION AND MATERIALS CHEMISTRY GROUP OF THE ÅBO AKADEMI PROCESS CHEMISTRY CENTRE:

RECENT REPORTS FROM THE COMBUSTION AND MATERIALS CHEMISTRY GROUP OF THE ÅBO AKADEMI PROCESS CHEMISTRY CENTRE:

PROCESS CHEMISTRY CENTRE